

Electronic Supplementary Information (ESI)

Anti-Schistosomal Activity and ADMET Properties of 1,2,5-Oxadiazinane-Containing Compound Synthesized by Visible-Light Photoredox Catalysis

Kennosuke Itoh,^{*a,b} Hiroki Nakahara,^a Atsushi Takashino,^a Aya Hara,^a Akiho Katsuno,^a Yuriko Abe,^a Takaaki Mizuguchi,^{a,b} Fumika Karaki,^{a,b} Shigeto Hirayama,^{a,b} Kenichiro Nagai,^b Reiko Seki,^b Noriko Sato,^b Kazuki Okuyama,^c Masashi Hashimoto,^c Ken Tokunaga,^d Hitoshi Ishida,^e Fusako Mikami,^f Kofi Dadzie Kwofie,^f Hayato Kawada,^f Bangzhong Lin,^g Kazuto Nunomura,^g Toshio Kanai,^g Takeshi Hatta,^f Naotoshi Tsuji,^f Junichi Haruta,^g and Hideaki Fujii^{*a,b}

- a. *Laboratory of Medicinal Chemistry, School of Pharmacy, Kitasato University, 5-9-1 Shirokane, Minato-ku, Tokyo 108-8641, Japan.*
Corresponding author. E-mail: itok@pharm.kitasato-u.ac.jp
- b. *Medicinal Research Laboratories, School of Pharmacy, Kitasato University, 5-9-1 Shirokane, Minato-ku, Tokyo 108-8641, Japan.*
- c. *Department of Material Science, Graduate School of Science, Josai University, 1-1 Keyakidai, Sakado, Saitama 350-0295, Japan.*
- d. *Division of Liberal Arts, Center for Promotion of Higher Education, Kogakuin University, 2665-1 Nakano-machi, Hachioji, Tokyo 192-0015, Japan.*
- e. *Graduate School of Science and Engineering, Department of Chemistry, Materials and Bioengineering, Kansai University, 3-3-35 Yamate-cho, Suita, Osaka, 564-8680, Japan.*
- f. *Department of Parasitology and Tropical Medicine, Kitasato University School of Medicine, 1-15-1 Kitazato, Minami-ku, Sagami-hara, Kanagawa 252-0374, Japan.*
- g. *Drug Innovation Center Lead Exploration Unit, Graduate School of Pharmaceutical Sciences, Osaka University, 1-6 Yamadagaoka, Suita, Osaka 565-0871, Japan.*

Table of Contents

1. General information	S3
1. Instruments	S3
2. Materials	S3
3. Reaction Monitoring and Purification	S3
2. Synthesis of Ir^{III} Complex IX	S4
3. Synthesis of Nitrone 1i	S4
4. Small-Scale Photochemical Reactions	S5
1. Equipment for Small-Scale Photochemical Reaction	S5
2. General Procedure	S5
5. Photochemical Flow Reaction	S6
1. Photochemical Flow Reactor for Multi-Gram Scale Synthesis	S6
2. Procedure for Multi-Gram Scale Synthesis of 3tb	S6
6. Synthesis of <i>anti</i>-Schistosomal Molecule 4	S7
7. Characterization of Products	S8
1. Characterization of Ir ^{III} Complex IX	S8
2. Characterization of Nitrones 1h and 1i	S8
3. Characterization of Previously Reported 1,2,5-Oxadiazinanes Acquired in this Research	S8
4. Characterization of Novel 1,2,5-Oxadiazinanes	S10
5. Characterization of <i>Anti</i> -Schistosomal Molecule 4	S13
8. NMR Spectra	S14
9. Quenching Experiment	S54
10. Determination of Quantum Yield	S54
11. Determination of Redox Potential and Excited-State Potential of Ir^{III} complex VIII and IX	S55
12. Computation of Dipole Moment	S58
13. Single Crystal X-Ray Diffraction of 3ab	S61
14. Biological Assay	S64
15. ADMET Assay	S64
1. Solubility and LogD	S64
2. Caco-2 Assay	S64
3. LC-MS/MS Analysis	S64
4. Acid Stability Assay	S64
5. Metabolic Stability in Microsomes	S64
6. Cytotoxicity Assay	S65
7. Cardiotoxicity Assay	S65
16. References	S66

1. General Information

1.1. Instruments

Proton NMR spectra were recorded using Agilent 400 MR (400 MHz) and Agilent 600 MR (600 MHz) spectrometers. Chemical shifts were reported in parts per million (ppm) downfield (δ) relative to internal tetramethylsilane (TMS, δ = 0.00) or/with the solvent reference as the internal standard (CDCl_3 , δ = 7.26; CD_3OD , δ = 3.31; $[\text{D}_6]\text{Acetone}$, δ = 2.05; $[\text{D}_6]\text{DMSO}$, δ = 2.50). Data were presented as follows: chemical shift, multiplicity (s = singlet, d = doublet, t = triplet, q = quartet, quint = quintet, sept = septet, br = broad, m = multiplet), coupling constants (Hz), integration, and assignment. Carbon NMR spectra were recorded using Agilent 400 MR (100 MHz) and Agilent 600 MR (600 MHz) spectrometers with complete proton decoupling. Chemical shifts were reported in ppm downfield (δ) relative to the respective solvent reference as the internal standard (CDCl_3 , δ = 77.16; CD_3OD , δ = 49.00; $[\text{D}_6]\text{Acetone}$, δ = 29.84; $[\text{D}_6]\text{DMSO}$, δ = 39.52). Fluorine-19 NMR spectra were recorded using Agilent 400 MR (376 MHz) and Agilent 600 MR (600 MHz) spectrometers without complete proton decoupling. Chemical shifts were reported in ppm downfield (δ) relative to the respective solvent reference as the external standard (CFCl_3 , δ = 0.00) in CDCl_3 . Infrared (IR) spectra were recorded using a JASCO FT/IR-5300 IR spectrophotometer, with ν_{max} given in cm^{-1} . Mass spectra were obtained using JEOL JMS-T100LP AccuTOF and JEOL JMS-700 MStation spectrometers. Melting points were recorded using a YANAKO MP-S3 apparatus. X-ray diffraction measurements for the 1,2,5-oxadiazinane **3ab** were performed at 93K using a Rigaku R-Axis RAPID diffractometer with graphite monochromated Cu K α radiation (λ = 1.54187 Å). Elemental analysis (C, H and N) of the *anti*-Schistosomal molecule **4** was performed using a J-SCIENCE LAB MICRO CORDER JM11. The absorption spectrum of the Ir^{III} complex **IX** was measured using a JASCO V-730 spectrophotometer. The emission spectra of the Ir^{III} complex **IX** at ambient temperature and 77K were recorded using a JASCO FP-8300 spectrophotometer. Electrochemical measurements for the Ir^{III} complexes **VIII** and **IX** were conducted using an electrochemical analyzer (Als/CHI, model 760D) equipped with a single-compartment cell under an argon atmosphere.

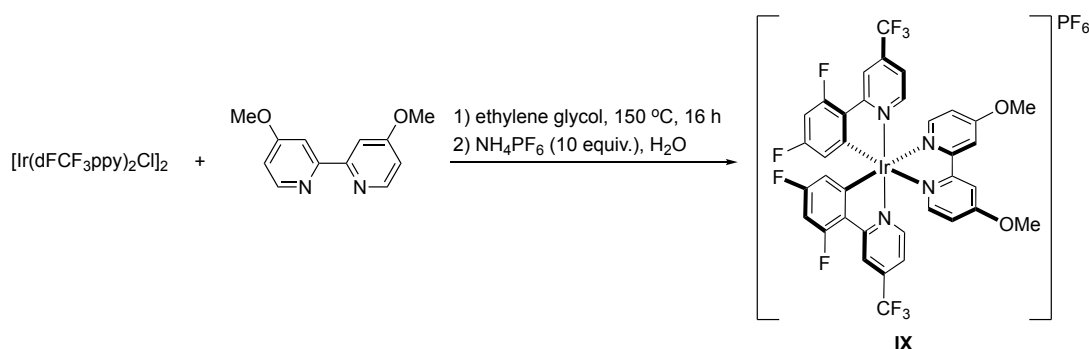
1.2. Materials

All reaction solvents were anhydrous and were purchased from FUJIFILM Wako Pure Chemical Corporation. Deuterated solvents for NMR spectroscopic measurements were obtained from KANTO CHEMICAL Co., Inc. Ir^{III} and Ru^{II} complexes **I–XI** were prepared using previously reported procedures.^{1,2} A novel Ir^{III} complex **IX** was synthesized using $[\text{Ir}(\text{dFCF}_3\text{ppy})_2\text{Cl}]_2$ and 2-(2,4-difluorophenyl)-4-(trifluoromethyl)pyridine³ following the known method mentioned above. Nitrones **1a–1u** were prepared according to previously reported methods.⁴ *N,N,N',N'*-Tetramethyldiaminomethane (**2a**) was purchased from Tokyo Chemical Industry Co., Ltd., while other *N,N,N',N'*-tetraalkyldiaminomethanes **2b–2e** were prepared using previously reported procedures.⁵

1.3. Reaction Monitoring and Purification

All reaction were monitored performed by thin layer chromatography (TLC), using glass TLC plate, silica gel coated with fluorescent indicator F254. The TLC was visualized by UV-quenching and oxidative staining with phosphomolybdic acid (PMA) / ethanol solution. Flash chromatography was performed using Silica Gel (PSQ-60B) purchased from Fuji Silysia Chemical, LTD. Organic solvents and volatile compounds were removed by evaporation at 40 °C.

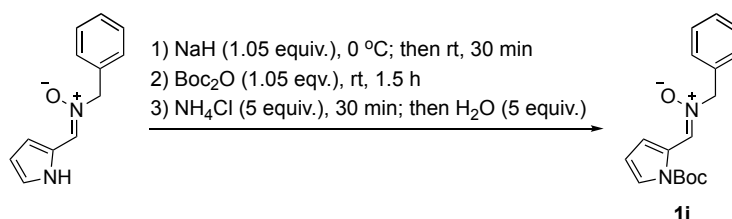
2. Synthesis of Ir^{III} Complex IX



Scheme S1.

To a 30 mL eggplant flask equipped with a stir bar, [Ir(dFCF₃ppy)₂Cl]₂ (180 mg, 0.121 mmol, 1.00 equiv.), 4,4'-dimethoxy-2,2'-bipyridine (60.0 mg, 0.277 mmol, 2.29 equiv.), and ethylene glycol (8.20 mL) were added under a stream of argon. The resulting suspension was heated to 150 °C and stirred for 16 hours. The resulting yellowish solution was cooled to room temperature and poured into aqueous NH₄PF₆ (197 mg, 1.21 mmol, 10.0 equiv.) / water (5.00 mL) solution was added. The resulting suspension was stirred for overnight, and then the bright yellow precipitates was collected by filtration followed by washing with water (20.0 mL). The yellow precipitates was purified by flash chromatography (stationary phase: silica gel, eluent: gradient from 50% AcOEt / *n*-hexane to 100% AcOEt) to afford 220 mg (85%) of IX as a bright yellow solid.

3. Synthesis of Nitron 1i



Scheme S2.

To a 50 mL single-neck round-bottom flask equipped with a stir bar, (Z)-N-benzyl-1-(1H-pyrrol-2-yl)methanimine oxide (500 mg, 2.50 mmol, 1.00 equiv.) and THF (12.5 mL) were added under a stream of argon. The resulting colorless solution was cooled to 0 °C and stirred for 10 minutes, after which NaH (60% dispersion in mineral oil) (175 mg, 2.62 mmol, 1.05 equiv.) was added. The resulting suspension, containing grayish-white precipitates, was warmed to room temperature and stirred until hydrogen gas evolution ceased. Boc₂O (572 mg, 2.62 mmol, 1.05 equiv.), pre-weighed as a solid before melting, was then added to the suspension and stirred for 1.5 hours. Upon completion of the reaction, NH₄Cl (668 mg, 12.5 mmol, 5.00 equiv.) was added to the reaction mixture with vigorous stirring for 30 minutes to form a suspension with white precipitates, followed by the addition of water (225 mg, 12.5 mmol, 5.00 equiv.). The resulting suspension was evaporated, yielding white precipitates as the crude product. The crude product was purified directly by flash chromatography (stationary phase: spherical silica gel; eluent: 10% → 25% → 50% ethyl acetate/*n*-hexane) to afford 677 mg (90%) of (Z)-N-benzyl-1-(1-(tert-butoxycarbonyl)-1H-pyrrol-2-yl)methanimine oxide (1i) as colorless flakes.

4. Small-Scale Photochemical Reactions

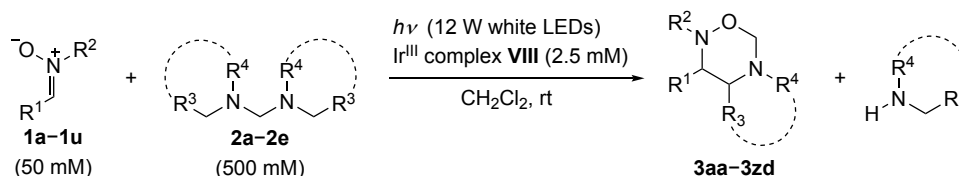
4.1. Equipment for Small-Scale Photochemical Reaction



Figure S1.

Small-scale photochemical reactions (Table 1, Scheme 2) were conducted employing a 12 W white LED tape light sourced from Akiba LED PIKARI-KAN (<https://www.akiba-led.jp/product/1019>). The LED tape light, measuring 10 mm in width and 1 m in length, features SAMSUNG 5630, LM561B LED chips with a color temperature of 5000 K. A DOSHISHA FST-106U WH cooling fan was utilized, and the LED tape was affixed around a PET bottle with slits.

4.2. General Procedure



Scheme S3.

To a test tube equipped with a stir bar were added nitron **1a** (50.0 mg, 237 μmol , 1.00 equiv.), CH_2Cl_2 (4.74 mL), Ir^{III} complex **VIII** (12.7 mg, 11.8 μmol , 0.0500 equiv.), and *N,N,N',N'*-tetramethyldiaminomethane (**2a**) (323 μL , 2.37 mmol, 10.0 equiv.). The resulting solution was degassed by bubbling with argon for 15 min under stirring. External irradiation was performed using a homemade photochemical reactor equipped with a 12 W white LED tape light (Figure S1). The resulting bright yellow solution was stirred at room temperature for 6 h, after which the volatile compounds were removed through evaporation. The crude product was purified through flash chromatography (stationary phase: spherical silica gel; eluent: gradient ranging from 20% ethyl acetate/*n*-hexane) to afford 54.9 mg (86%) of (\pm)-2-benzyl-5-methyl-3-phenyl-1,2,5-oxadiazinane (**3aa**) as a colorless solid.

5. Photochemical Flow Reaction

5.1. Photochemical Flow Reactor for Multi-Gram Scale Synthesis

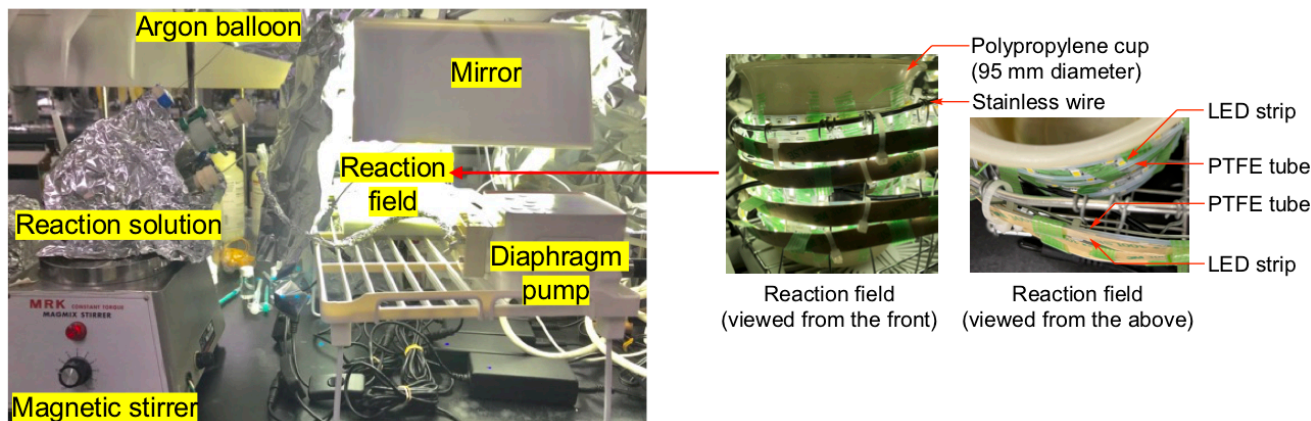
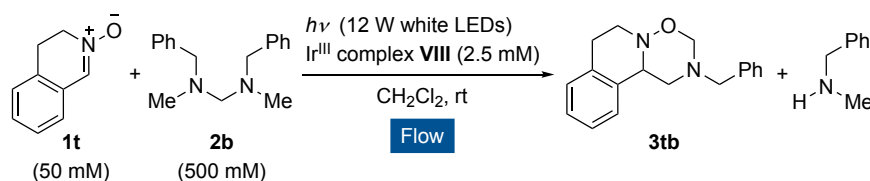


Figure S2.

For the gram-scale photoflow synthesis of **3tb** (Scheme 3), a dedicated photochemical flow system was constructed. Specifications and conditions for the photoflow synthesis are as follows: LED tapes measuring 4 meters in length (60 LEDs/m), PTFE tube with an outer diameter of 1.59 mm and inner diameter of 0.8 mm, spanning 3.75 meters, diaphragm pump model TAKUMINA Q-5-KR-UP-S.

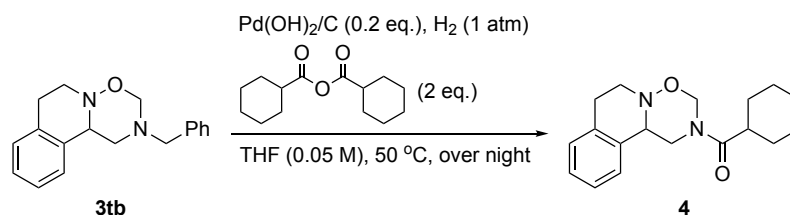
5.2. Procedure for Multi-Gram Scale Synthesis of **3tb**



Scheme S4.

To a 500 mL three-neck round-bottom flask equipped with a stir bar were added nitron **1t** (1.70 g, 11.6 mmol, 1.00 equiv.), CH₂Cl₂ (231 mL), Ir^{III} complex **VIII** (618 mg, 0.578 mmol, 0.0500 equiv.), and *N,N*-dibenzyl-*N',N'*-dimethylmethanediamine (**2b**) (29.4 g, 116 mmol, 10.0 equiv.). The resulting bright yellow solution was degassed by bubbling argon through it for 15 minutes while stirring. Using a diaphragm pump, the resulting CH₂Cl₂ solution was transferred to the reaction field for irradiation (Figure S2). The residence time was set to 45 minutes, resulting in an average flow rate of 0.0420 mL/min. During the flow reaction, the 500 mL three-neck round-bottom flask was filled with argon using an argon balloon. The CH₂Cl₂ solution, which turned brownish, was collected into a 500 mL single-neck round-bottom flask. After completing the flow, CH₂Cl₂ (115 mL) was added to the 500 mL three-neck round-bottom flask. The resulting CH₂Cl₂ solution in the 500 mL three-neck round-bottom flask, containing a small amount of reagents, was then delivered to the reaction field for irradiation at the same flow rate mentioned above and collected into the same 500 mL single-neck round-bottom flask. The combined brownish solution in the 500 mL single-neck round-bottom flask was evaporated, yielding a brownish oil as the crude product. The crude product was dissolved in Et₂O (115 mL), and then acetic acid (13.3 mL, 231 mmol, 20.0 equiv.) was added. After stirring for 30 minutes, a colorless solid precipitated. The resulting precipitate was removed by filtration and washed with Et₂O. The filtrate was evaporated, yielding a pale brown oil, which was purified through flash chromatography (stationary phase: spherical silica gel; eluent: 9% ethyl acetate/*n*-hexane) to afford 1.88 g (58%) of (±)-2-Benzyl-1,2,3,6,7,11b-hexahydro-[1,2,5]oxadiazino[3,2-*a*]isoquinoline (**3tb**) as a colorless viscous oil. The ratio of the eluent was changed to 50% ethyl acetate/*n*-hexane, yielding some fractions containing the Ir^{III} complex. The counter anion was possibly altered from PF₆ of **VIII** to another, which needs to be determined. We have been attempting to establish the regeneration method of **VIII**. Next, the colorless solid was added to a saturated aqueous solution of NaHCO₃, followed by extraction with AcOEt to recover unreacted **2b**. The recovered **2b** was purified by distillation under reduced pressure, yielding 13.2 g (48%) of **2b** as a colorless oil, which was reusable.

6. Synthesis of *anti*-Schistosomal Molecule 4

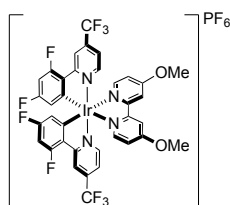


Scheme S5.

To a 200 mL single-neck round-bottom flask equipped with a stir bar were added (±)-2-Benzyl-1,2,3,6,7,11b-hexahydro-[1,2,5]oxadiazino[3,2-a]isoquinoline (**3tb**) (518 mg, 1.85 mmol, 1.00 equiv.), cyclohexanecarboxylic anhydride (880 mg, 3.69 mmol, 2.00 equiv.), and THF (37.0 mL). The resulting solution was conditioned under reduced pressure using a low-pressure hand pump, then filled with argon via an argon balloon. Pd(OH)₂/C (20 wt%, dry basis) (259 mg, 0.369 mmol, 0.200 equiv.) was then added to the THF solution, which was again conditioned under reduced pressure using a low-pressure hand pump, followed by the introduction of H₂ gas to the reaction mixture using a balloon. The mixture was stirred overnight. The suspension was filtered, and the filtrate was evaporated, yielding a pale yellow oil as the crude product. The crude product was purified by flash chromatography (stationary phase: spherical silica gel; eluent: 9% ethyl acetate/*n*-hexane) to afford 333 mg (60%) of (±)-cyclohexyl(1,6,7,11b-tetrahydro-[1,2,5]oxadiazino[3,2-a]isoquinolin-2(3*H*)-yl)methanone (**4**) as a colorless solid.

7. Characterization of Products

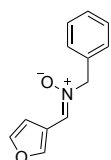
7.1. Characterization of Ir^{III} Complex



(4,4'-Dimethoxy-2,2'-bipyridine)bis[3,5-difluoro-2-[4-(trifluoromethyl)-2-pyridinyl-κN]phenyl-κC]iridium(III) hexafluorophosphate (IX)

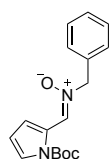
Bright yellow solid; ¹H NMR (600 MHz, [D₆]Acetone, 22 °C, TMS, ppm): δ = 8.57–8.49 (2H, m), 8.41 (2H, d, *J* = 2.7 Hz), 8.30 (2H, d, *J* = 6.3 Hz), 7.96 (2H, d, *J* = 6.5 Hz), 7.56 (2H, dd, *J* = 6.3, 2.0 Hz), 7.27 (2H, dd, *J* = 6.5, 2.7 Hz), 6.85 (2H, ddd, *J* = 12.9, 8.8, 2.4 Hz), 5.96 (2H, dd, *J* = 8.8, 2.4 Hz), 4.1 (6H, s); ¹³C NMR (150 MHz, [D₆]Acetone, 22 °C, TMS, ppm): δ = 166.5, 165.2 (dd, *J* = 261.2, 13.2 Hz), 163.0 (dd, *J* = 258.2, 12.5 Hz), 156.1 (d, *J* = 7.3 Hz), 152.9, 152.2, 140.6 (q, *J* = 34.5 Hz), 127.9 (dd, *J* = 8.9, 2.9 Hz), 123.3 (q, *J* = 273.1 Hz), 120.7 (dd, *J* = 6.0, 3.1 Hz), 119.9 (q, *J* = 21.3 Hz), 115.4, 115.1 (dd, *J* = 14.7, 2.9 Hz), 112.8, 99.9 (dd, *J* = 27.1, 27.1 Hz), 57.4; ¹⁹F (564 MHz, [D₆]Acetone, 23 °C, TMS, ppm): δ = –109.2 (1F, dt, *J* = 12.1, 4.2 Hz), –105.7 (1F, td, *J* = 11.2, 9.0 Hz), –65.8 (3F, s); HRMS (ESI): *m/z* Calcd for C₃₆H₂₂F₁₀IrN₄O₂ [M]⁺: 925.1216; Found: 925.1213.

7.2. Characterization of Novel Nitrones 1h and 1i



(Z)-N-Benzyl-1-(furan-3-yl)methanimine oxide (1h)

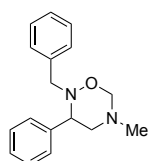
Pale brown solid; M.p. 98–99 °C; ¹H NMR (400 MHz, CDCl₃, 22 °C, TMS, ppm): δ = 8.90 (1H, s), 7.54–7.36 (6H, m), 7.33 (1H, s), 5.03 (2H, s); ¹³C NMR (100 MHz, CDCl₃, 22 °C, TMS, ppm): δ = 146.3, 142.8, 133.1, 129.4, 129.2 (2C), 127.8, 116.8, 109.4, 69.4; IR (KBr): ν = 3076, 1591, 1457, 1430, 1135, 1018, 818 cm^{–1}; HRMS (FAB): *m/z* Calcd for C₁₂H₁₂NO₂: 202.0868 [M+H]⁺; Found: 202.0868.



(Z)-N-Benzyl-1-(1-(tert-butoxycarbonyl)-1H-pyrrol-2-yl)methanimine oxide (1i)

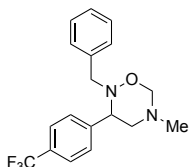
Colorless flake; M.p. 131–132 °C; ¹H NMR (400 MHz, CDCl₃, 22 °C, TMS, ppm): δ = 8.70 (1H, s), 8.15 (1H, dd, *J* = 3.6, 1.6 Hz), 7.53–7.43 (2H, m), 7.43–7.31 (4H, m), 6.29 (1H, dd, *J* = 3.6, 3.6 Hz), 5.03 (2H, s), 1.59 (9H, s); ¹³C NMR (100 MHz, CDCl₃, 22 °C, TMS, ppm): δ = 149.4, 133.9, 129.1, 129.0, 128.8, 126.6, 126.4, 124.6, 120.2, 112.0, 84.8, 70.6, 28.1; IR (KBr): ν = 3156, 2983, 2950, 1751, 1566, 1471, 1327, 1296, 1127, 835, 737 cm^{–1}; HRMS (ESI): *m/z* Calcd for C₁₇H₂₁N₂O₃: 301.1552 [M+H]⁺; Found: 301.1547.

7.3. Characterization of Previously Reported 1,2,5-Oxadiazinanes Acquired in this Research



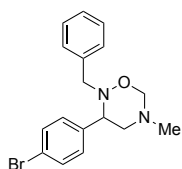
(±)-2-Benzyl-5-methyl-3-phenyl-1,2,5-oxadiazinane (3aa)

¹H NMR (400 MHz, CDCl₃, 22 °C, TMS, ppm): δ = 7.60–7.07 (m, 10H), 4.65 (d, *J* = 9.7 Hz, 1H), 4.40 (dd, *J* = 9.7, 1.8 Hz, 1H), 4.03 (dd, *J* = 10.6, 2.3 Hz, 1H), 3.88 (d, *J* = 14.6 Hz, 1H), 3.55 (d, *J* = 14.6 Hz, 1H), 3.05 (dd, *J* = 13.0, 10.6 Hz, 1H), 2.87 (ddd, *J* = 13.0, 2.3, 1.8 Hz, 1H), 2.52 (s, 3H); ¹³C NMR (100 MHz, CDCl₃, 22 °C, TMS, ppm): δ = 139.8, 138.3, 128.9, 128.5, 128.1, 128.0, 127.9, 126.9, 87.0, 65.0, 60.0, 59.6, 39.7; HRMS (ESI): *m/z* Calcd for C₁₇H₂₁N₂O: 269.1654 [M+H]⁺; found: 269.1652. The spectral characteristics were consistent with spectral data previously reported.^{5b}



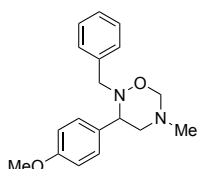
(±)-2-Benzyl-5-methyl-3-(4-(trifluoromethyl)phenyl)-1,2,5-oxadiazinane (3ba)

¹H NMR (400 MHz, CDCl₃, 22 °C, TMS, ppm): δ = 7.61 (d, *J* = 8.2 Hz, 2H), 7.52 (br d, *J* = 7.0 Hz, 1H), 7.36–7.15 (m, 5H), 4.67 (d, *J* = 10.0 Hz, 1H), 4.41 (dd, *J* = 10.0, 2.0 Hz, 1H), 4.10 (dd, *J* = 10.6, 3.0 Hz, 1H), 3.82 (d, *J* = 14.7 Hz, 1H), 3.58 (d, *J* = 14.7 Hz, 1H), 3.03 (dd, *J* = 13.2, 10.6 Hz, 1H), 2.86 (ddd, *J* = 13.2, 3.0, 2.0 Hz, 1H), 2.53 (s, 3H); ¹³C NMR (100 MHz, CDCl₃, 22 °C, TMS, ppm): δ = 143.9, 137.8, 130.3 (q, *J* = 32.5 Hz), 128.5, 128.2 (2C), 127.1, 125.9 (q, *J* = 3.7 Hz), 124.1 (q, *J* = 272.2 Hz), 86.9, 64.4, 59.85, 59.81, 39.6; ¹⁹F NMR (376 MHz, CDCl₃, 23 °C, TMS, ppm): δ = –62.6; HRMS (ESI): *m/z* Calcd for C₁₈H₂₀F₃N₂O: 337.1528 [M+H]⁺; found: 337.1520. The spectral characteristics were consistent with spectral data previously reported.^{5b}



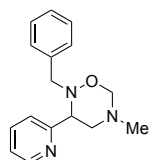
(±)-2-Benzyl-3-(4-bromophenyl)-5-methyl-1,2,5-oxadiazinane (3ca)

^1H NMR (400 MHz, CDCl_3 , 22 °C, TMS, ppm): δ = 7.53–7.41 (m, 2H), 7.39–7.14 (m, 7H), 4.63 (d, J = 10.0 Hz, 1H), 4.40 (dd, J = 10.0, 1.9 Hz, 1H), 4.00 (dd, J = 10.5, 3.0 Hz, 1H), 3.82 (d, J = 14.6 Hz, 1H), 3.55 (d, J = 14.6 Hz, 1H), 2.98 (dd, J = 13.1, 10.5 Hz, 1H), 2.85 (ddd, J = 13.1, 3.0, 1.9 Hz, 1H), 2.51 (s, 3H); ^{13}C NMR (100 MHz, CDCl_3 , 22 °C, TMS, ppm): δ = 138.8, 138.0, 132.1, 129.5, 128.6, 128.2, 127.1, 121.9, 87.0, 64.2, 59.9, 59.6, 39.7; HRMS (ESI): m/z Calcd for $\text{C}_{17}\text{H}_{20}^{81}\text{BrN}_2\text{O}$: 349.0739 $[M+H]^+$; found: 349.0751. The spectral characteristics were consistent with spectral data previously reported.^{5b}



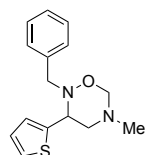
(±)-2-Benzyl-3-(4-methoxyphenyl)-5-methyl-1,2,5-oxadiazinane (3da)

^1H NMR (400 MHz, CDCl_3 , 22 °C, TMS, ppm): δ = 7.43–7.13 (m, 7H), 6.97–6.78 (m, 2H), 4.62 (d, J = 9.8 Hz, 1H), 4.39 (dd, J = 9.8, 1.9 Hz, 1H), 3.98 (dd, J = 10.7, 3.0 Hz, 1H), 3.89 (d, J = 14.8 Hz, 1H), 3.79 (s, 3H), 3.53 (d, J = 14.8 Hz, 1H), 3.00 (dd, J = 12.7, 10.7 Hz, 1H), 2.85 (ddd, J = 12.7, 3.0, 1.9 Hz, 1H), 2.51 (s, 3H); ^{13}C NMR (100 MHz, CDCl_3 , 22 °C, TMS, ppm): δ = 159.4, 138.4, 131.7, 129.0, 128.5, 128.2, 126.9, 114.3, 87.0, 64.3, 60.0, 59.4, 55.4, 39.7; HRMS (ESI): m/z Calcd for $\text{C}_{18}\text{H}_{23}\text{N}_2\text{O}_2$: 299.1760 $[M+H]^+$; found: 299.1758. The spectral characteristics were consistent with spectral data previously reported.^{5b}



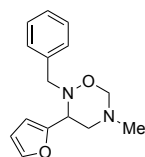
(±)-2-Benzyl-5-methyl-3-(pyridin-2-yl)-1,2,5-oxadiazinane (3ea)

^1H NMR (400 MHz, CDCl_3 , 22 °C, TMS, ppm): δ = 8.63–8.52 (m, 1H), 7.67 (ddd, J = 7.7, 7.7, 1.8 Hz, 1H), 7.47 (d, J = 7.7 Hz, 1H), 7.35–7.16 (m, 6H), 4.78 (d, J = 10.2 Hz, 1H), 4.41 (dd, J = 10.2, 2.0 Hz, 1H), 4.30 (dd, J = 10.7, 2.9 Hz, 1H), 3.81 (d, J = 14.9 Hz, 1H), 3.69 (d, J = 14.9 Hz, 1H), 3.18 (dd, J = 13.2, 10.7 Hz, 1H), 2.99 (ddd, J = 13.2, 2.9, 2.0 Hz, 1H), 2.58 (s, 3H); ^{13}C NMR (100 MHz, CDCl_3 , 22 °C, TMS, ppm): δ = 159.4, 149.6, 137.9, 137.0, 128.5, 128.2, 127.0, 122.9, 122.4, 86.8, 66.0, 60.1, 58.3, 39.6; HRMS (ESI): m/z Calcd for $\text{C}_{16}\text{H}_{20}\text{N}_3\text{O}$: 270.1606 $[M+H]^+$; found: 270.1609. The spectral characteristics were consistent with spectral data previously reported.^{5b}



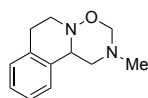
(±)-2-Benzyl-5-methyl-3-(thiophen-2-yl)-1,2,5-oxadiazinane (3fa)

^1H NMR (400 MHz, CDCl_3 , 22 °C, TMS, ppm): δ = 7.41–7.18 (m, 6H), 7.03 (br d, J = 3.6 Hz, 1H), 6.96 (dd, J = 5.1, 3.6 Hz, 1H), 4.63 (d, J = 10.0 Hz, 1H), 4.37 (d, J = 10.4 Hz, 1H), 4.36 (d, J = 10.0 Hz, 1H), 3.96 (d, J = 14.7 Hz, 1H), 3.56 (d, J = 14.7 Hz, 1H), 3.11 (dd, J = 12.9, 10.4 Hz, 1H), 2.97 (br d, J = 12.9 Hz, 1H), 2.51 (s, 3H); ^{13}C NMR (100 MHz, CDCl_3 , 22 °C, TMS, ppm): δ = 141.9, 138.1, 128.7, 128.2, 127.0, 126.6, 125.7, 125.6, 87.0, 60.7, 60.1, 59.6, 39.6; HRMS (ESI): m/z Calcd for $\text{C}_{15}\text{H}_{19}\text{N}_2\text{OS}$: 275.1218 $[M+H]^+$; found: 275.1228. The spectral characteristics were consistent with spectral data previously reported.^{5b}



(±)-2-Benzyl-3-(furan-2-yl)-5-methyl-1,2,5-oxadiazinane (3ga)

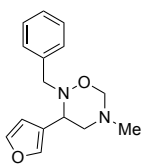
^1H NMR (400 MHz, $[\text{D}_6]\text{Acetone}$, 22 °C, TMS, ppm): δ = 7.57–7.53 (dd, J = 1.6, 0.8 Hz, 1H), 7.33–7.12 (m, 5H), 6.52–6.38 (m, 2H), 4.54 (d, J = 9.6 Hz, 1H), 4.27 (d, J = 9.6 Hz, 1H), 4.18 (dd, J = 11.1, 2.5 Hz, 1H), 3.78 (d, J = 14.7 Hz, 1H), 3.62 (d, J = 14.7 Hz, 1H), 3.24 (dd, J = 13.5, 11.1 Hz, 1H), 2.88 (ddd, J = 13.5, 2.5, 2.0 Hz, 1H), 2.47s (s, 3H); ^{13}C NMR (100 MHz, $[\text{D}_6]\text{Acetone}$, 22 °C, TMS, ppm): δ = 153.4, 143.2, 139.3, 129.3, 128.7, 127.4, 111.3, 109.2, 87.4, 60.4, 58.3, 57.0, 39.5; HRMS (ESI): m/z Calcd for $\text{C}_{15}\text{H}_{19}\text{N}_2\text{O}_2$: 259.1447 $[M+H]^+$; Found: 259.1458. The spectral characteristics were consistent with spectral data previously reported.^{5b}



(±)-2-Methyl-1,2,3,6,7,11b-hexahydro-[1,2,5]oxadiazino[3,2-a]isoquinoline (3ta)

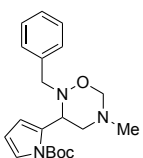
^1H NMR (400 MHz, CDCl_3 , 22 °C, TMS, ppm): δ = 7.21–7.14 (2H, m), 7.13–7.02 (2H, m), 4.62 (1H, d, J = 9.4 Hz), 4.47 (1H, dd, J = 9.4, 1.6 Hz), 4.05 (1H, d, J = 9.6 Hz), 3.50 (1H, dd, J = 10.6, 6.5 Hz), 3.42 (1H, d, J = 10.6 Hz), 3.28 (1H, ddd, J = 12.0, 10.4, 4.5 Hz), 3.02 (1H, ddd, J = 12.0, 10.4, 4.5 Hz), 2.90–2.70 (2H, m), 2.56 (3H, s); ^{13}C NMR (100 MHz, CDCl_3 , 22 °C, TMS, ppm): δ = 134.5, 134.1, 128.9, 127.1, 126.3, 123.8, 87.0, 60.8, 55.9, 52.8, 40.2, 29.1; HRMS (ESI): m/z Calcd for $\text{C}_{12}\text{H}_{17}\text{N}_2\text{O}$: 205.1341 $[M+H]^+$; Found: 205.1307. The spectral characteristics were consistent with spectral data previously reported.^{5b}

7.4. Characterization of Novel 1,2,5-Oxadiazinanes



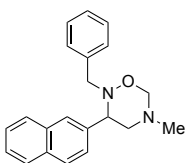
(±)-2-Benzyl-3-(furan-3-yl)-5-methyl-1,2,5-oxadiazinane (3ha)

Pale yellow oil; ^1H NMR (400 MHz, CD_3OD , 22 $^\circ\text{C}$, TMS, ppm): δ = 7.57 (1H, s), 7.49 (1H, dd, J = 1.1, 1.1 Hz), 7.29–7.14 (5H, m), 6.51 (1H, d, J = 1.1 Hz), 4.41 (1H, d, J = 9.8 Hz), 4.39–4.28 (1H, m), 4.06 (1H, dd, J = 10.2, 3.2 Hz), 3.94 (1H, d, J = 14.4 Hz), 3.53 (1H, d, J = 14.4 Hz), 2.91 (1H, dd, J = 12.7, 10.2 Hz), 2.85 (1H, ddd, J = 12.7, 3.2, 1.7 Hz), 2.41 (3H, s); ^{13}C NMR (100 MHz, CD_3OD , 22 $^\circ\text{C}$, TMS, ppm): δ = 144.7, 141.9, 138.9, 129.7, 128.7, 127.6, 124.2, 109.9, 87.3, 60.1, 59.5, 57.5, 39.1; IR (neat): ν = 2939, 1497, 1454, 1159, 1021 cm^{-1} ; HRMS (ESI): m/z Calcd for $\text{C}_{15}\text{H}_{19}\text{N}_2\text{O}$: 259.1447 $[M+\text{H}]^+$; Found: 259.1456. To prevent the observation of broadened signals in the NMR measurement, we utilized CD_3OD as a deuterated solvent.



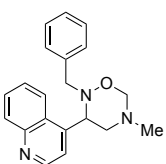
(±)-tert-Butyl 2-(2-benzyl-5-methyl-1,2,5-oxadiazinan-3-yl)-1H-pyrrole-1-carboxylate (3ia)

Pale yellow solid; M.p. 74–75 $^\circ\text{C}$; ^1H NMR (400 MHz, $[\text{D}_6]\text{Acetone}$, 22 $^\circ\text{C}$, TMS, ppm): δ = 7.35–7.14 (6H, m), 6.54–6.30 (1H, br s), 6.18 (1H, dd, J = 1.1, 1.1 Hz), 5.01 (1H, dd, J = 9.9, 3.1 Hz), 4.56 (1H, d, J = 9.8 Hz), 4.29 (1H, d, J = 9.8 Hz), 3.93 (1H, d, J = 14.7 Hz), 3.63 (1H, d, J = 14.7 Hz), 3.03 (1H, br d, J = 12.6 Hz), 2.91 (1H, dd, J = 12.6, 9.9 Hz), 2.48 (3H, s), 1.63 (9H, s); ^{13}C NMR (100 MHz, $[\text{D}_6]\text{Acetone}$, 22 $^\circ\text{C}$, TMS, ppm): δ = 150.1, 139.6, 134.2, 129.3, 128.7, 127.4, 122.3, 113.3, 111.3, 87.4, 84.9, 59.9, 59.6, 56.8, 39.6, 28.1; IR (KBr): ν = 3169, 2971, 2932, 1735, 1321, 969, 732 cm^{-1} ; HRMS (ESI): m/z $\text{C}_{20}\text{H}_{28}\text{N}_3\text{O}_3$: 358.2131 $[M+\text{H}]^+$; Found: 358.2114. To prevent the observation of broadened signals in the NMR measurement, we utilized $[\text{D}_6]\text{Acetone}$ as a deuterated solvent.



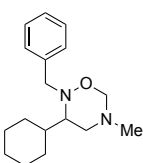
(±)-2-Benzyl-5-methyl-3-(naphthalen-2-yl)-1,2,5-oxadiazinane (3ja)

Colorless oil; ^1H NMR (400 MHz, CDCl_3 , 22 $^\circ\text{C}$, TMS, ppm): δ = 7.93–7.74 (4H, m), 7.65–7.52 (br s, 1H), 7.50–7.40 (2H, m), 7.32–7.16 (5H, m), 4.71 (1H, d, J = 9.9 Hz), 4.44 (1H, dd, J = 9.9, 2.2 Hz), 4.21 (1H, dd, J = 10.7, 2.7 Hz), 3.92 (1H, d, J = 14.8 Hz), 3.62 (1H, d, J = 14.8 Hz), 3.16 (1H, dd, J = 12.2, 10.7 Hz), 2.93 (1H, ddd, J = 12.2, 2.7, 2.2 Hz), 2.56 (3H, s); ^{13}C NMR (100 MHz, CDCl_3 , 22 $^\circ\text{C}$, TMS, ppm): δ = 138.2, 137.3, 133.5, 133.3, 128.7, 128.6, 128.2, 127.9, 127.8, 127.1, 127.0, 126.4, 126.2, 125.5, 87.1, 65.0, 59.9, 59.8, 39.7; IR (neat): ν = 2940, 1509, 1048, 700 cm^{-1} ; HRMS (ESI): m/z Calcd for $\text{C}_{21}\text{H}_{23}\text{N}_2\text{O}$ $[M+\text{H}]^+$: 319.1810; Found: 319.1825.



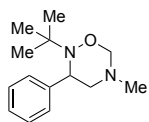
(±)-2-Benzyl-5-methyl-3-(quinolin-4-yl)-1,2,5-oxadiazinane (3ka)

Colorless oil; ^1H NMR (400 MHz, $[\text{D}_6]\text{DMSO}$, 80 $^\circ\text{C}$, ppm): δ = 8.86 (1H, d, J = 4.5 Hz), 8.46 (1H, br s), 8.05 (1H, d, J = 8.5, 1.0 Hz), 7.76 (1H, ddd, J = 8.5, 6.6, 1.2 Hz), 7.65 (1H, ddd, J = 8.5, 6.6, 1.0 Hz), 7.64 (1H, d, J = 4.5 Hz), 7.26–7.17 (5H, m), 4.88 (1H, br d, J = 10.7 Hz), 4.68 (1H, d, J = 10.0 Hz), 4.43 (1H, dd, J = 10.0, 2.2 Hz), 3.74 (1H, J = 14.9 Hz), 3.64 (1H, J = 14.9 Hz), 3.13 (1H, br dd, J = 13.1, 10.7 Hz), 2.93 (1H, ddd, J = 13.1, 3.6, 2.2 Hz), 2.54 (3H, s); ^{13}C NMR (100 MHz, $[\text{D}_6]\text{DMSO}$, 80 $^\circ\text{C}$, ppm): δ = 149.8, 147.9, 144.5, 137.3, 129.6, 128.8, 127.9, 127.4, 126.24, 126.20, 125.4, 123.1, 119.6, 85.9, 58.9 (2C), 57.7, 38.5; IR (neat): ν = 3029, 2938, 2884, 1586, 1508, 1050, 966, 759 cm^{-1} ; HRMS (ESI): m/z Calcd for $\text{C}_{20}\text{H}_{22}\text{N}_3\text{O}$ $[M+\text{H}]^+$: 320.1763; Found: 320.1768. The ^1H NMR spectrum and ^{13}C NMR spectrum were measured at room temperature, where signals from conformational isomers were observed. Therefore, the measurement was conducted at 80 $^\circ\text{C}$ to coalesce the signals of the conformational isomers.



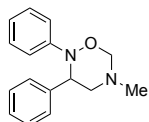
(±)-2-Benzyl-3-cyclohexyl-5-methyl-1,2,5-oxadiazinane (3la)

Pale yellow solid; M.p. 57–58 $^\circ\text{C}$; ^1H NMR (400 MHz, CDCl_3 , 22 $^\circ\text{C}$, TMS, ppm): δ = 7.44–7.352 (2H, m), 7.350–7.27 (2H, m), 7.27–7.21 (1H, m), 4.33–4.18 (3H, m), 3.62 (1H, d, J = 14.8 Hz), 2.94 (1H, ddd, J = 10.1, 3.6, 3.6 Hz), 2.78 (1H, ddd, J = 12.2, 3.6, 1.2 Hz), 2.76 (1H, dd, J = 12.2, 10.1 Hz), 2.36 (3H, s), 1.89–1.593 (5H, m), 1.592–1.44 (1H, m), 1.37–0.96 (5H, m); ^{13}C NMR (100 MHz, CDCl_3 , 22 $^\circ\text{C}$, TMS, ppm): δ = 138.6, 128.5, 128.2, 126.9, 86.7, 63.5, 58.3, 52.5, 39.8, 39.1, 30.1, 27.2, 26.9, 26.8, 26.4; IR (KBr): ν = 2953, 2925, 2849, 1452, 1047, 969 cm^{-1} ; HRMS (ESI): m/z Calcd for $\text{C}_{17}\text{H}_{27}\text{N}_2\text{O}$ $[M+\text{H}]^+$: 275.2123; Found: 275.2122.



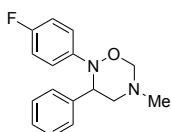
(±)-2-(*tert*-Butyl)-5-methyl-3-phenyl-1,2,5-oxadiazinane (3ma)

Pale yellow solid; M.p. 39–40 °C; ¹H NMR (400 MHz, CDCl₃, 22 °C, TMS, ppm): δ = 7.36 (2H, d, *J* = 6.7 Hz), 7.31–7.19 (3H, m), 4.54 (1H, d, *J* = 9.4 Hz), 4.44 (1H, dd, *J* = 9.4, 2.5 Hz), 4.24 (1H, dd, *J* = 10.0, 2.5 Hz), 2.95 (1H, dd, *J* = 12.6, 10.0 Hz), 2.72 (1H, ddd, *J* = 12.6, 2.5, 2.5 Hz), 2.42 (3H, s), 0.91 (9H, s), ¹³C NMR (100 MHz, CDCl₃, 22 °C, TMS, ppm): δ = 141.6, 128.7, 128.3, 127.7, 87.0, 61.2, 61.0, 60.3, 39.5, 27.3; IR (KBr): ν = 2971, 2920, 2886, 1359, 1048, 978 cm⁻¹; HRMS (ESI): *m/z* Calcd for C₁₄H₂₃N₂O [*M*+H]⁺: 235.1810; Found: 235.1799.



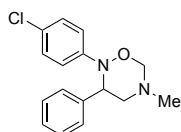
(±)-5-Methyl-2,3-diphenyl-1,2,5-oxadiazinane (3na)

Colorless solid; M.p. 41–42 °C; ¹H NMR (400 MHz, CDCl₃, 22 °C, TMS, ppm): δ = 7.35–6.95 (10H, m), 4.93 (1H, d, *J* = 9.8 Hz), 4.60 (1H, dd, *J* = 9.8, 1.9 Hz), 4.51 (1H, dd, *J* = 9.5, 3.0 Hz), 3.23 (1H, dd, *J* = 13.0, 9.5 Hz), 3.00 (1H, ddd, *J* = 13.0, 3.0, 1.9 Hz), 2.60 (3H, s); ¹³C NMR (100 MHz, CDCl₃, 22 °C, TMS, ppm): δ = 149.1, 138.8, 128.4, 128.3 (2C), 127.7, 125.7, 123.2, 87.6, 64.3, 59.5, 39.6; IR (KBr): ν = 2940, 2800, 1490, 696 cm⁻¹; HRMS (ESI): *m/z* Calcd for C₁₆H₁₉N₂O [*M*+H]⁺: 255.1502; Found: 255.1497.



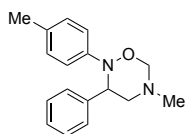
(±)-2-(4-Fluorophenyl)-5-methyl-3-phenyl-1,2,5-oxadiazinane (3oa)

Pale yellow solid; M.p. 41–42 °C; ¹H NMR (400 MHz, CDCl₃, 22 °C, TMS, ppm): δ = 7.06–7.28 (7H, m), 6.76–6.86 (2H, m), 4.91 (1H, d, *J* = 9.8 Hz), 4.59 (1H, dd, *J* = 9.8, 2.0 Hz), 4.43 (1H, dd, *J* = 10.3, 3.0 Hz), 3.23 (1H, dd, *J* = 13.4, 10.3 Hz), 2.99 (1H, ddd, *J* = 13.4, 3.0, 2.0 Hz), 2.62 (3H, s); ¹³C NMR (100 MHz, CDCl₃, 22 °C, TMS, ppm): δ = 160.8 (d, *J* = 245 Hz), 145.2 (d, *J* = 2.9 Hz), 138.5, 128.5 (d, *J* = 10.5 Hz), 128.0, 125.7, 125.6, 115.1 (d, *J* = 22.4 Hz), 87.7, 65.2, 59.6, 39.7; ¹⁹F (376 MHz, CDCl₃, 23 °C, TMS, ppm): δ = -116.2 (3F, s); IR (KBr): ν = 2942, 1505, 1208, 700 cm⁻¹; HRMS (ESI): *m/z* Calcd for C₁₆H₁₈FN₂O [*M*+H]⁺: 273.1393; Found: 273.1403.



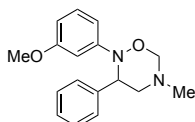
(±)-2-(4-Chlorophenyl)-5-methyl-3-phenyl-1,2,5-oxadiazinane (3pa)

Pale yellow solid; M.p. 57–58 °C; ¹H NMR (400 MHz, CDCl₃, 22 °C, TMS, ppm): δ = 7.25–7.16 (5H, m), 7.13–7.05 (2H, m), 7.05–6.98 (2H, m), 7.00–6.90 (2H, m), 4.91 (1H, d, *J* = 9.9 Hz), 4.60 (1H, dd, *J* = 9.9, 1.9 Hz), 4.44 (1H, dd, *J* = 9.9, 3.0 Hz), 3.23 (1H, dd, *J* = 13.1, 9.9 Hz), 2.99 (1H, ddd, *J* = 13.1, 3.0, 1.9 Hz), 2.60 (3H, s); ¹³C NMR (100 MHz, CDCl₃, 22 °C, TMS, ppm): δ = 146.5, 139.0, 135.7, 128.9, 128.3, 128.2, 127.6, 123.6, 87.5, 64.2, 59.8, 39.6, 20.9; IR (KBr): ν = 2941, 1488, 1087, 700 cm⁻¹; HRMS (ESI): *m/z* Calcd for C₁₆H₁₈ClN₂O [*M*+H]⁺: 289.1107; Found: 289.1107.



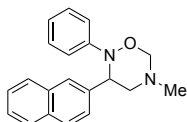
(±)-5-Methyl-3-phenyl-2-(*p*-tolyl)-1,2,5-oxadiazinane (3qa)

White solid; M.p. 40–41 °C; ¹H NMR (400 MHz, CDCl₃, 22 °C, TMS, ppm): δ = 7.27–7.13 (5H, m), 7.06–7.00 (2H, m), 7.00–6.90 (2H, m), 4.91 (1H, d, *J* = 9.9 Hz), 4.58 (1H, dd, *J* = 9.9, 1.9 Hz), 4.50 (1H, dd, *J* = 10.1, 3.0 Hz), 3.20 (1H, dd, *J* = 13.0, 10.1 Hz), 3.00 (1H, ddd, *J* = 13.0, 3.0, 1.9 Hz), 2.60 (3H, s), 2.20 (3H, s); ¹³C NMR (100 MHz, CDCl₃, 22 °C, TMS, ppm): δ = 146.5, 139.0, 135.7, 128.9, 128.3, 128.2, 127.6, 123.6, 87.5, 64.2, 59.8, 39.6, 20.9; IR (KBr): ν = 2940, 1454, 969, 743 cm⁻¹; HRMS (ESI): *m/z* Calcd for C₁₇H₂₂N₂O [*M*+H]⁺: 269.1654; Found: 269.1654.



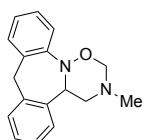
(±)-2-(3-Methoxyphenyl)-5-methyl-3-phenyl-1,2,5-oxadiazinane (3ra)

Pale yellow oil; ¹H NMR (400 MHz, CDCl₃, 22 °C, TMS, ppm): δ = 7.29–7.15 (5H, m), 7.03 (1H, dd, *J* = 8.0, 8.0 Hz), 6.70 (1H, ddd, *J* = 8.1, 1.5, 1.5 Hz), 6.64 (1H, dd, *J* = 1.5, 1.5 Hz), 6.56 (1H, dd, *J* = 8.1, 1.5 Hz), 4.91 (1H, d, *J* = 9.8 Hz), 4.60 (1H, dd, *J* = 9.8, 1.2 Hz), 4.49 (1H, dd, *J* = 9.8, 2.5 Hz), 3.62 (3H, s), 3.23 (1H, dd, *J* = 12.9, 9.8 Hz), 3.00 (1H, ddd, *J* = 12.9, 2.5, 1.2 Hz), 2.58 (3H, s); ¹³C NMR (100 MHz, CDCl₃, 22 °C, TMS, ppm): δ = 159.6, 150.5, 139.0, 129.0, 128.5, 128.4, 127.8, 115.0, 111.6, 108.4, 87.6, 64.5, 59.4, 55.2, 39.7; IR (neat): ν = 2940, 2801, 1602, 1489, 1452, 1046, 698 cm⁻¹; HRMS (ESI): *m/z* Calcd for C₁₇H₂₁N₂O₂ [*M*+H]⁺: 285.1603; Found: 285.1616.



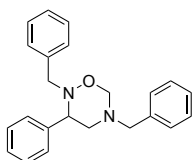
(±)-5-Methyl-3-(naphthalen-2-yl)-2-phenyl-1,2,5-oxadiazinane (3sa)

Colorless solid; M.p. 72–73 °C; ¹H NMR (400 MHz, CDCl₃, 22 °C, TMS, ppm): δ = 7.79–7.64 (4H, m), 7.49–7.35 (3H, m), 7.21–7.04 (4H, m), 7.02–6.92 (1H, m), 4.95 (1H, d, *J* = 9.9 Hz), 4.70 (1H, dd, *J* = 9.9, 3.0 Hz), 4.63 (1H, dd, *J* = 9.9, 1.9 Hz), 3.32 (1H, dd, *J* = 13.1, 9.9 Hz), 3.05 (1H, ddd, *J* = 13.1, 3.0, 1.9 Hz), 2.63 (3H, s); ¹³C NMR (100 MHz, CDCl₃, 22 °C, TMS, ppm): δ = 149.2, 136.7, 133.3, 133.0, 128.5, 128.2, 128.0, 127.7, 127.4, 126.1 (2C), 126.0, 125.9, 123.3, 87.7, 64.3, 59.7, 39.8; IR (KBr): ν = 2933, 1491, 1056, 693 cm⁻¹; HRMS (ESI): *m/z* Calcd for C₂₀H₂₁N₂O [*M*+H]⁺: 305.1654; Found: 305.1654.



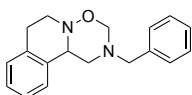
(±)-3-Methyl-3,4,4a,9-tetrahydro-2H-dibenzo[c,f][1,2,5]oxadiazino[2,3-a]azepine (3ua)

Colorless solid; 131–132 °C; ¹H NMR (400 MHz, CDCl₃, 22 °C, TMS, ppm): δ = 7.48–7.41 (1H, m), 7.29–7.04 (5H, m), 6.98–6.89 (2H, m), 4.84 (1H, d, *J* = 9.6 Hz), 4.69 (1H, d, *J* = 13.7 Hz), 4.65 (1H, dd, *J* = 9.6, 1.9 Hz), 4.62 (1H, dd, *J* = 10.5, 2.5 Hz), 3.35 (1H, d, *J* = 13.7 Hz), 3.21 (1H, dd, *J* = 13.0, 10.5 Hz), 3.02 (1H, ddd, *J* = 13.0, 2.5, 1.9 Hz), 2.66 (3H, s); ¹³C NMR (100 MHz, CDCl₃, 22 °C, TMS, ppm): δ = 147.9, 138.3, 136.4, 134.8, 129.0, 128.6, 127.4, 127.1, 126.6, 126.5, 123.7, 116.9, 87.7, 64.7, 61.2, 39.9, 38.9; IR (KBr): ν = 2491, 1485, 1053, 752 cm⁻¹; HRMS (ESI): *m/z* Calcd for C₁₇H₁₉N₂O [*M*+H]⁺: 267.1497; Found: 267.1485.



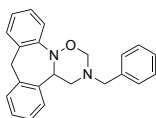
(±)-2,5-Dibenzyl-3-phenyl-1,2,5-oxadiazinane (3ab)

Colorless plate; M.p. 110–111 °C; ¹H NMR (400 MHz, CDCl₃, 22 °C, TMS, ppm): δ = 7.49–7.16 (15H, m), 4.77 (1H, d, *J* = 10.2 Hz), 4.49 (1H, dd, *J* = 10.2, 2.5 Hz), 4.07 (1H, dd, *J* = 10.6, 2.5 Hz), 3.94 (2H, s), 3.89 (1H, d, *J* = 14.8 Hz), 3.59 (1H, d, *J* = 14.8 Hz), 3.09 (1H, dd, *J* = 13.4, 10.6 Hz), 2.93 (1H, ddd, *J* = 13.4, 2.5, 2.5 Hz); ¹³C NMR (100 MHz, CDCl₃, 22 °C, TMS, ppm): δ = 139.8, 138.4 (2C), 129.1, 128.9, 128.6, 128.5, 128.2, 128.0, 127.9, 127.3, 126.9, 85.4, 65.1, 59.7, 57.5, 55.9; IR (KBr): ν = 3031, 2909, 2845, 1493, 1454, 1357, 965, 736, 697 cm⁻¹; HRMS (ESI): *m/z* Calcd for C₂₃H₂₅N₂O [*M*+H]⁺: 345.1967; Found: 345.1974. The single crystal of this compound was obtained by recrystallization from *n*-hexane / ethyl acetate, and its structure was analyzed by single-crystal X-ray crystallography.



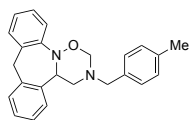
(±)-2-Benzyl-1,2,3,6,7,11b-hexahydro-[1,2,5]oxadiazino[3,2-a]isoquinoline (3tb)

Colorless oil; ¹H NMR (400 MHz, CDCl₃, 22 °C, TMS, ppm): δ = 7.69–7.27 (5H, m), 7.22–7.04 (3H, m), 7.02–6.87 (1H, m), 4.80 (1H, d, *J* = 10.0 Hz), 4.53 (1H, dd, *J* = 10.0, 1.6 Hz), 4.12 (1H, br d, *J* = 10.2 Hz), 3.98 (1H, br d, *J* = 13.3 Hz), 3.96 (1H, br d, *J* = 13.3 Hz), 3.61–3.38 (2H, m), 3.29 (1H, ddd, *J* = 14.5, 11.7, 5.7 Hz), 3.05 (1H, ddd, *J* = 14.5, 9.8, 4.3 Hz), 2.99–2.75 (2H, m); ¹³C NMR (100 MHz, CDCl₃, 22 °C, TMS, ppm): δ = 138.4, 134.5, 134.2, 129.2, 128.9, 128.6, 127.5, 127.1, 126.2, 123.9, 85.5, 60.6, 56.5, 53.3, 52.9, 29.1; IR (neat): ν = 2922, 2830, 1493, 1358, 1022, 743 cm⁻¹; HRMS (ESI): *m/z* Calcd for C₁₈H₂₁N₂O [*M*+H]⁺: 281.1654; Found: 281.1647.



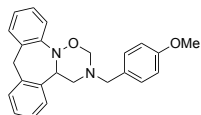
(±)-3-Benzyl-3,4,4a,9-tetrahydro-2H-dibenzo[c,f][1,2,5]oxadiazino[2,3-a]azepine (3ub)

Colorless amorphous; ¹H NMR (400 MHz, CDCl₃, 22 °C, TMS, ppm): δ = 7.54–7.17 (7H, m), 7.16–7.00 (4H, m), 6.94 (1H, ddd, *J* = 7.4, 7.4, 1.2 Hz), 6.85–6.75 (1H, m), 4.98 (1H, d, *J* = 10.5 Hz), 4.73 (1H, dd, *J* = 10.5, 2.0 Hz), 4.70 (1H, d, *J* = 13.8 Hz), 4.66 (1H, dd, *J* = 10.6, 2.3 Hz), 4.13 (1H, d, *J* = 13.3 Hz), 4.07 (1H, d, *J* = 13.3 Hz), 3.34 (1H, d, *J* = 13.8 Hz), 3.27 (1H, dd, *J* = 13.4, 10.6 Hz), 3.05 (1H, ddd, *J* = 13.4, 2.3, 2.0 Hz); ¹³C NMR (100 MHz, CDCl₃, 22 °C, TMS, ppm): δ = 147.9, 138.2, 138.0, 136.3, 134.7, 129.0, 128.8, 128.5, 128.3, 127.3, 127.2, 126.9, 126.4 (2C), 123.5, 116.7, 86.0, 64.4, 58.5, 56.0, 38.7; IR (neat): ν = 3024, 2851, 1486, 753 cm⁻¹; HRMS (ESI): *m/z* Calcd for C₂₃H₂₃N₂O [*M*+H]⁺: 343.1810; Found: 343.1817.



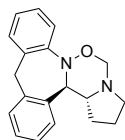
(±)-3-(4-Methylbenzyl)-3,4,4a,9-tetrahydro-2H-dibenzo[c,f][1,2,5]oxadiazino[2,3-a]azepine (3uc)

Pale yellow oil; ^1H NMR (400 MHz, CDCl_3 , 22 °C, TMS, ppm): δ = 7.46 (1H, dd, J = 8.0, 0.9 Hz), 7.31 (2H, d, J = 7.9 Hz), 7.22 (1H, ddd, J = 7.7, 7.7, 1.4 Hz), 7.18 (2H, d, J = 7.9 Hz), 7.15–7.00 (4H, m), 6.94 (1H, ddd, J = 7.4, 7.4, 1.2 Hz), 6.85–6.76 (1H, m), 4.97 (1H, d, J = 10.0 Hz), 4.73 (1H, dd, J = 10.0, 2.0 Hz), 4.70 (1H, d, J = 13.7 Hz), 4.66 (1H, dd, J = 10.5, 2.4 Hz), 4.09 (1H, d, J = 13.2 Hz), 4.04 (1H, d, J = 13.2 Hz), 3.34 (1H, d, J = 13.7 Hz), 3.25 (1H, dd, J = 13.3, 10.5 Hz), 3.05 (1H, ddd, J = 13.3, 2.4, 2.0 Hz), 2.36 (3H, s); ^{13}C NMR (100 MHz, CDCl_3 , 22 °C, TMS, ppm): δ = 147.9, 138.0, 137.0, 136.3, 135.0, 134.7, 129.2, 129.0, 128.7, 128.3, 127.2, 126.8, 126.4 (2C), 123.4, 116.7, 85.9, 64.4, 58.4, 55.7, 38.7, 21.1; IR (neat): ν = 2921, 1485, 1032, 753 cm^{-1} ; HRMS (ESI): m/z Calcd for $\text{C}_{24}\text{H}_{25}\text{N}_2\text{O}$ $[M+\text{H}]^+$: 357.1967; Found: 357.1979.



(±)-3-(4-Methoxybenzyl)-3,4,4a,9-tetrahydro-2H-dibenzo[c,f][1,2,5]oxadiazino[2,3-a]azepine (3ud)

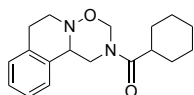
Colorless solid; M.p. 72–73 °C; ^1H NMR (400 MHz, CDCl_3 , 22 °C, TMS, ppm): δ = 7.46 (1H, dd, J = 8.0, 1.0 Hz), 7.38–7.30 (1H, m), 7.23 (1H, ddd, J = 7.8, 7.8, 1.3 Hz), 7.13–6.99 (4H, m), 6.98–6.87 (3H, m), 6.86–6.77 (1H, m), 4.96 (1H, d, J = 10.2 Hz), 4.72 (1H, dd, J = 10.2, 2.1 Hz), 4.70 (1H, d, J = 13.2 Hz), 4.65 (1H, dd, J = 10.5, 2.4 Hz), 4.06 (1H, d, J = 13.0 Hz), 4.02 (1H, d, J = 13.0 Hz), 3.84 (3H, s), 3.34 (1H, d, J = 13.2 Hz), 3.25 (1H, dd, J = 13.3, 10.5 Hz), 3.04 (1H, ddd, J = 13.3, 2.4, 2.1 Hz); ^{13}C NMR (100 MHz, CDCl_3 , 22 °C, TMS, ppm): δ = 159.0, 148.0, 138.1, 136.4, 134.7, 130.3, 130.2, 128.8, 128.4, 128.3, 127.3, 126.9, 126.5, 126.4, 123.5, 116.7, 113.9, 85.8, 64.5, 55.4, 55.3, 38.8; IR (KBr): ν = 2950, 2835, 1513, 1247, 764 cm^{-1} ; HRMS (ESI): m/z Calcd for $\text{C}_{24}\text{H}_{25}\text{N}_2\text{O}_2$ $[M+\text{H}]^+$: 373.1916; Found: 373.1914.



(±)-1,2,3,3a,3b,8-Hexahydro-15H-dibenzo[c,f]pyrrolo[2',1':4,5][1,2,5]oxadiazino[2,3-a]azepine (3ue)

Pale yellow solid; M.p. 131–132 °C; ^1H NMR (400 MHz, CDCl_3 , 22 °C, TMS, ppm): δ = 7.34 (1H, d, J = 7.8 Hz), 7.20–6.92 (6H, m), 6.88 (1H, td, J = 7.4, 1.2 Hz), 5.20 (1H, d, J = 10.0 Hz), 4.86 (1H, d, J = 10.0 Hz), 4.80–4.30 (2H, br m), 3.72–3.18 (3H, br m), 3.01 (1H, td, J = 8.8, 4.4 Hz), 2.24–1.70 (4H, br m); ^{13}C NMR (100 MHz, CDCl_3 , 22 °C, TMS, ppm): δ = 146.5, 139.8, 135.3, 133.9, 130.4, 128.3, 127.4, 127.0, 126.0, 125.8, 122.9, 116.3, 84.0, 69.6, 65.1, 47.3, 39.0, 26.9, 21.9; IR (neat): ν = 2961, 2902, 2861, 1600, 1483, 1242, 938, 764 cm^{-1} ; HRMS (ESI): m/z Calcd for $\text{C}_{19}\text{H}_{21}\text{N}_2\text{O}$: 193.1654 $[M+\text{H}]^+$; Found: 293.1664. The relative stereochemistry was determined to be in the trans configuration by ROESY spectroscopy.

7.5. Characterization of Anti-Schistosomal Molecule 4

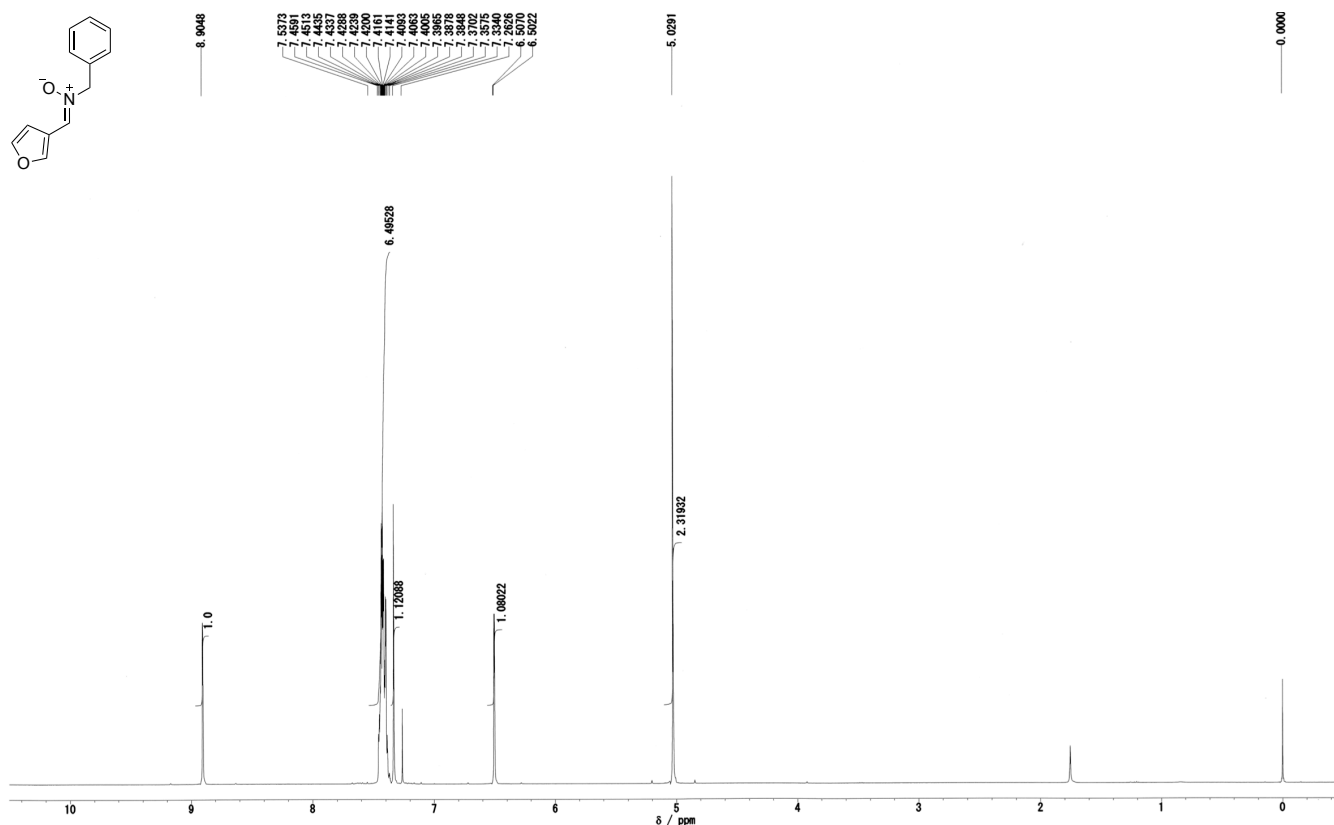


(±)-Cyclohexyl(1,6,7,11b-tetrahydro-[1,2,5]oxadiazino[3,2-a]isoquinolin-2(3H)-yl)methanone (4)

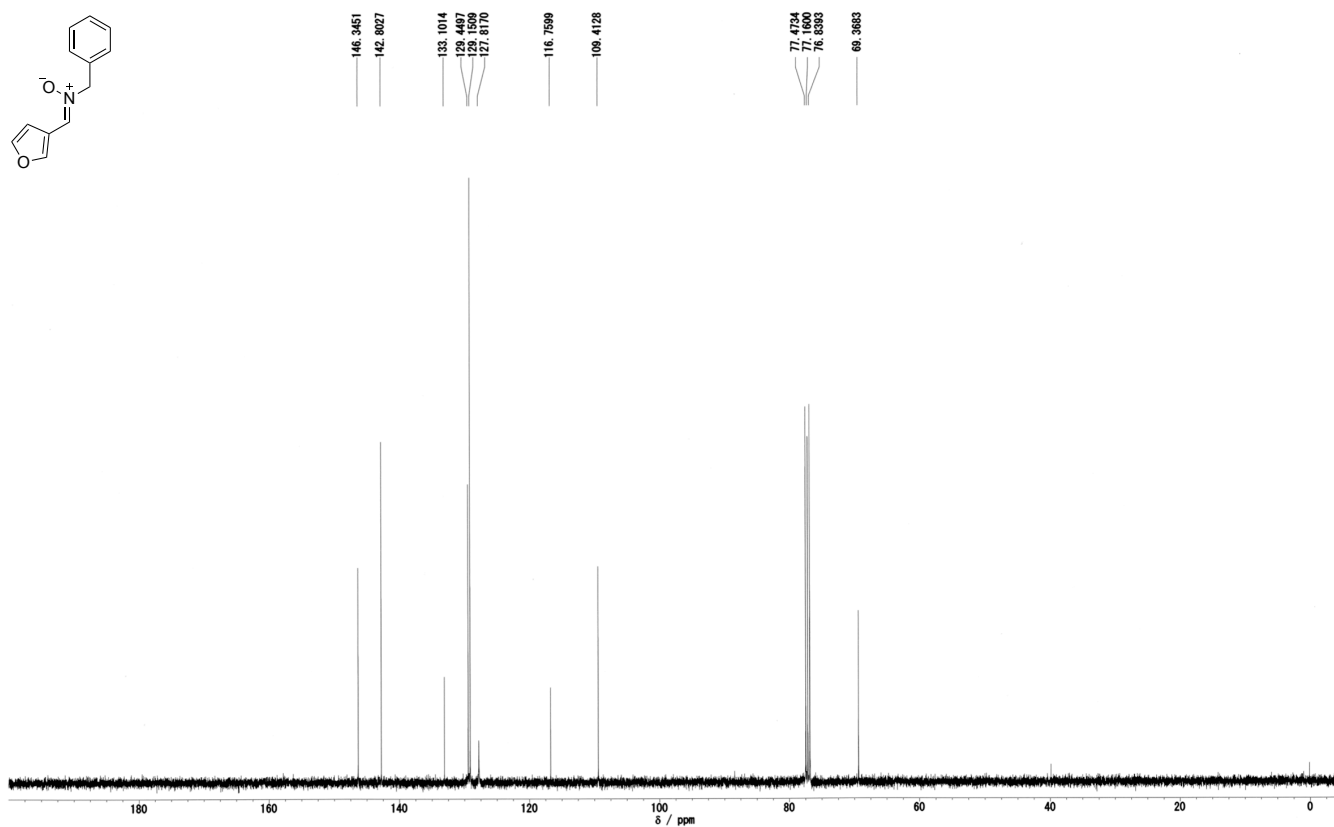
Colorless solid; M.p. 106–107 °C; ^1H NMR (400 MHz, $[\text{D}_6]\text{DMSO}$, 100 °C, TMS, ppm): δ = 7.30–7.08 (m, 4H), 5.60 (1H, br d, J = 10.0 Hz), 4.85 (1H, br d, J = 10.0 Hz), 4.73 (1H, br dd, J = 12.0, 2.0 Hz), 3.71 (1H, br dd, J = 10.0, 2.0 Hz), 3.45 (1H, ddd, J = 10.0, 6.5, 1.5 Hz), 3.22–3.02 (2H, m), 2.91 (1H, ddd, J = 12.0, 10.0, 4.5 Hz), 2.83 (1H, ddd, J = 16.0, 4.5, 1.5 Hz), 2.78–2.58 (1H, br m), 1.82–1.56 (5H, m), 1.50–1.29 (4H, m), 1.28–1.12 (1H, m); ^{13}C NMR (100 MHz, $[\text{D}_6]\text{DMSO}$, 100 °C, TMS, ppm): δ = 173.6, 133.3, 132.6, 127.9, 126.4, 125.5, 123.7, 76.2, 63.1, 51.4, 44.6, 38.7, 28.6, 28.5, 27.4, 25.0, 24.4; IR (KBr): ν = 2929, 2851, 1642, 1443, 1037, 743 cm^{-1} ; Elemental analysis calcd for $\text{C}_{18}\text{H}_{24}\text{N}_2\text{O}_2$: C 71.97, H 8.05, N 9.33, found: C 72.05, H 7.96, N 9.21. The ^1H , ^{13}C , ^1H – ^1H COSY, and HSQC NMR spectrum were measured at room temperature, where signals from conformational isomers were observed. Therefore, the measurements were conducted at 100 °C to coalesce the signals of the conformational isomers.

8. NMR Spectra

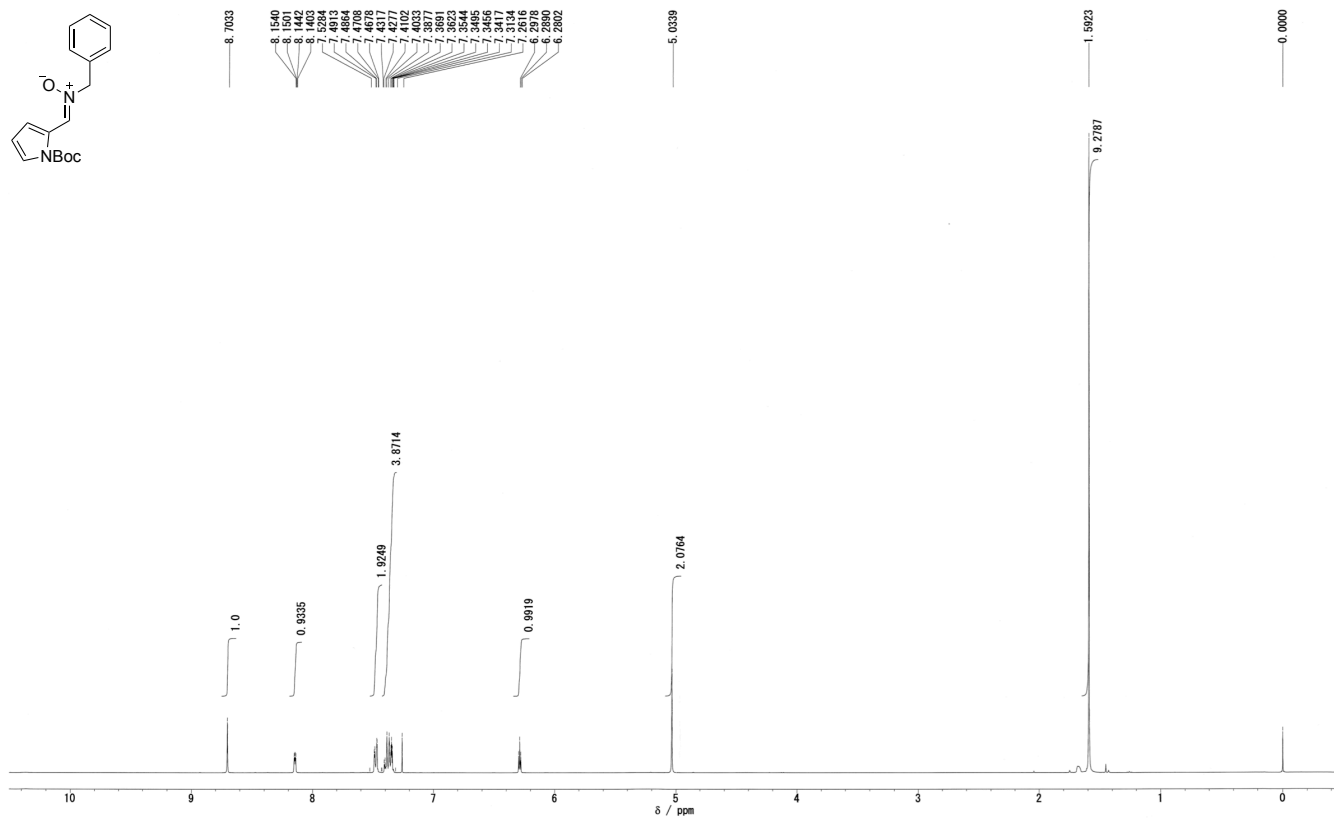
^1H NMR spectrum of (Z)-N-benzyl-1-(furan-3-yl)methanimine oxide (**1h**)



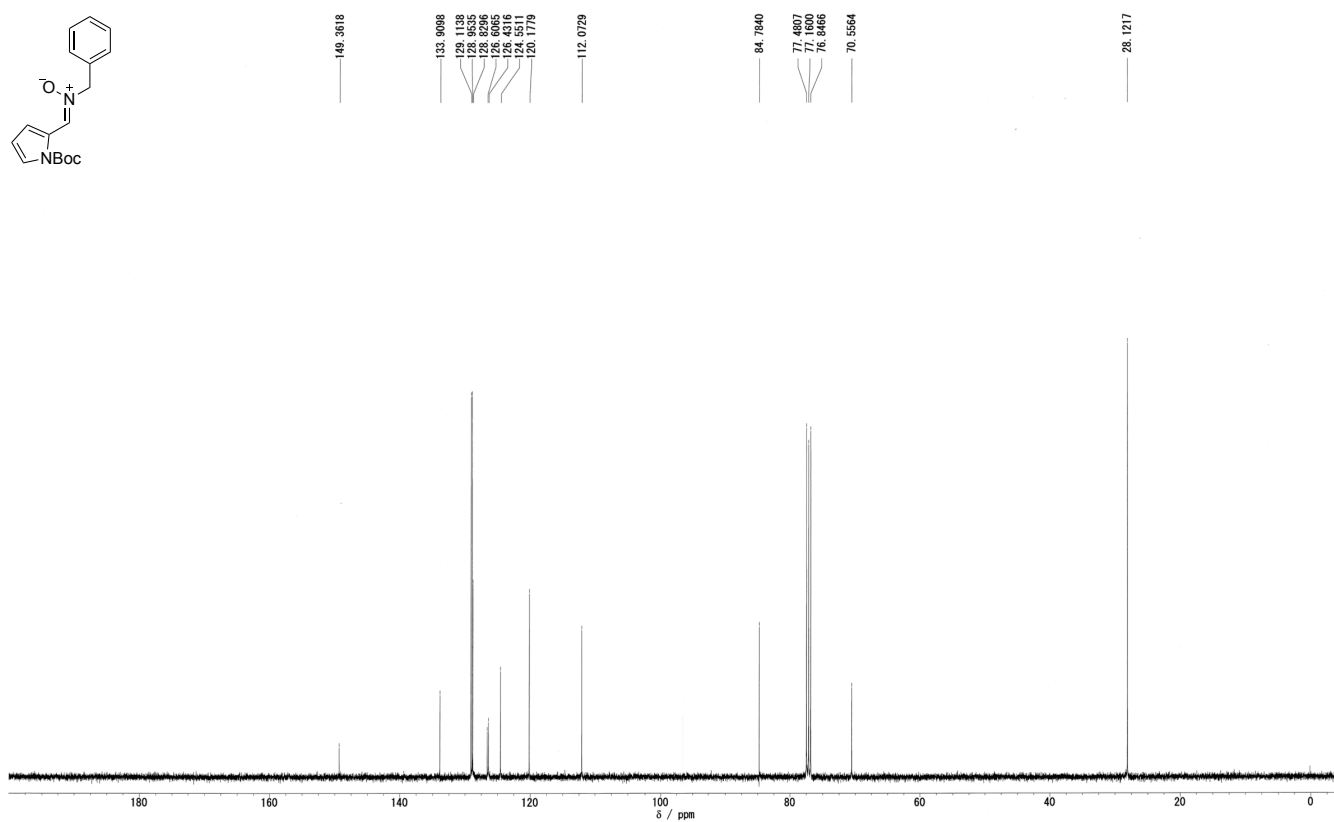
^{13}C NMR spectrum of (Z)-N-benzyl-1-(furan-3-yl)methanimine oxide (**1h**)



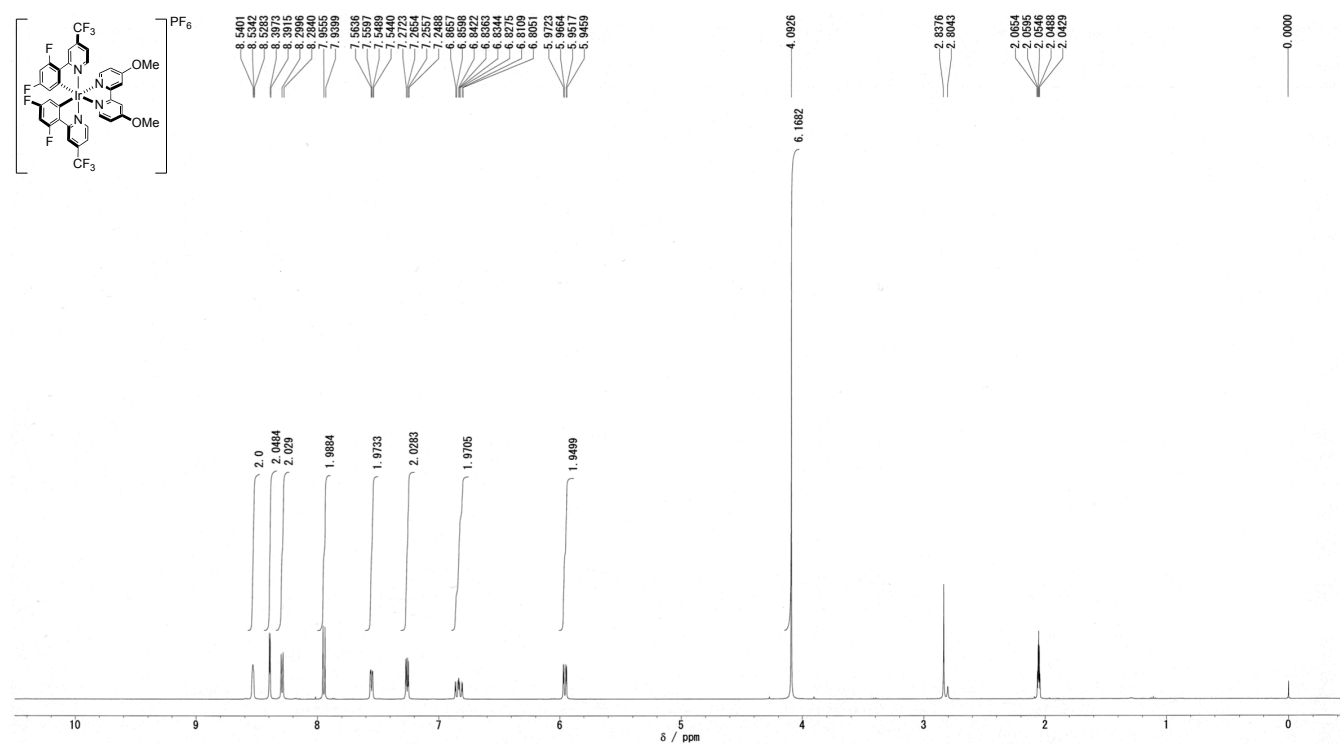
¹H NMR spectrum of (Z)-N-benzyl-1-(1-(*tert*-butoxycarbonyl)-1*H*-pyrrol-2-yl)methanimine oxide (**3i**)



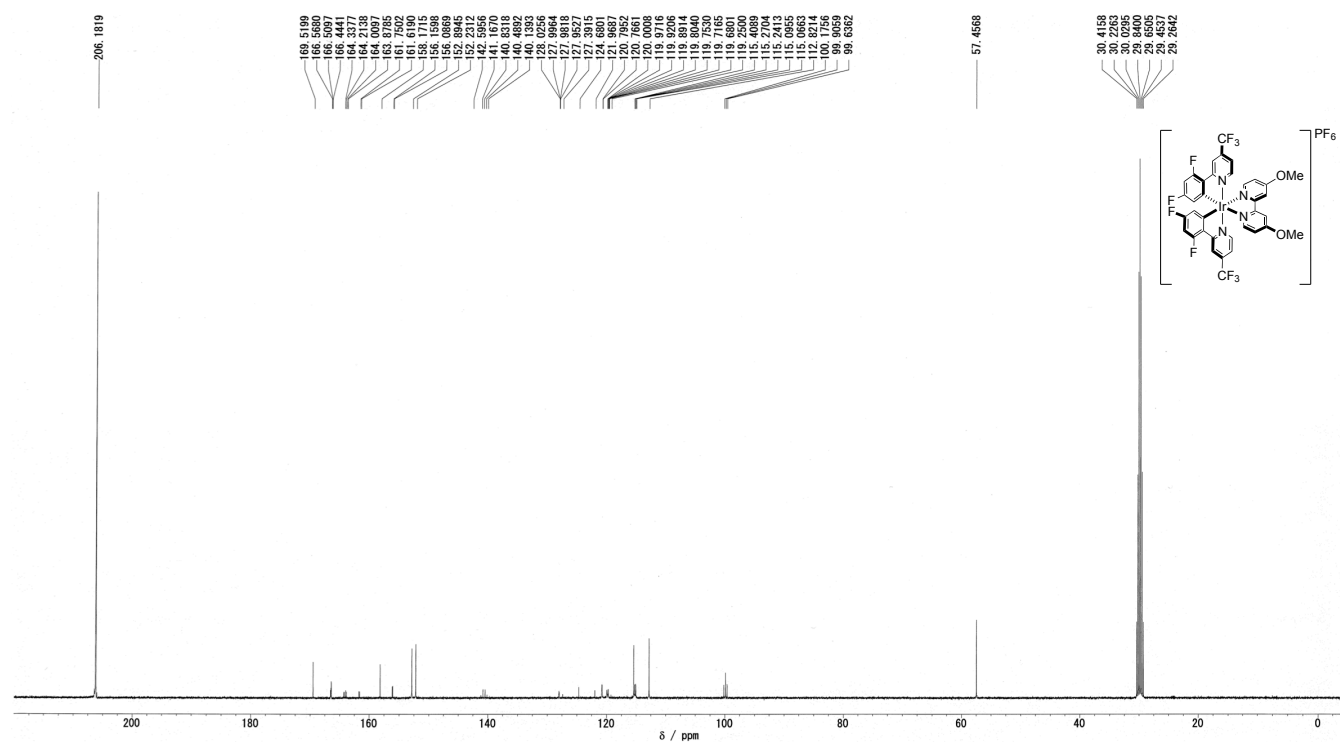
¹³C NMR spectrum of (Z)-N-benzyl-1-(1-(*tert*-butoxycarbonyl)-1*H*-pyrrol-2-yl)methanimine oxide (**3i**)



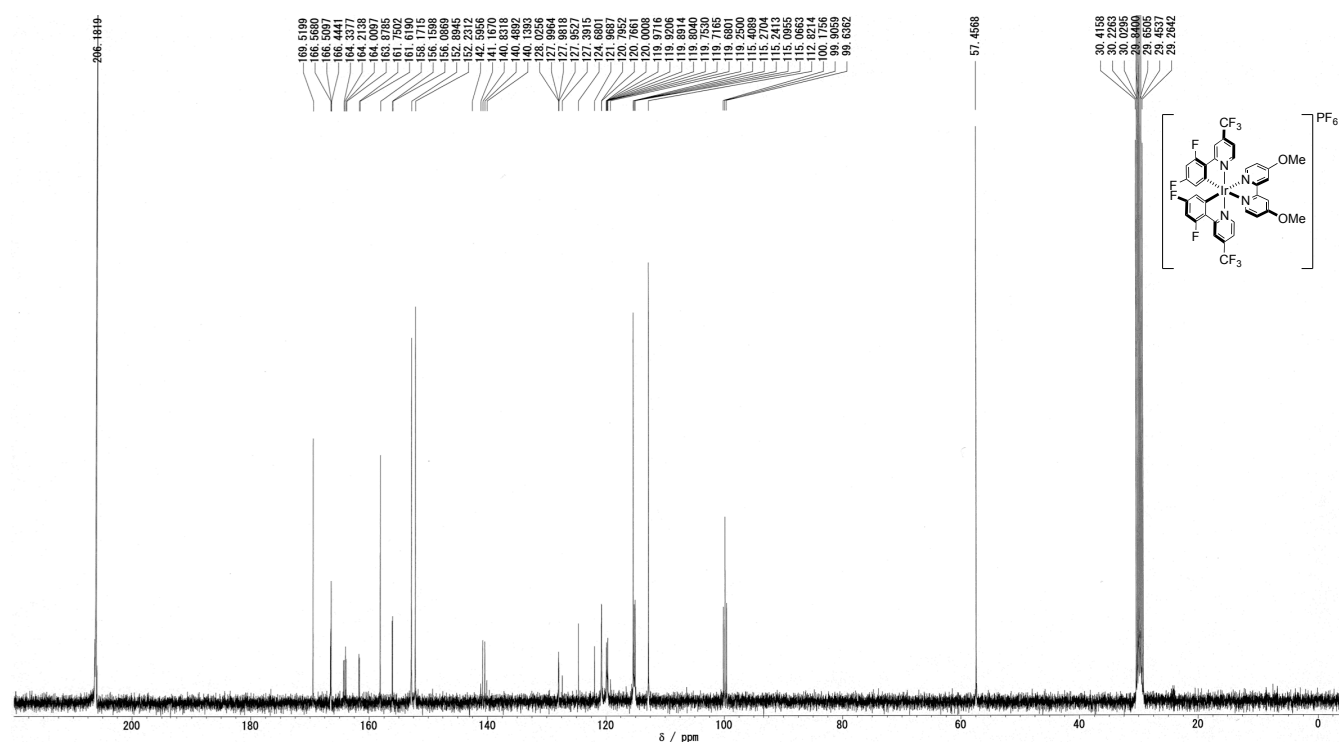
^1H NMR spectrum of (4,4'-Dimethoxy-2,2'-bipyridine)bis[3,5-difluoro-2-[4-trifluoromethyl-2-pyridinyl- κN]phenyl- κC]iridium(III) hexafluorophosphate (IX)



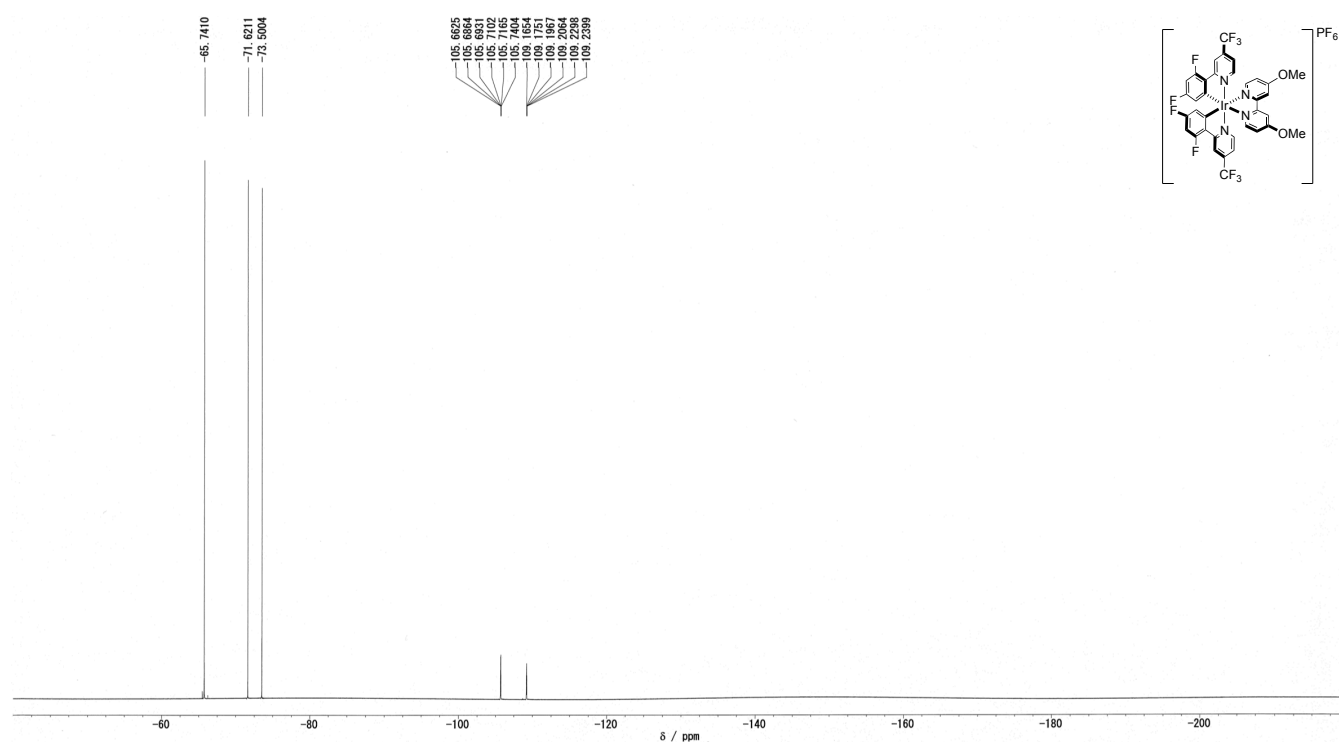
^{13}C NMR spectrum of (4,4'-Dimethoxy-2,2'-bipyridine)bis[3,5-difluoro-2-[4-trifluoromethyl-2-pyridinyl- κN]phenyl- κC]iridium(III) hexafluorophosphate (IX)

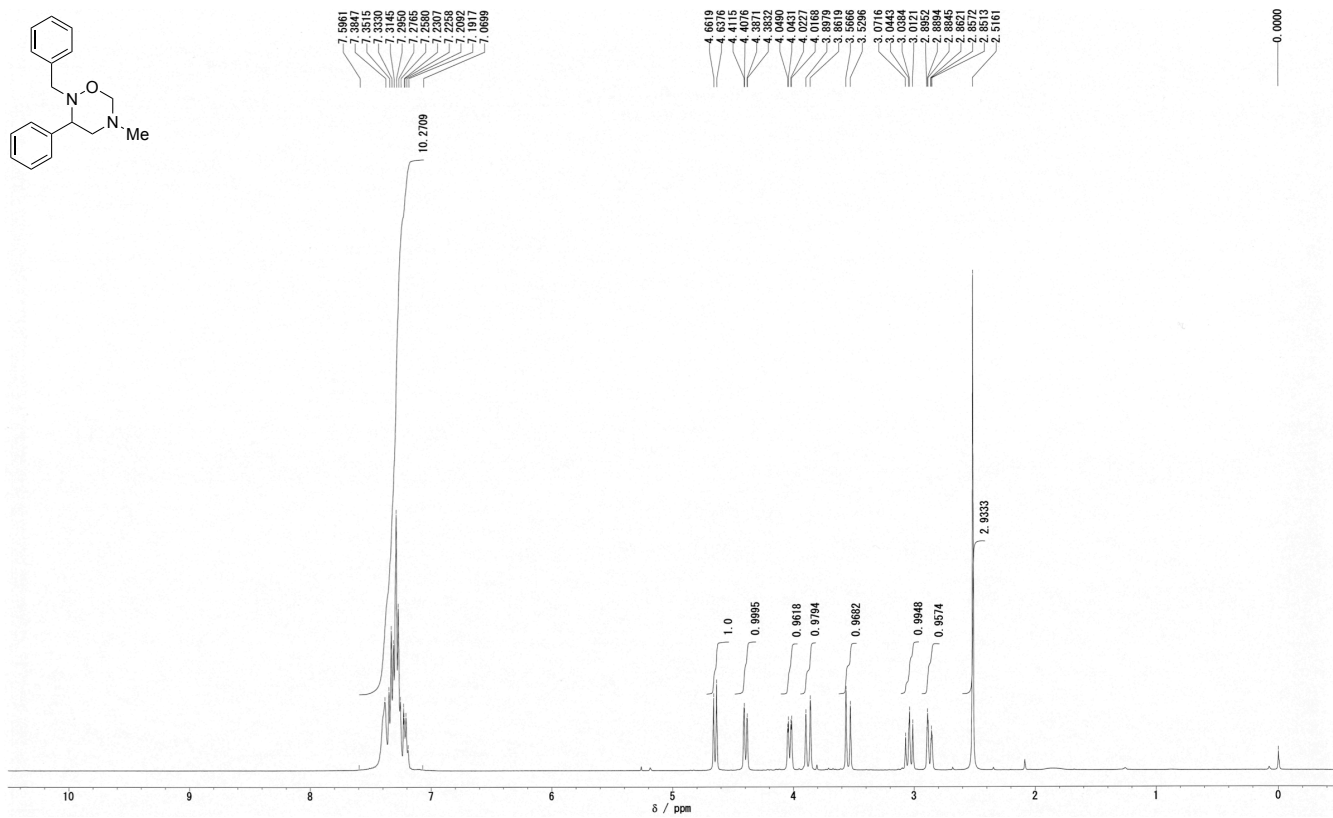


^{13}C NMR spectrum of (4,4'-Dimethoxy-2,2'-bipyridine)bis[3,5-difluoro-2-[4-trifluoromethyl-2-pyridinyl- κN]phenyl- κC]iridium(III) hexafluorophosphate (**IX**) (amplified y-axis)

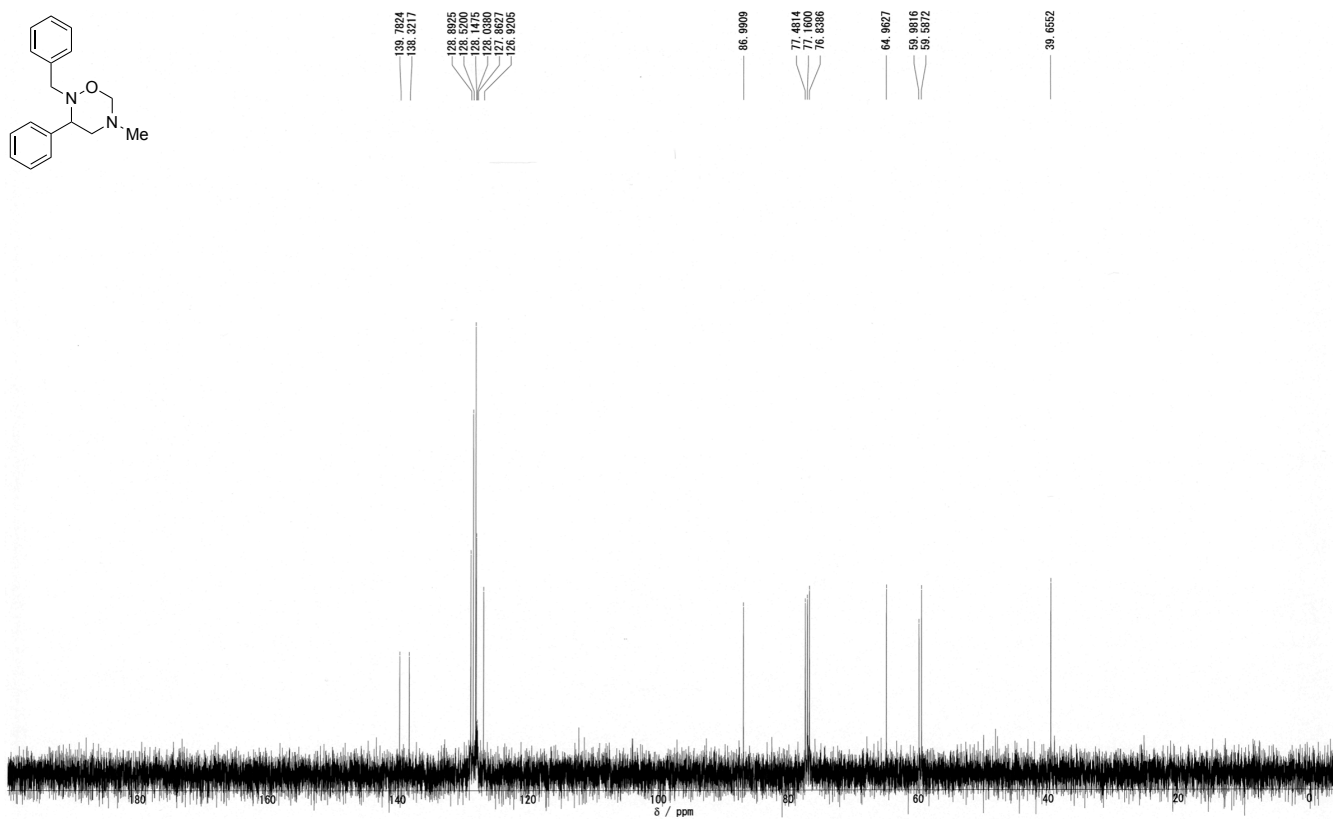


^{19}F NMR spectrum of (4,4'-Dimethoxy-2,2'-bipyridine)bis[3,5-difluoro-2-[4-trifluoromethyl-2-pyridinyl- κN]phenyl- κC]iridium(III) hexafluorophosphate (**IX**)

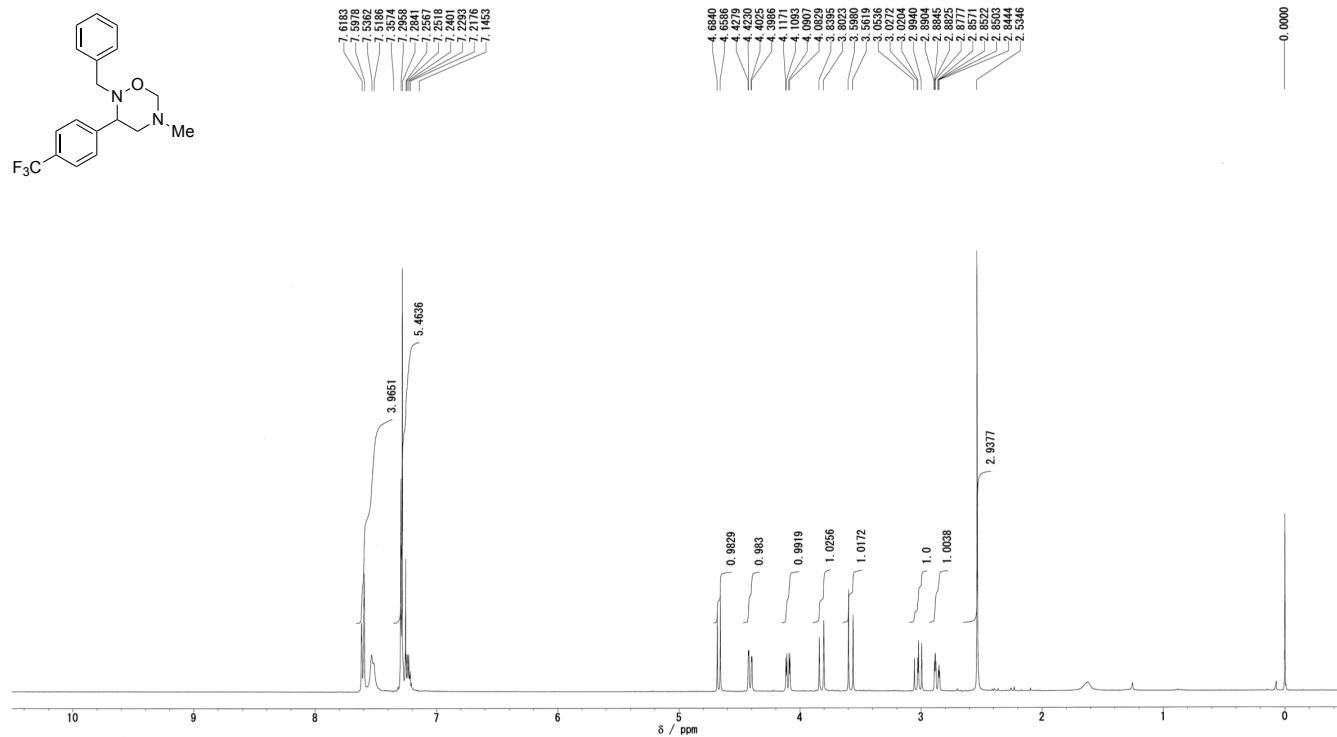


¹H NMR spectrum of (±)-2-benzyl-5-methyl-3-phenyl-1,2,5-oxadiazinane (**3aa**)

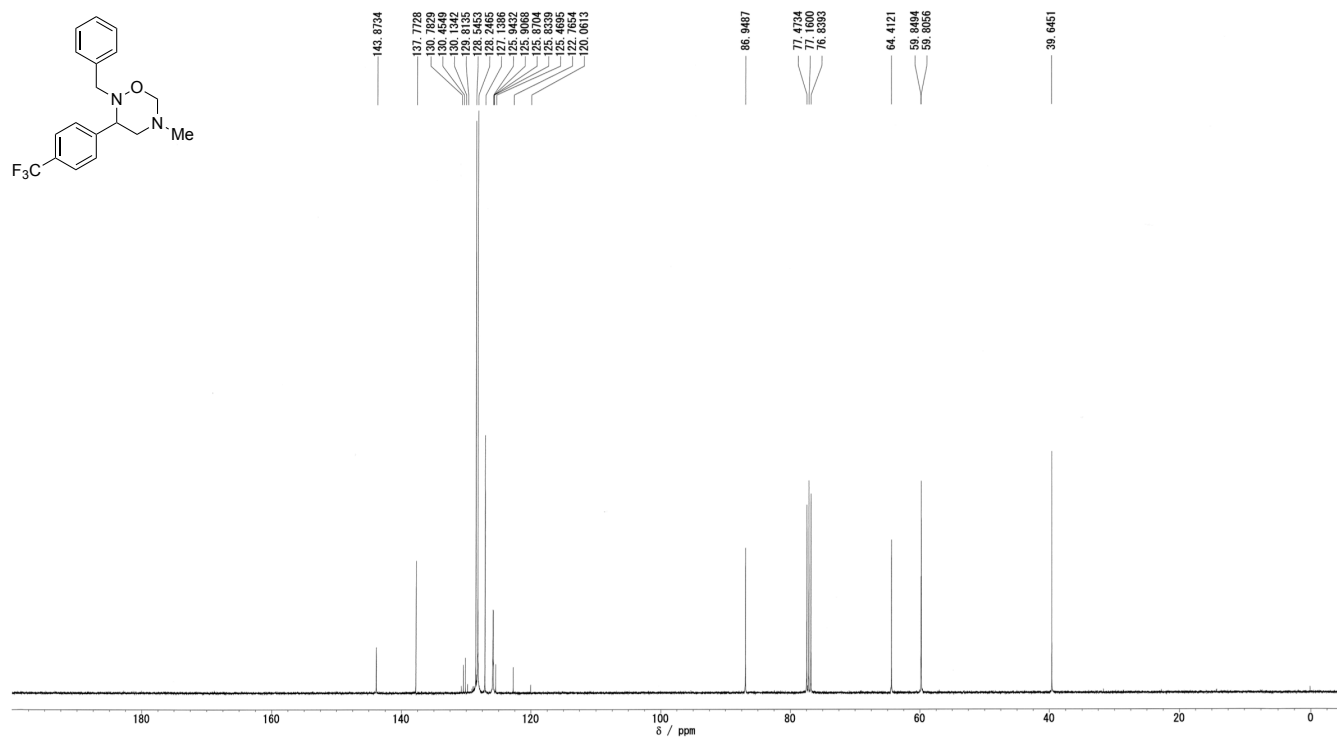
¹³C NMR spectrum of (±)-2-benzyl-5-methyl-3-phenyl-1,2,5-oxadiazinane (**3aa**)



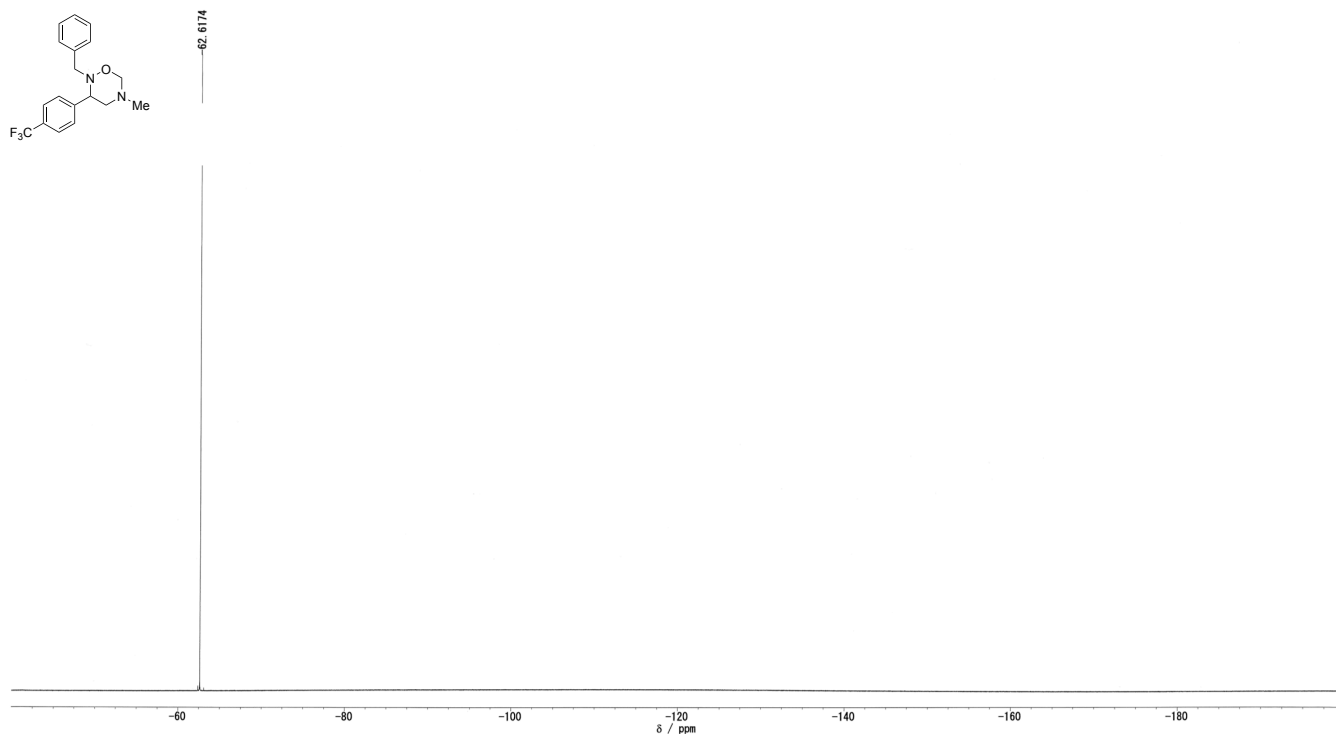
¹H NMR spectrum of (±)-2-benzyl-5-methyl-3-(4-(trifluoromethyl)phenyl)-1,2,5-oxadiazinane (**3ba**)



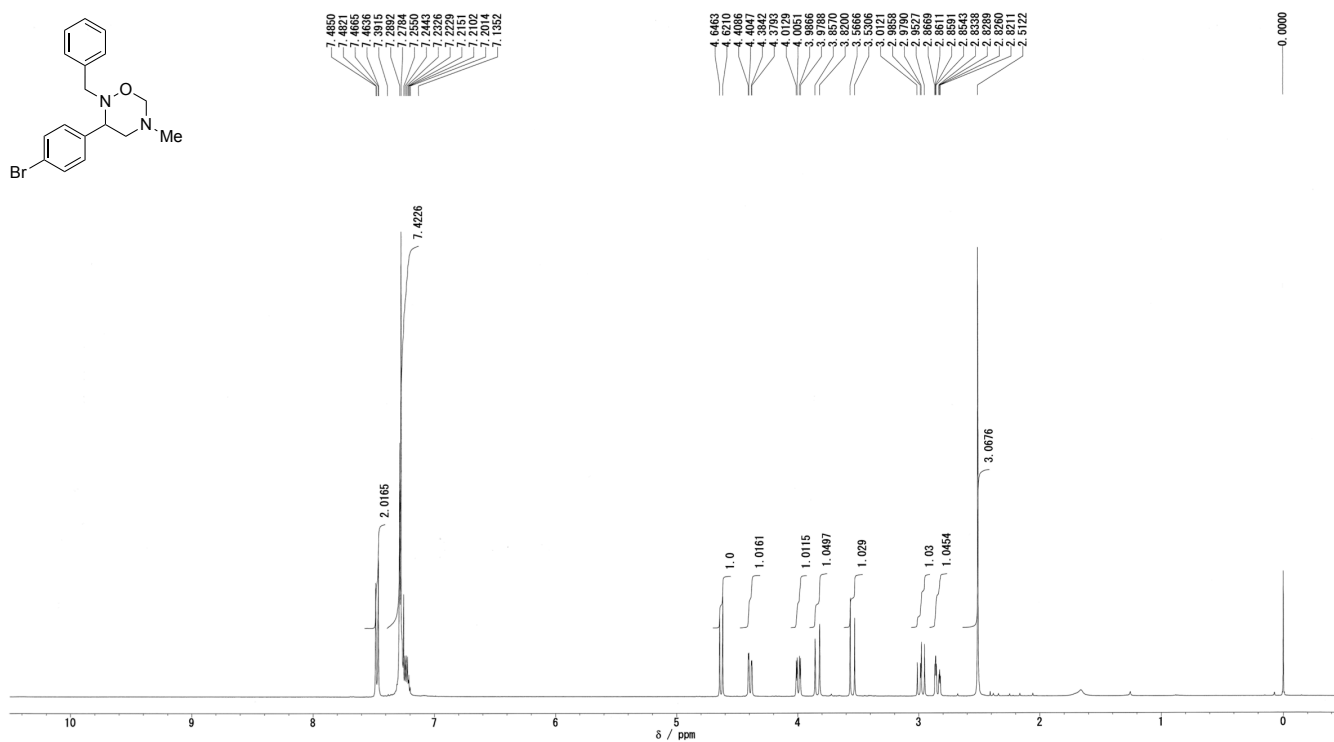
¹³C NMR spectrum of (±)-2-benzyl-5-methyl-3-(4-(trifluoromethyl)phenyl)-1,2,5-oxadiazinane (**3ba**)



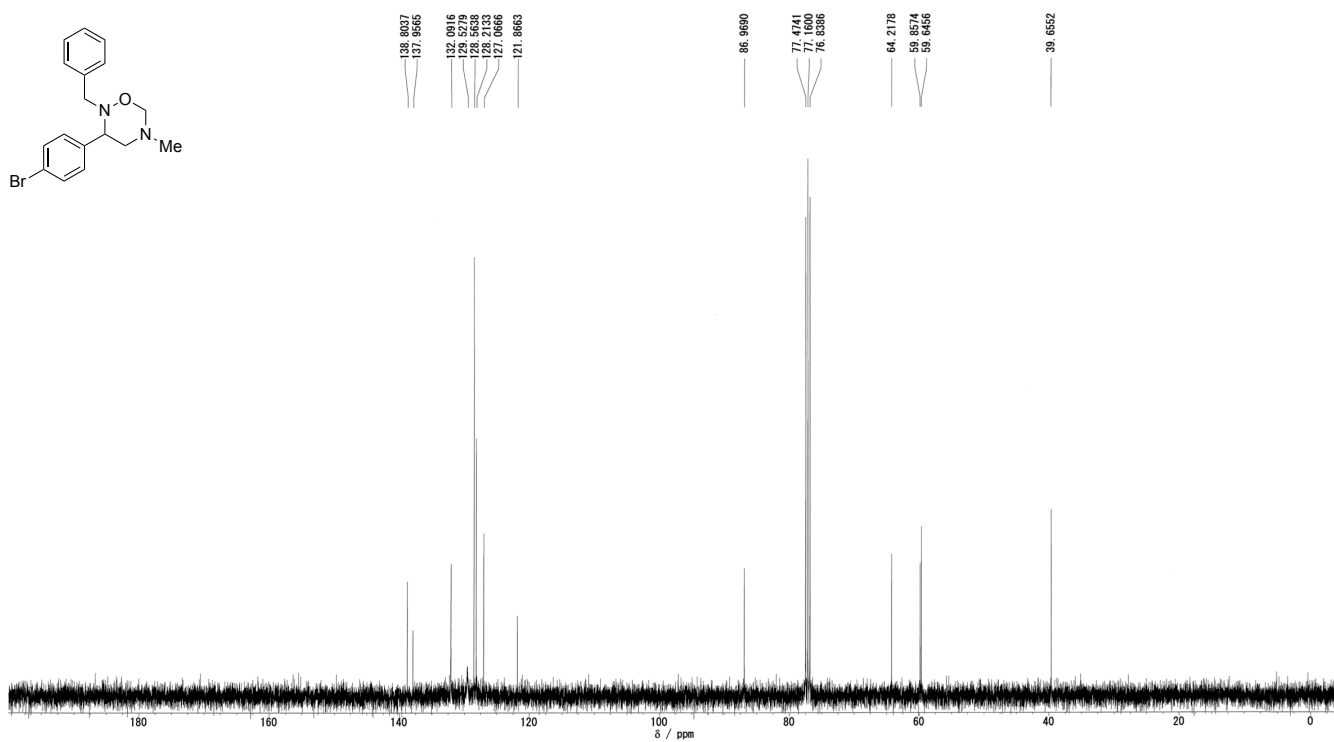
¹⁹F NMR spectrum of (±)-2-benzyl-5-methyl-3-(4-(trifluoromethyl)phenyl)-1,2,5-oxadiazinane (**3ba**)



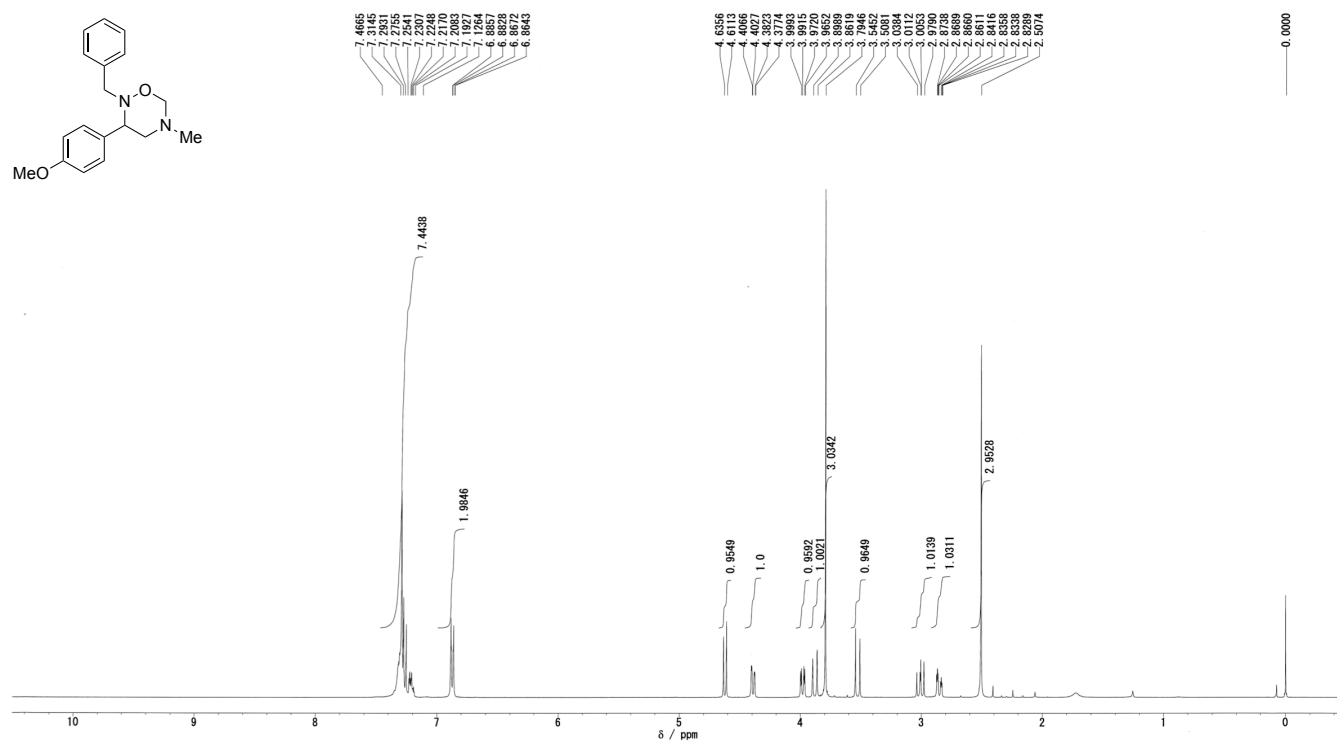
¹H NMR spectrum of (±)-2-benzyl-3-(4-bromophenyl)-5-methyl-1,2,5-oxadiazinane (**3ca**)



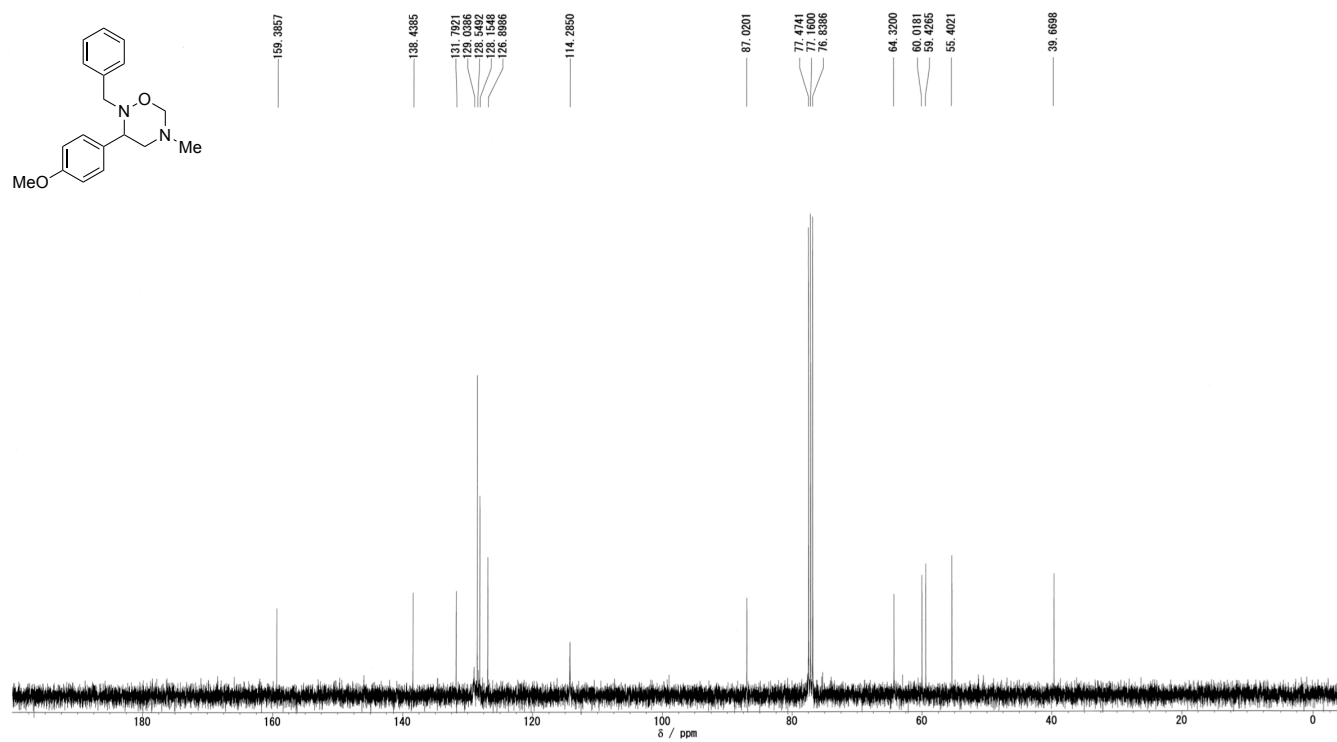
¹³C NMR spectrum of (±)-2-benzyl-3-(4-bromophenyl)-5-methyl-1,2,5-oxadiazinane (**3ca**)



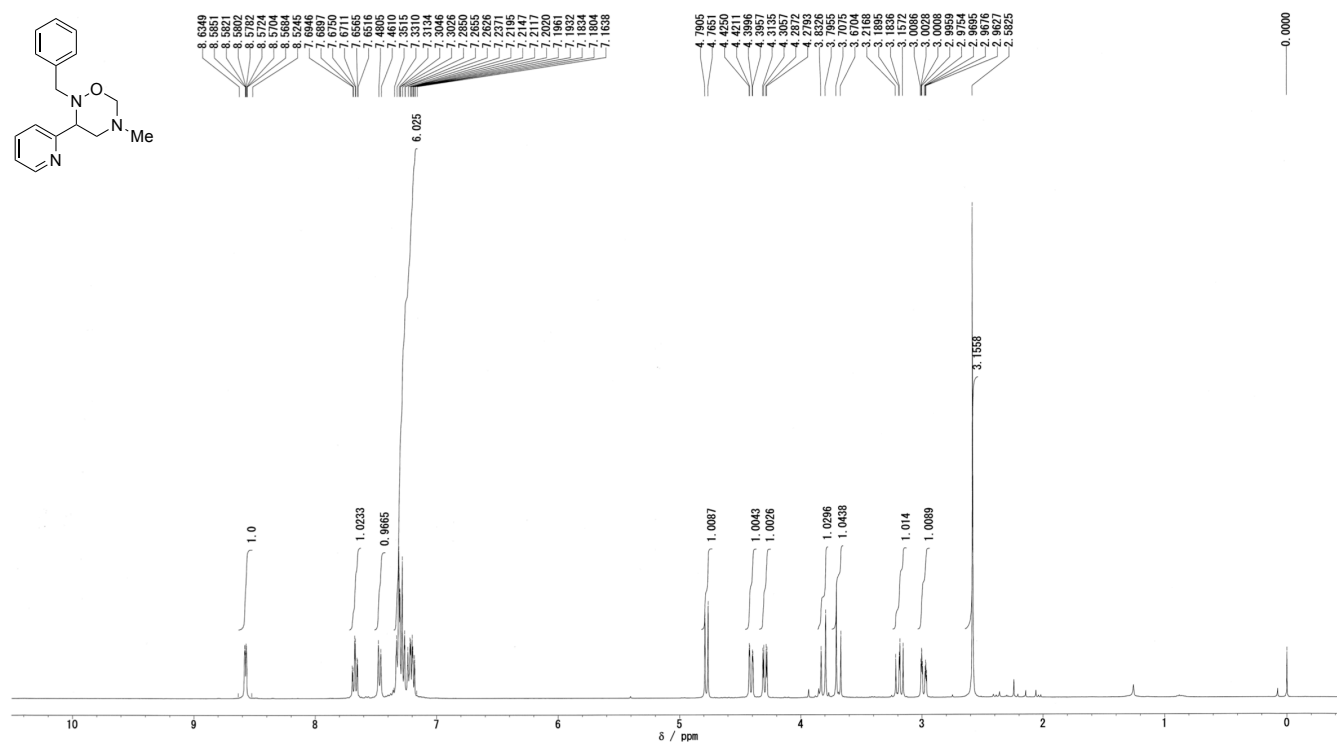
¹H NMR spectrum of (±)-2-benzyl-3-(4-methoxyphenyl)-5-methyl-1,2,5-oxadiazinane (**3da**)



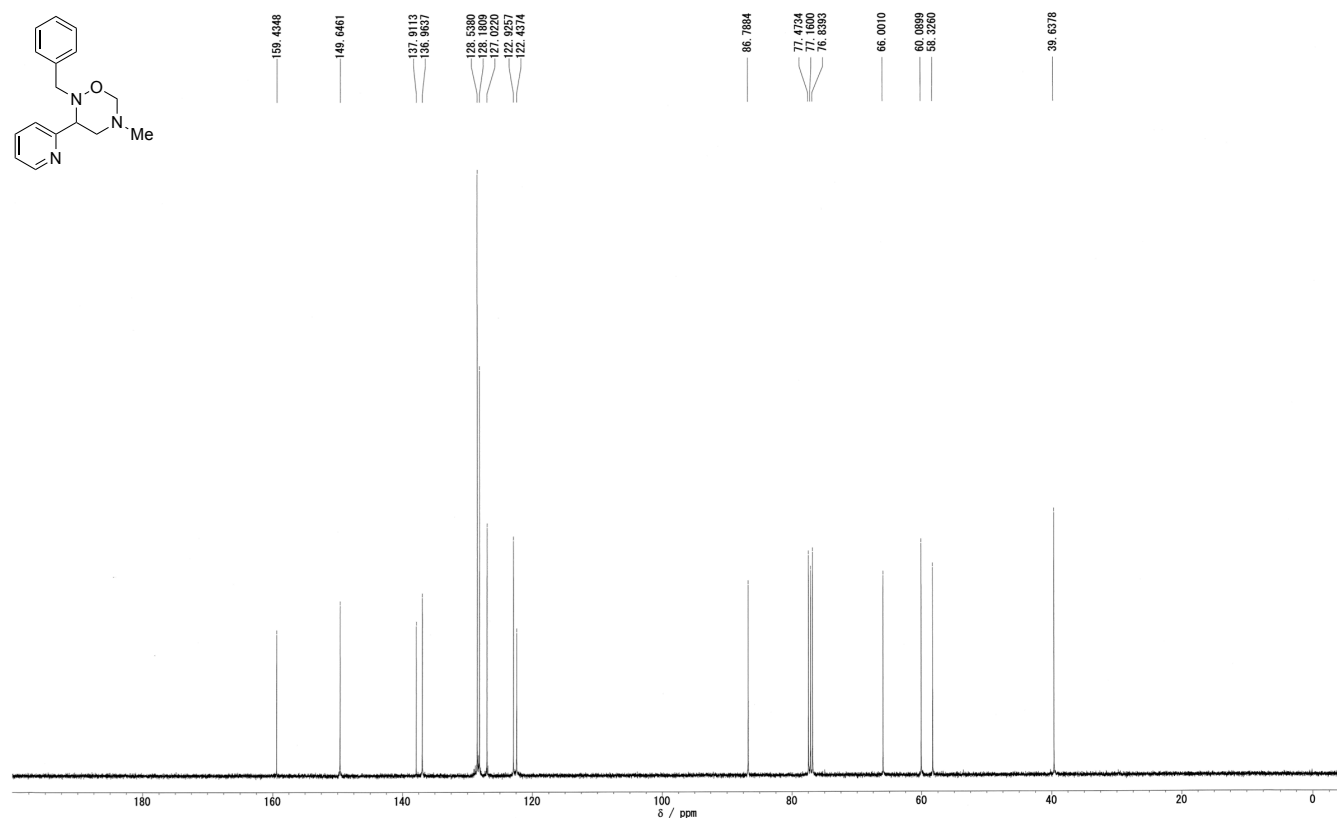
¹³C NMR spectrum of (±)-2-benzyl-3-(4-methoxyphenyl)-5-methyl-1,2,5-oxadiazinane (**3da**)



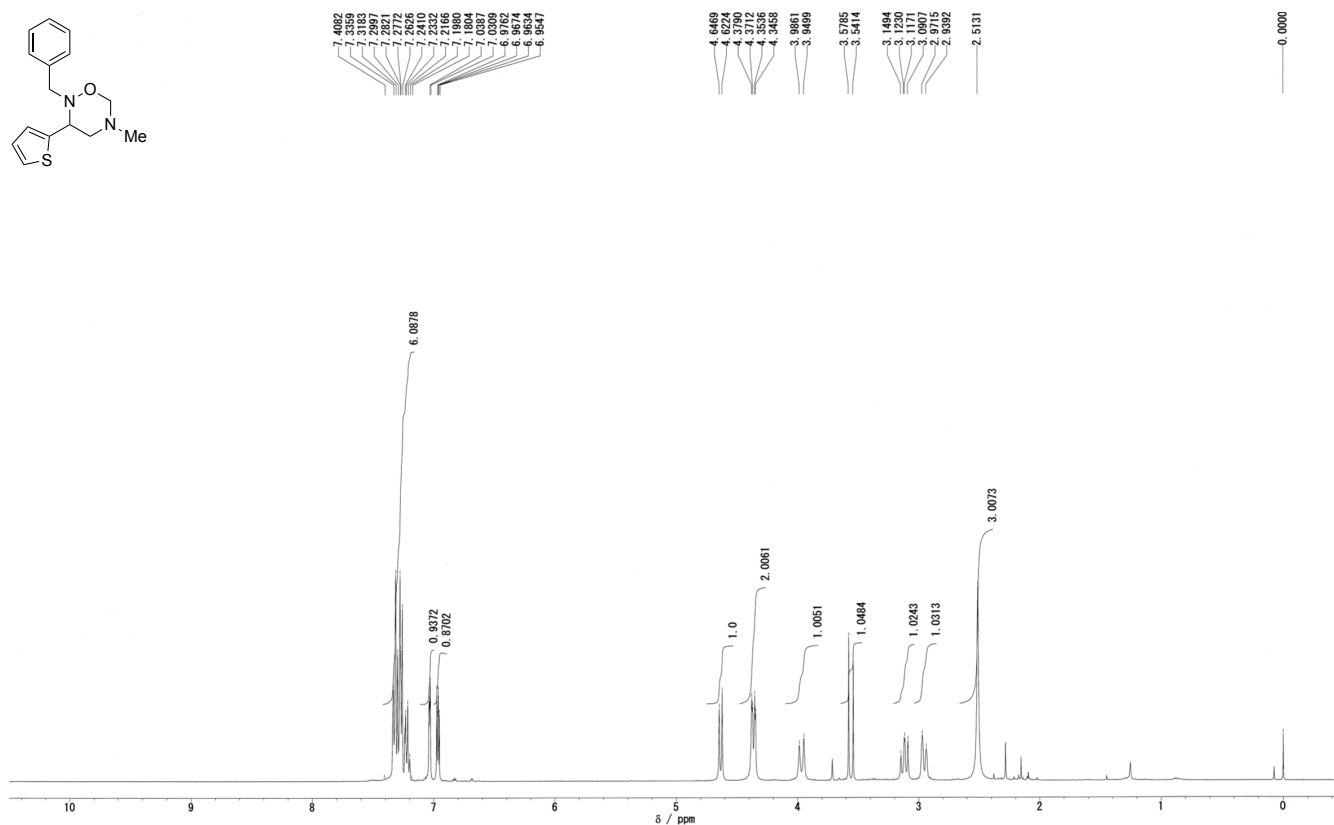
¹H NMR spectrum of (±)-2-benzyl-5-methyl-3-(pyridin-2-yl)-1,2,5-oxadiazinane (**3ea**)



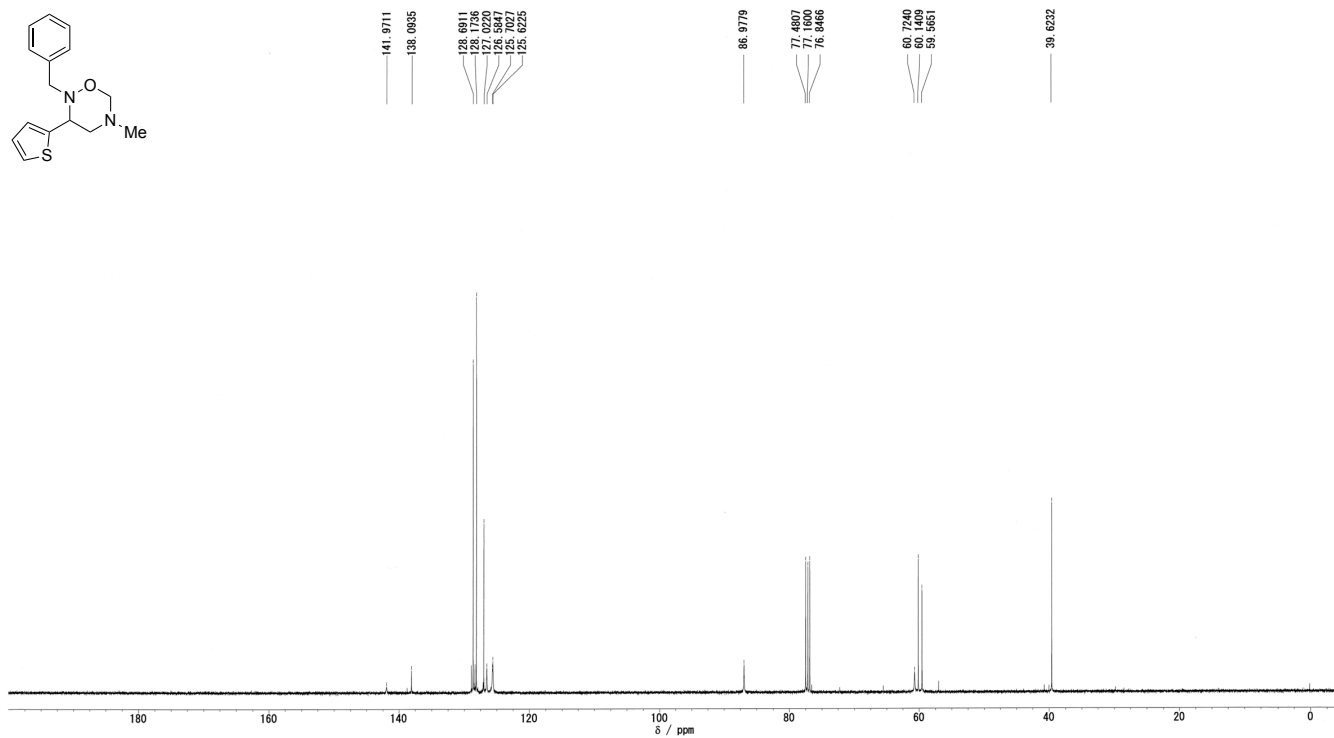
¹³C NMR spectrum of (±)-2-benzyl-5-methyl-3-(pyridin-2-yl)-1,2,5-oxadiazinane (**3ea**)



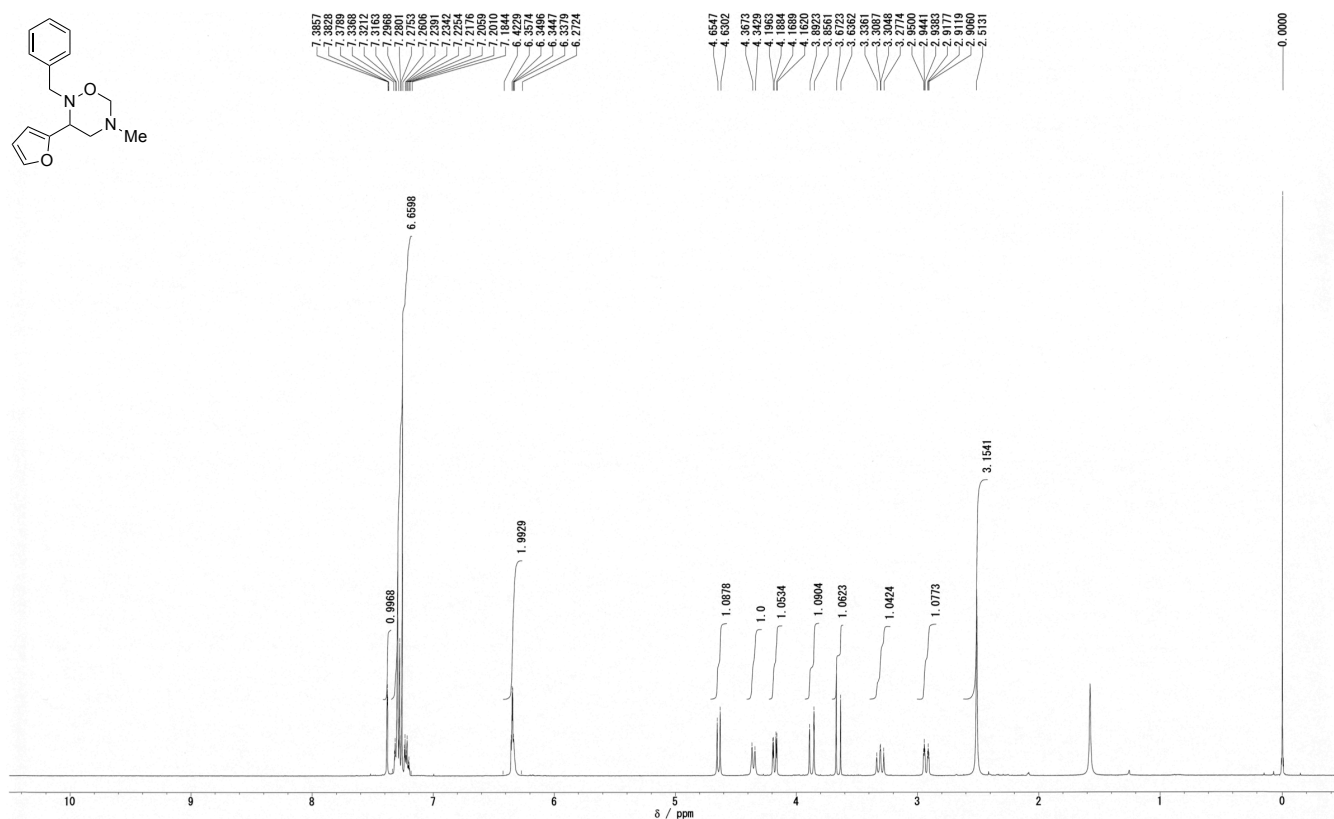
¹H NMR spectrum of (±)-2-benzyl-5-methyl-3-(thiophen-2-yl)-1,2,5-oxadiazinane (**3fa**)



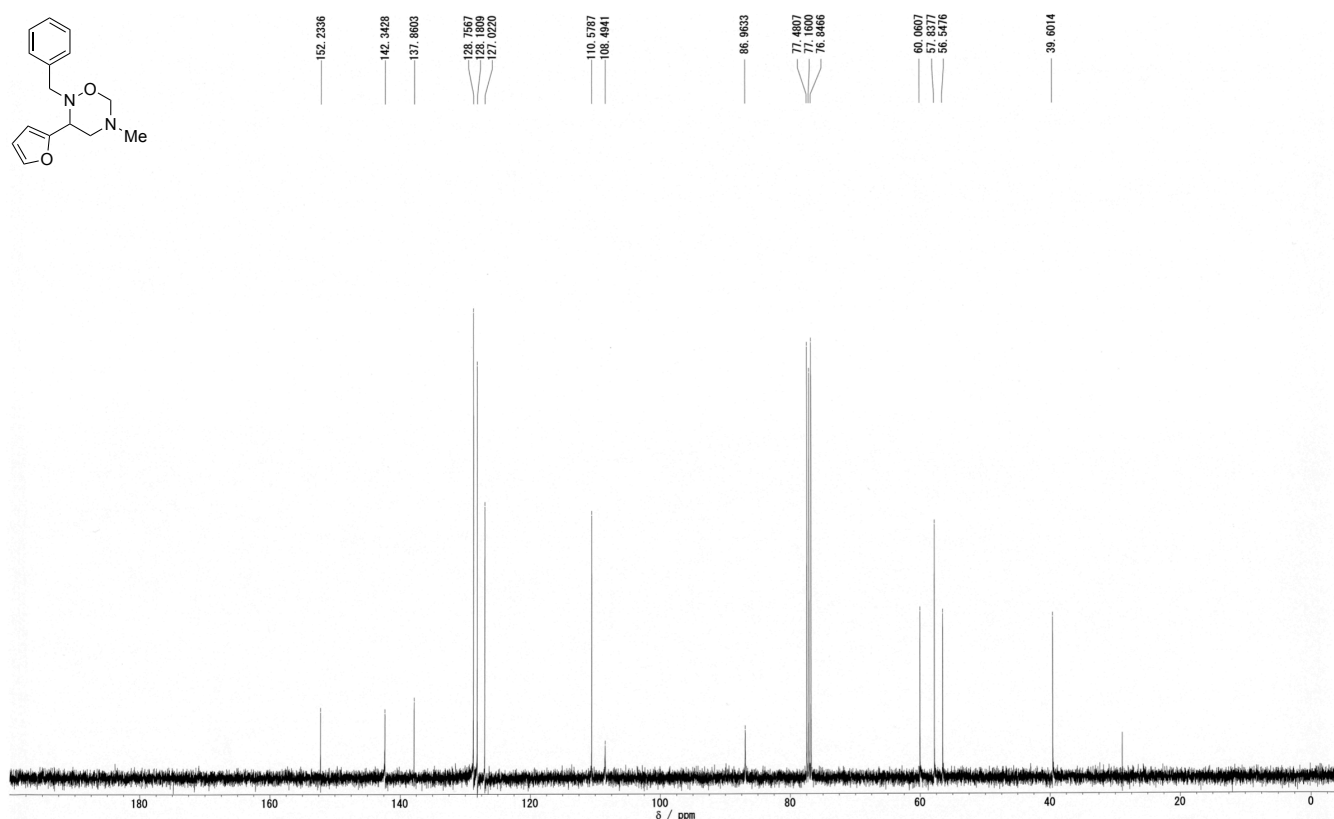
¹³C NMR spectrum of (±)-2-benzyl-5-methyl-3-(thiophen-2-yl)-1,2,5-oxadiazinane (**3fa**)



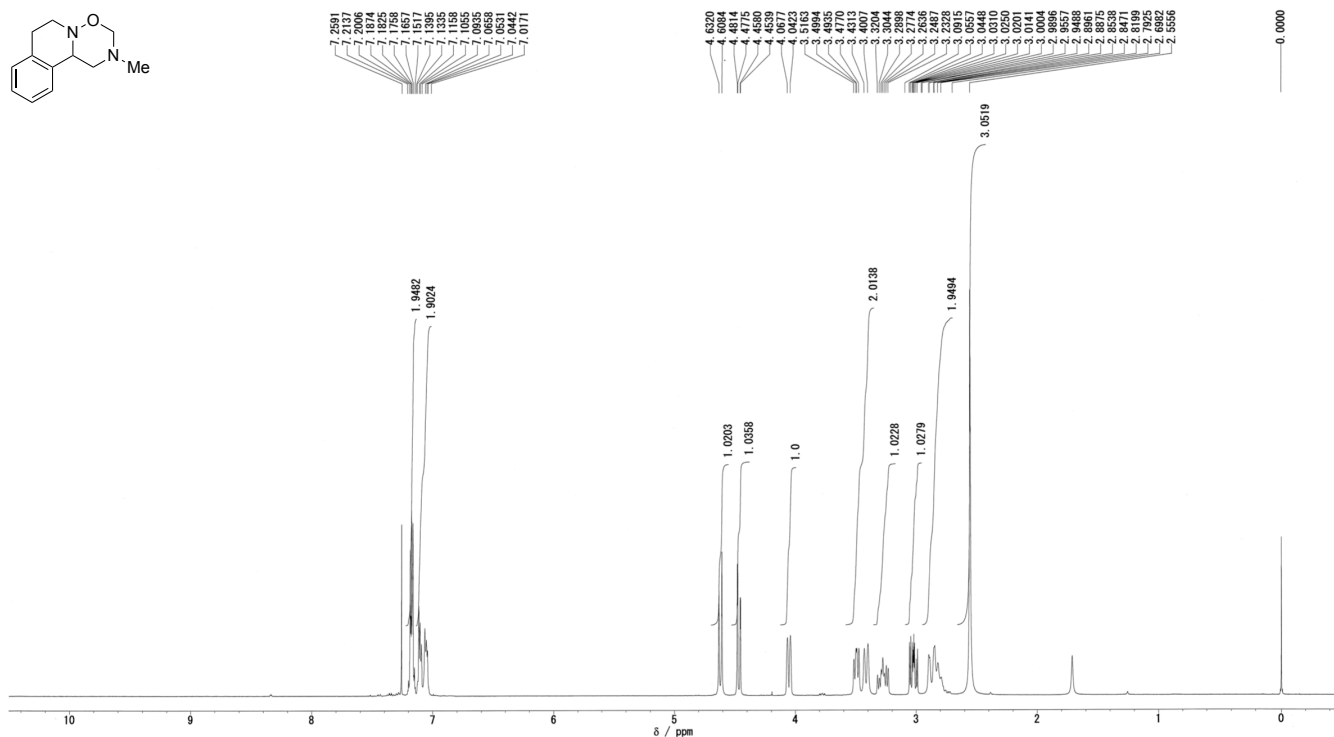
¹H NMR spectrum of (±)-2-benzyl-3-(furan-2-yl)-5-methyl-1,2,5-oxadiazinane (**3ga**)



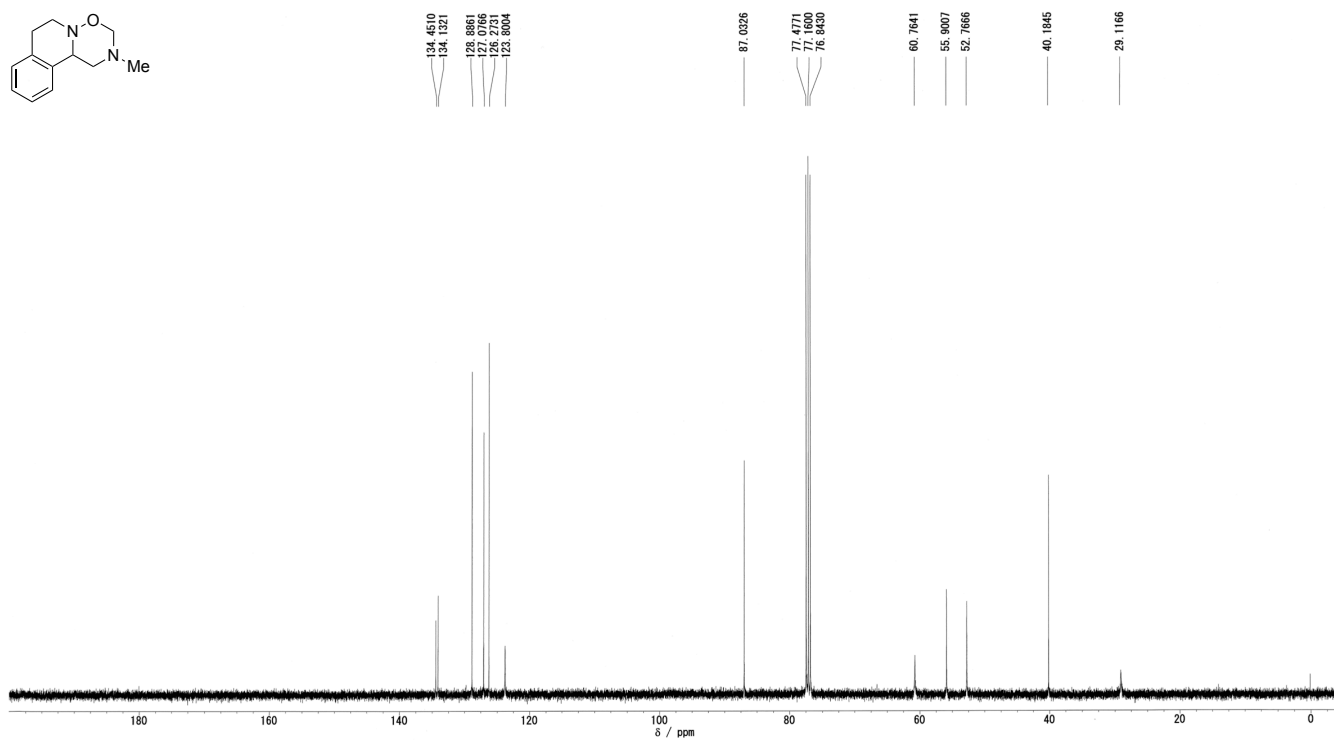
¹³C NMR spectrum of (±)-2-benzyl-3-(furan-2-yl)-5-methyl-1,2,5-oxadiazinane (**3ga**)

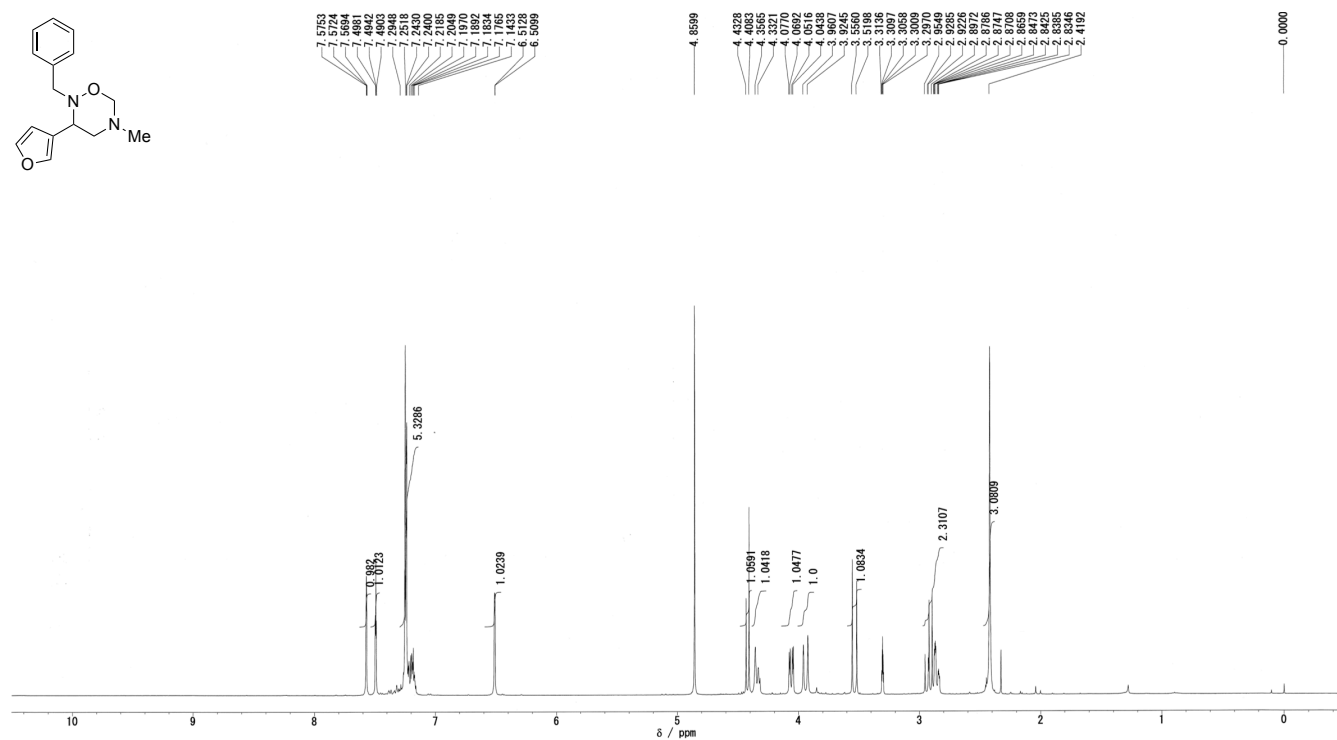
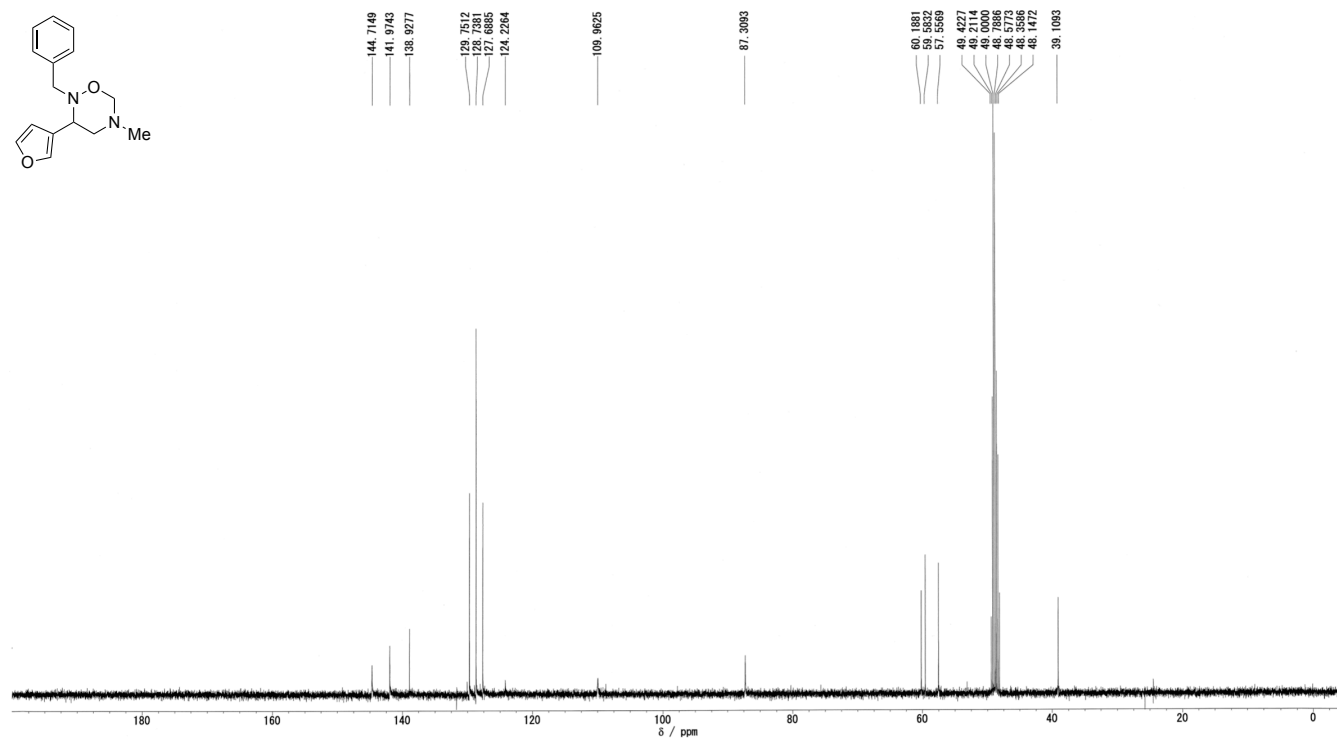


¹H NMR spectrum of (±)-2-methyl-1,2,3,6,7,11b-hexahydro-[1,2,5]oxadiazino[3,2-a]isoquinoline (**3ta**)

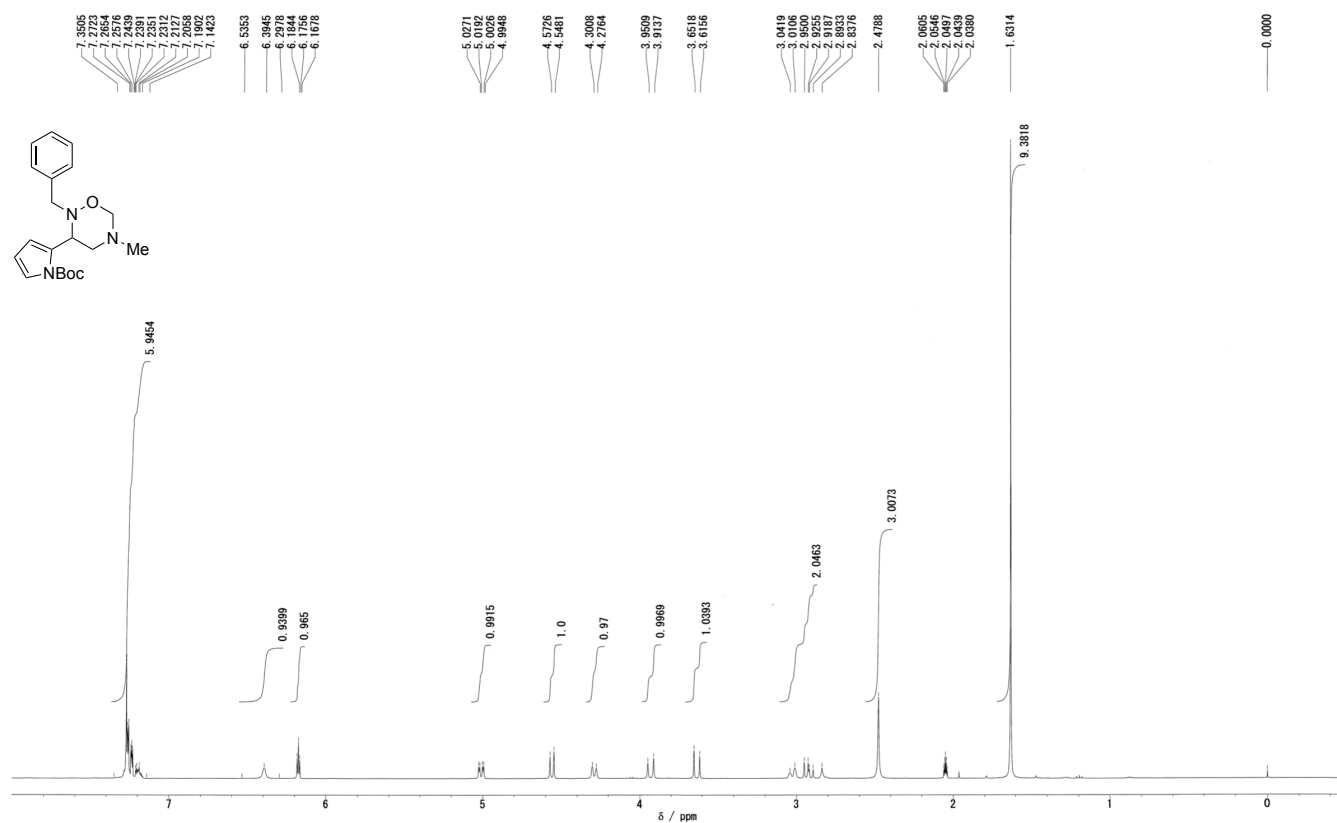


¹³C NMR spectrum of (±)-2-methyl-1,2,3,6,7,11b-hexahydro-[1,2,5]oxadiazino[3,2-a]isoquinoline (**3ta**)

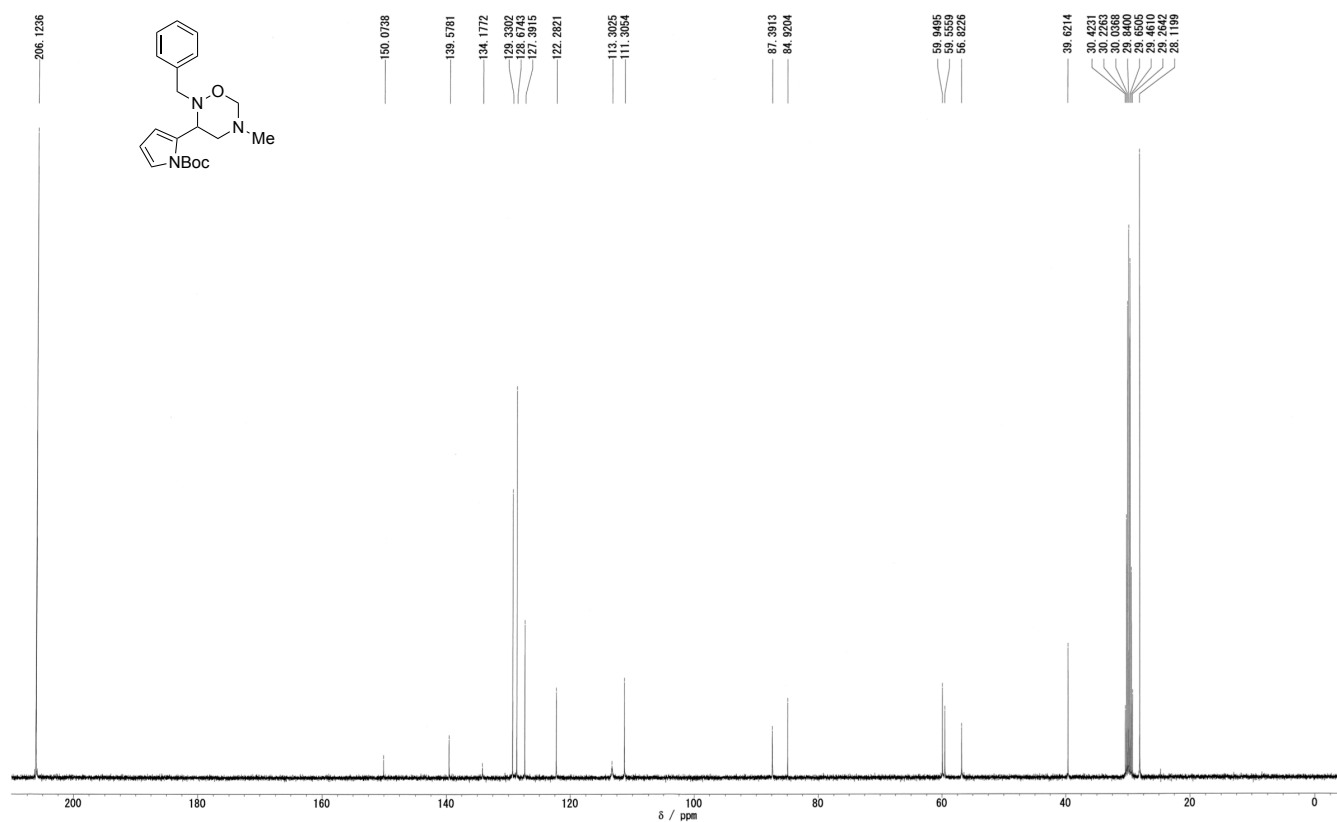


CN1CC2(C1)OC(C2)c3ccoc3Cc4ccccc4CN1CC2C(C1)C3=CC=CC=C3O2

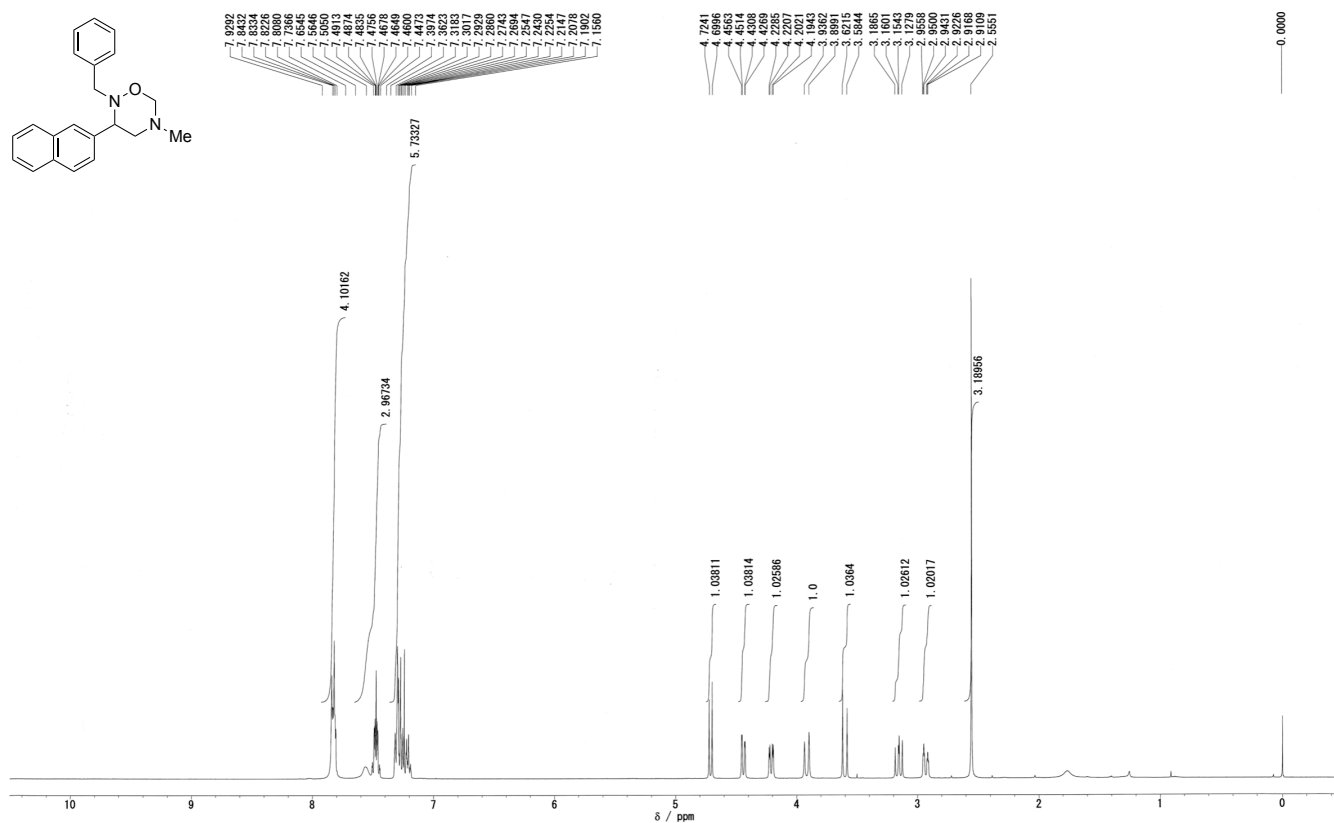
¹H NMR spectrum of (±)-*tert*-butyl 2-(2-benzyl-5-methyl-1,2,5-oxadiazinan-3-yl)-1*H*-pyrrole-1-carboxylate (**3ia**)



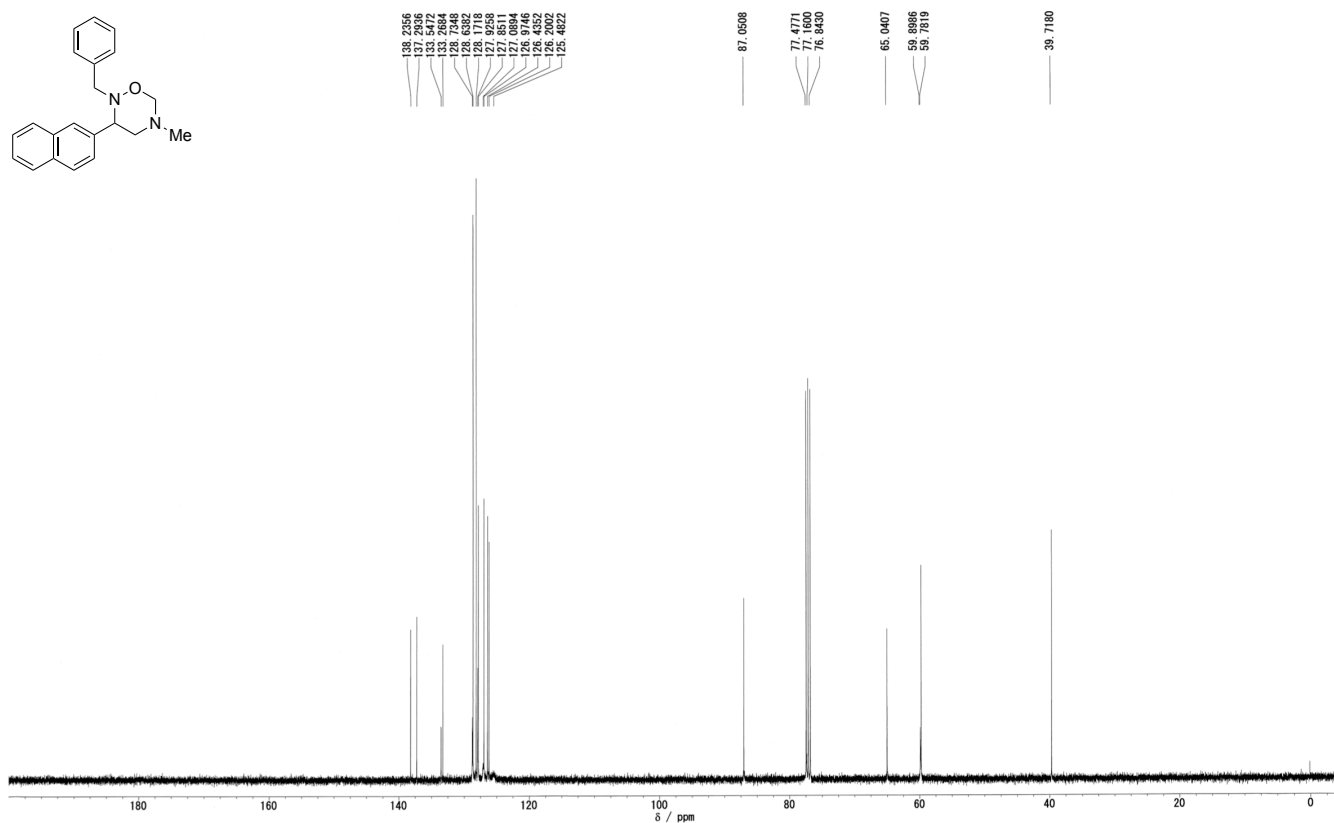
¹³C NMR spectrum of (±)-*tert*-butyl 2-(2-benzyl-5-methyl-1,2,5-oxadiazinan-3-yl)-1*H*-pyrrole-1-carboxylate (**3ia**)



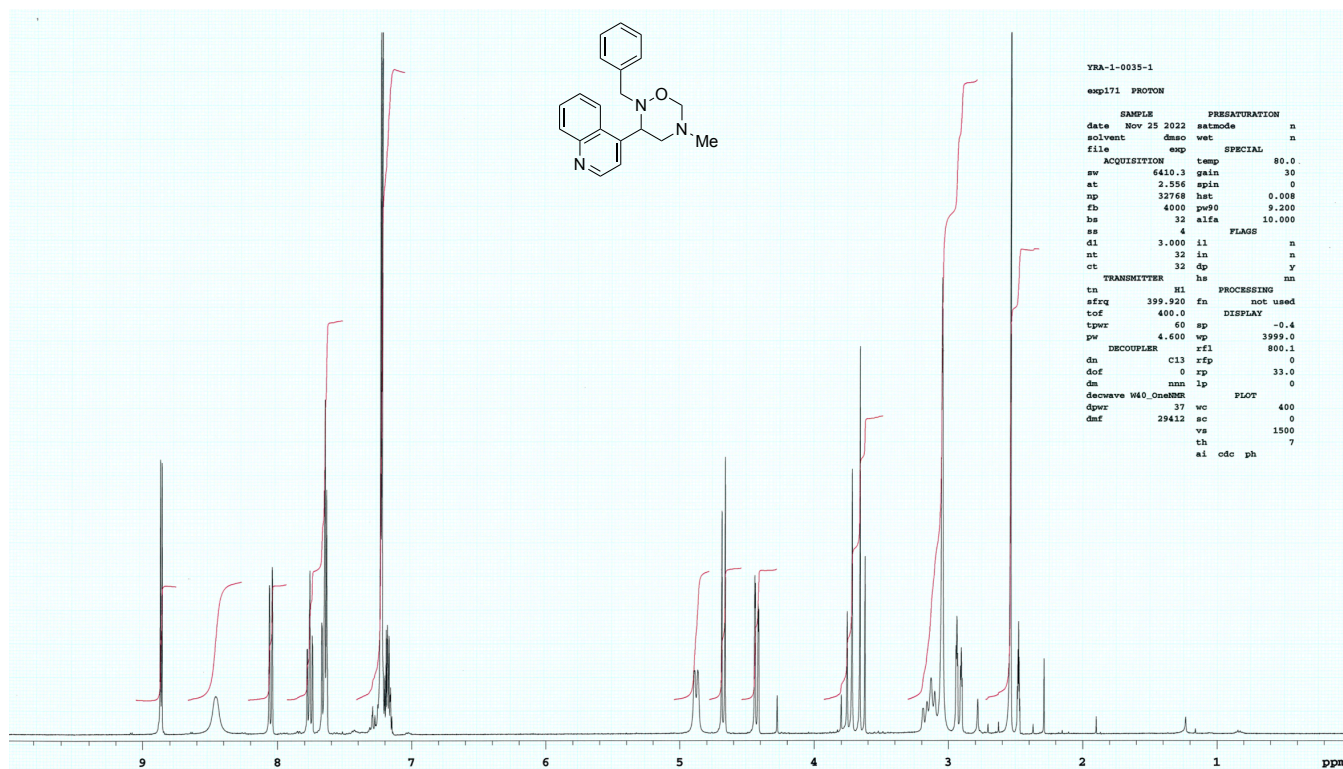
¹H NMR spectrum of (±)-2-benzyl-5-methyl-3-(naphthalen-2-yl)-1,2,5-oxadiazinane (**3ja**)



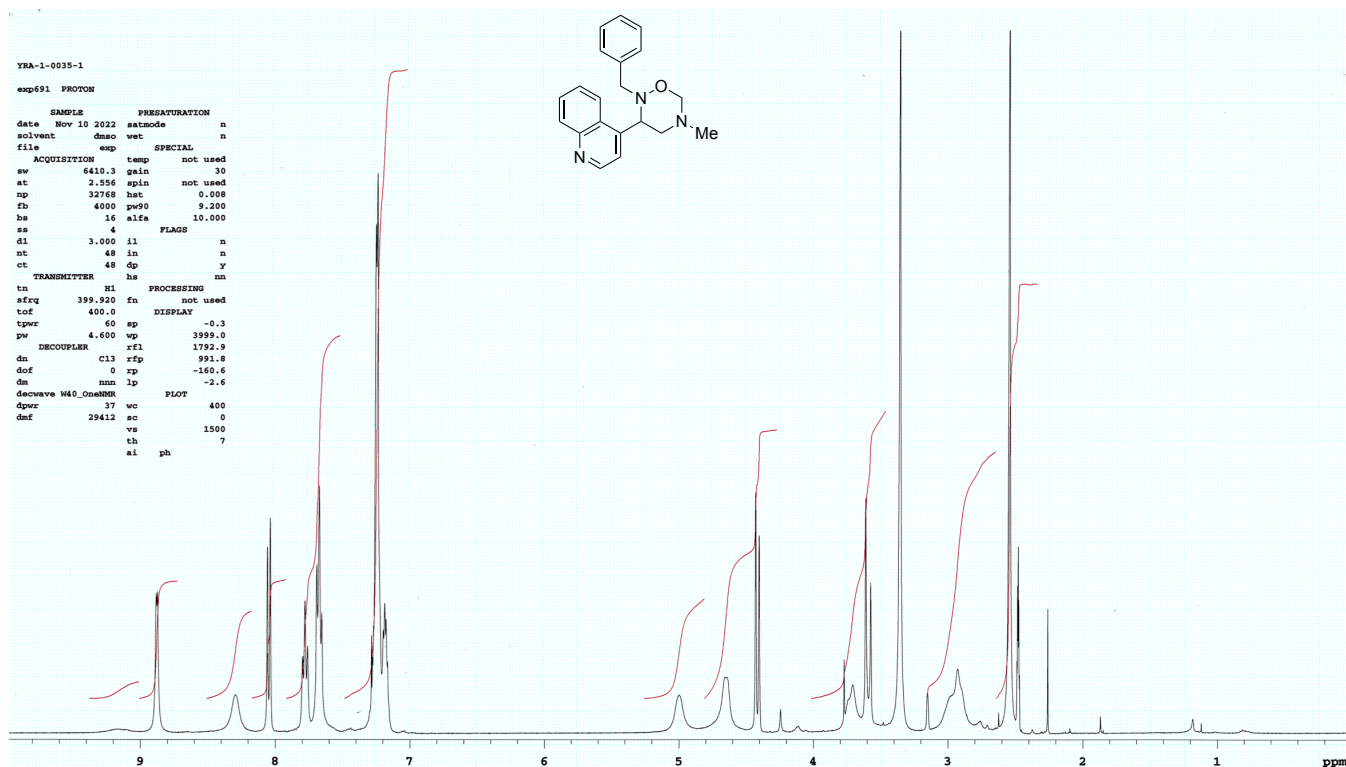
¹³C NMR spectrum of (±)-2-benzyl-5-methyl-3-(naphthalen-2-yl)-1,2,5-oxadiazinane (**3ja**)



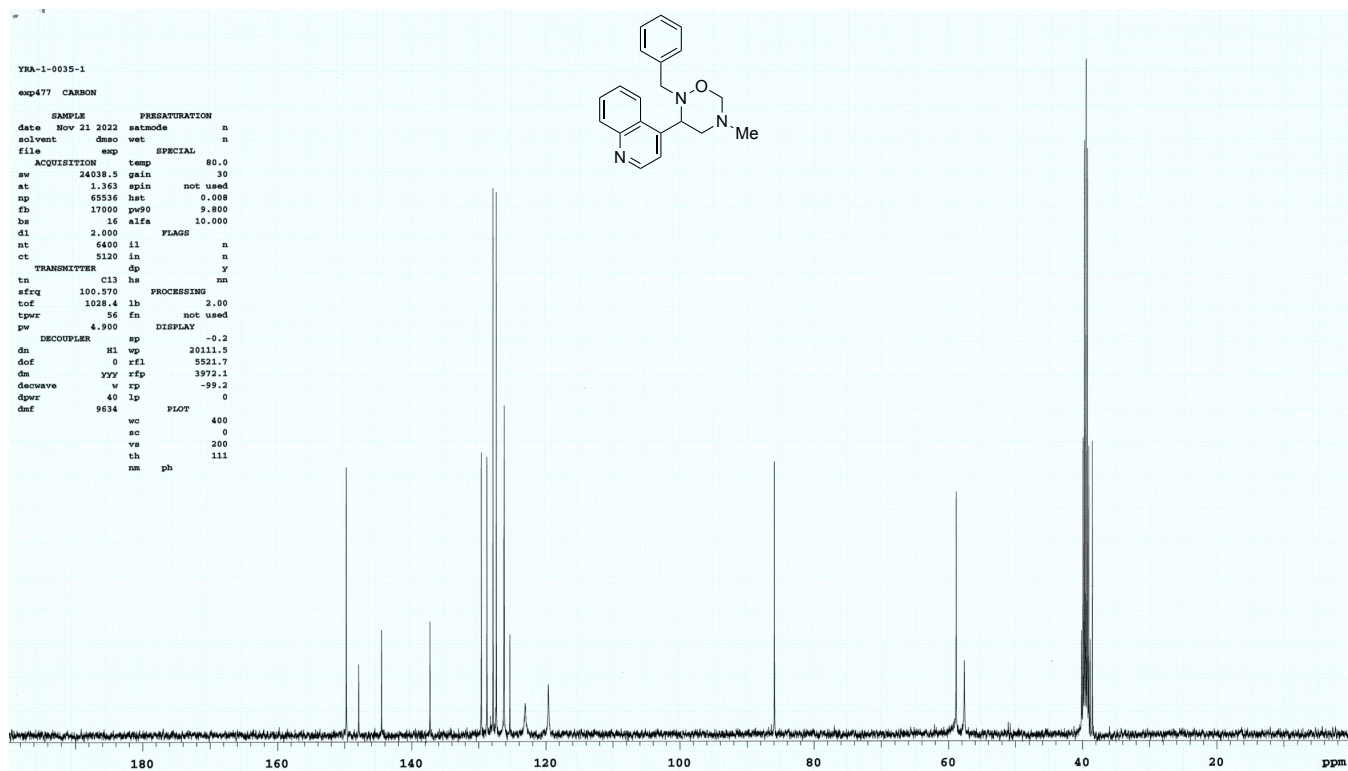
¹H NMR spectrum of (±)-2-benzyl-5-methyl-3-(quinolin-4-yl)-1,2,5-oxadiazinane (**3ka**) at 80 °C



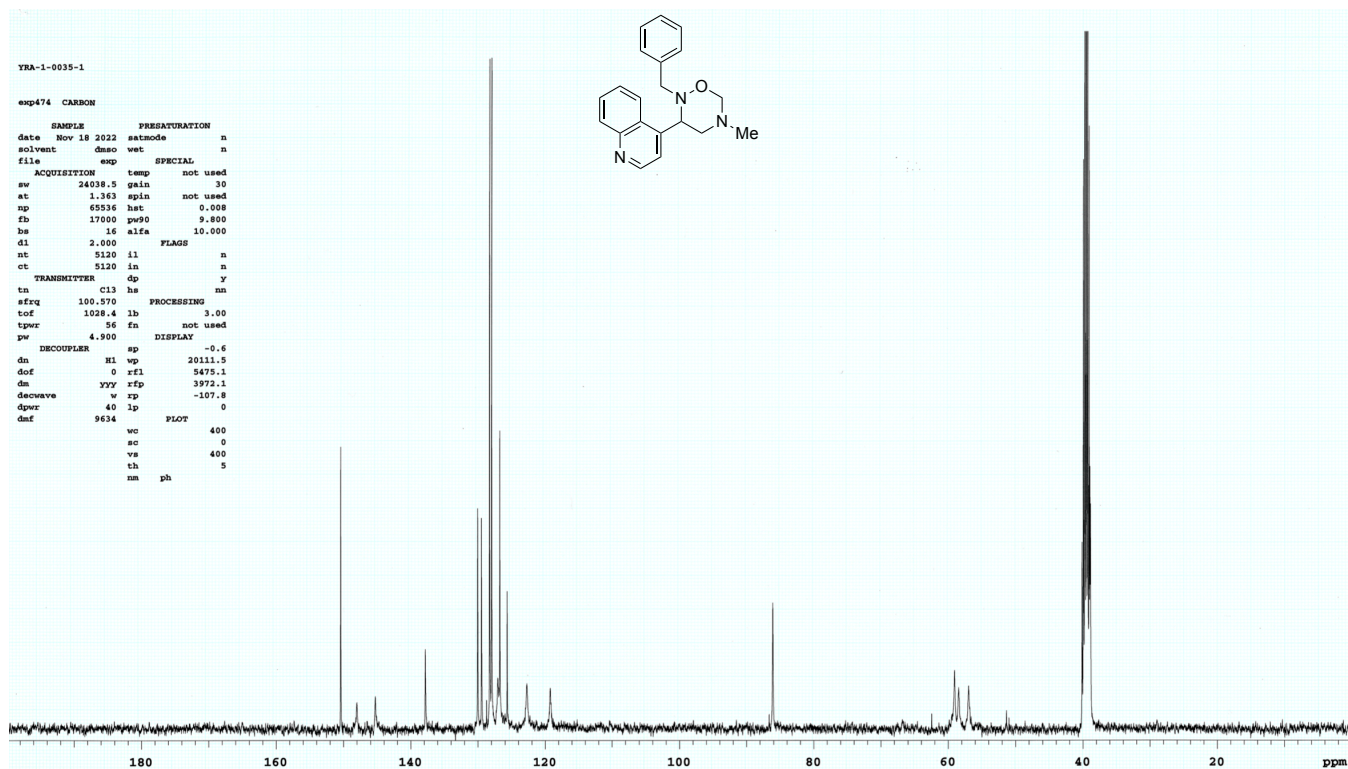
¹H NMR spectrum of (±)-2-benzyl-5-methyl-3-(quinolin-4-yl)-1,2,5-oxadiazinane (**3ka**) at rt



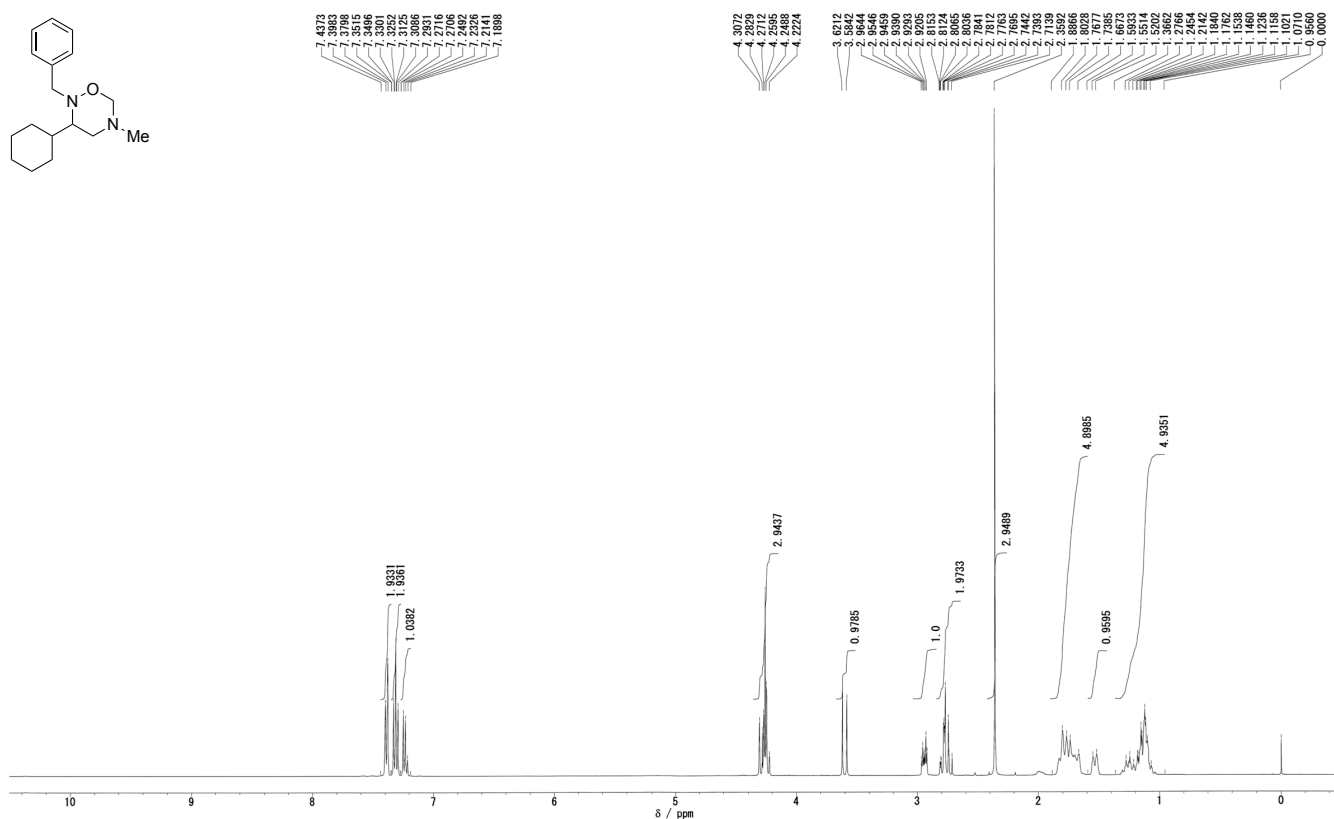
^{13}C NMR spectrum of (\pm)-2-benzyl-5-methyl-3-(quinolin-4-yl)-1,2,5-oxadiazinane (**3ka**) at 80 °C



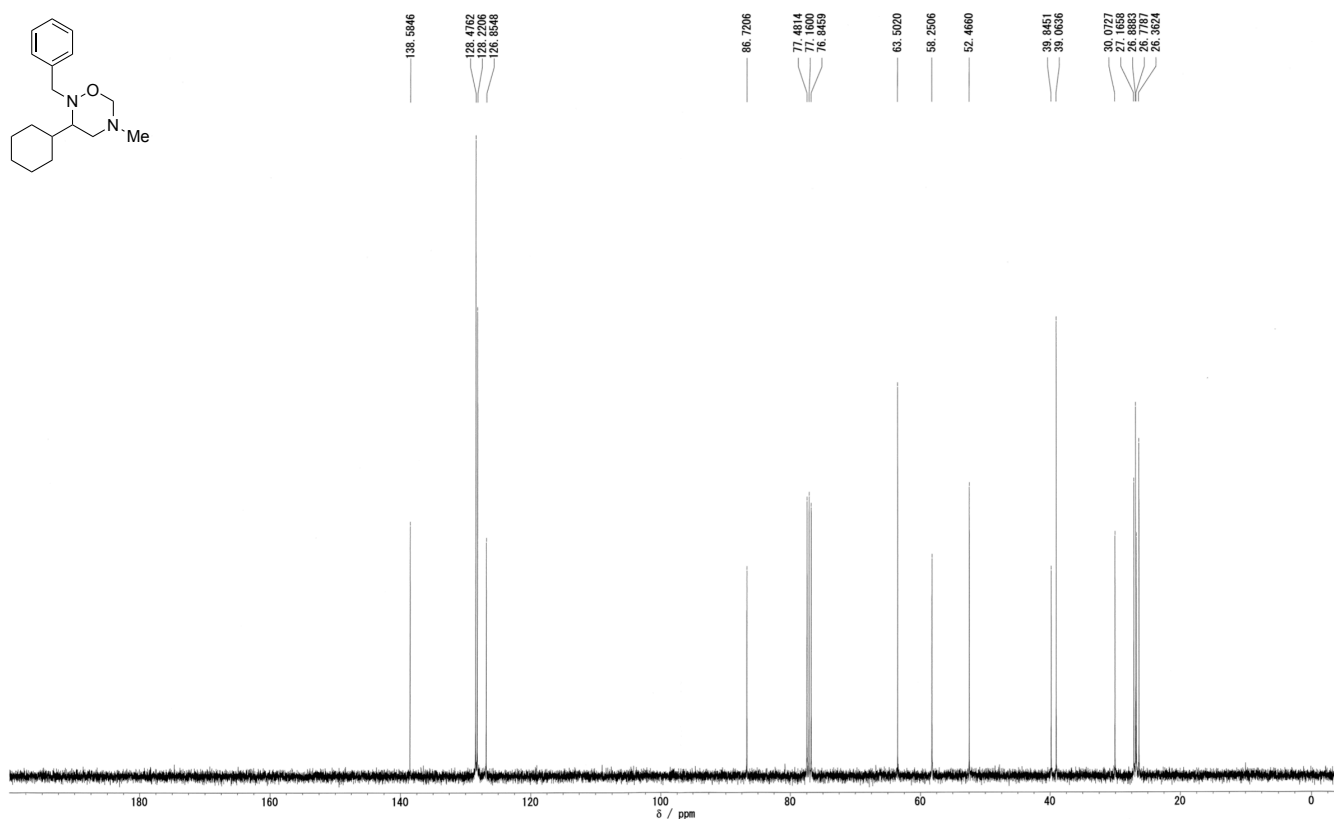
^{13}C NMR spectrum of (\pm)-2-benzyl-5-methyl-3-(quinolin-4-yl)-1,2,5-oxadiazinane (**3ka**) at rt



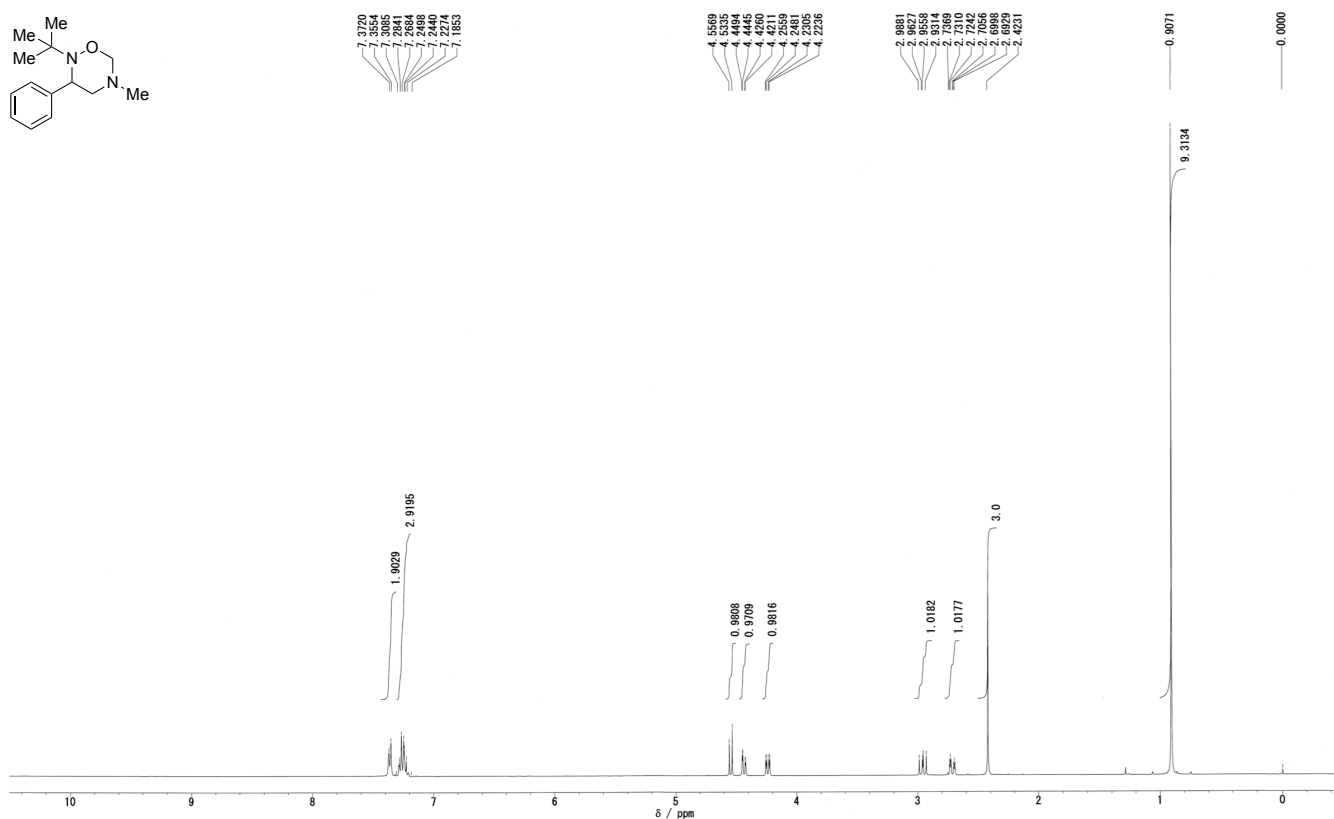
¹H NMR spectrum of (±)-2-benzyl-3-cyclohexyl-5-methyl-1,2,5-oxadiazinane (**31a**)



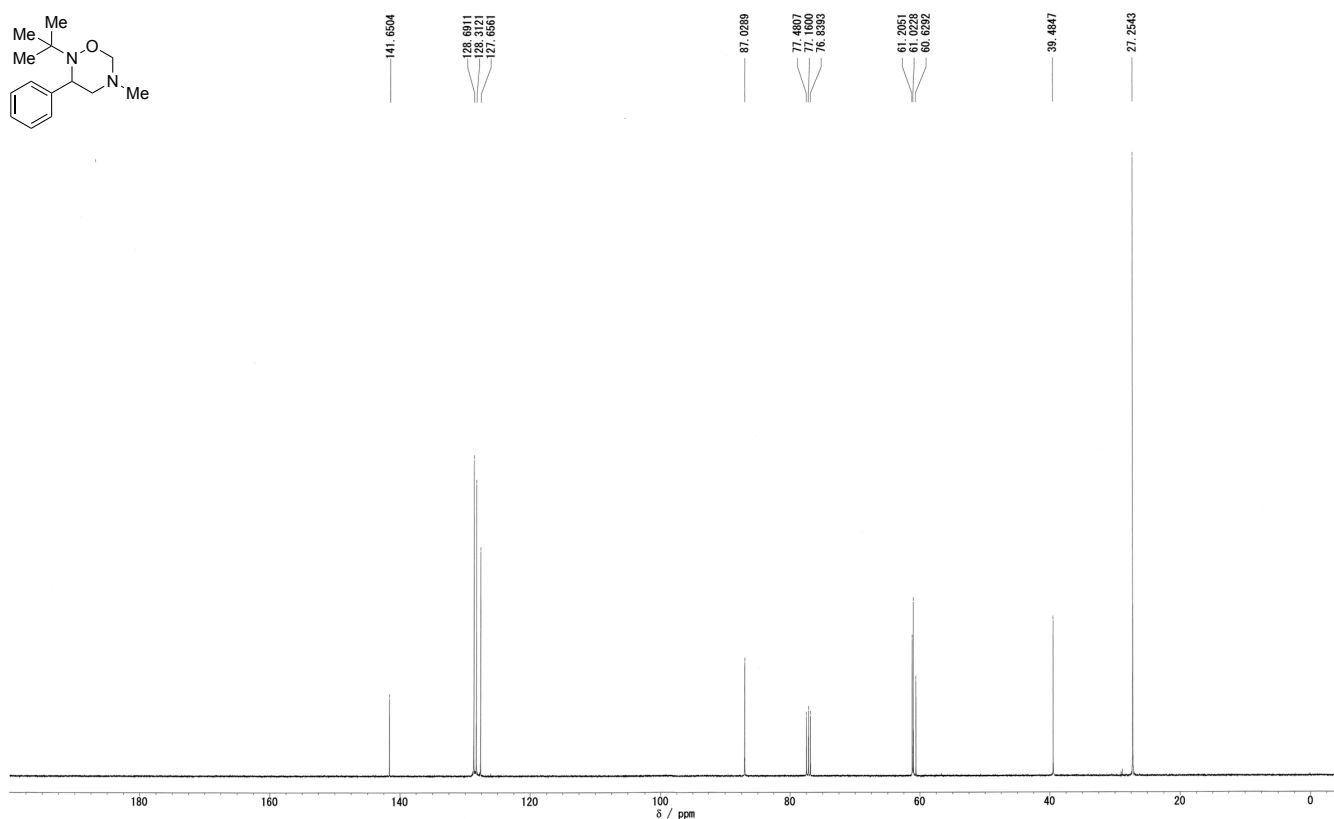
¹³C NMR spectrum of (±)-2-benzyl-3-cyclohexyl-5-methyl-1,2,5-oxadiazinane (**31a**)



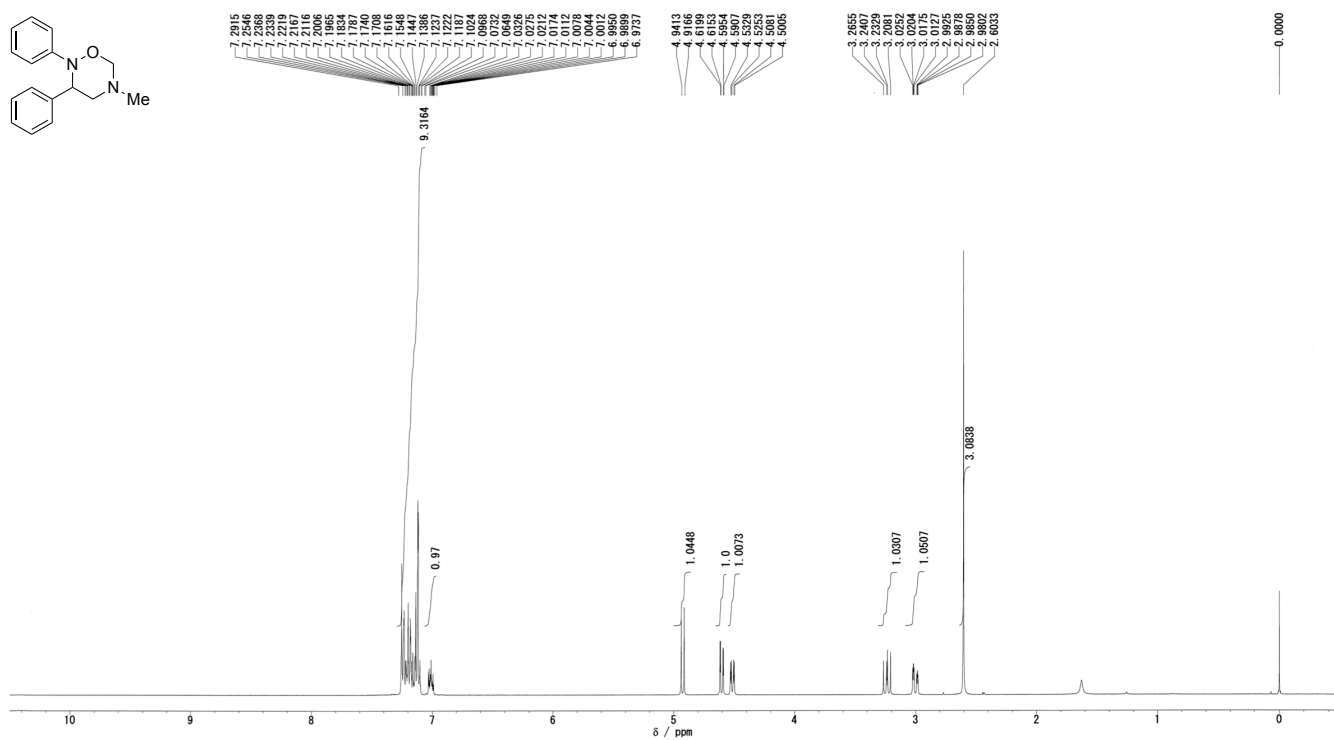
¹H NMR spectrum of (±)-2-(*tert*-butyl)-5-methyl-3-phenyl-1,2,5-oxadiazinane (**3ma**)



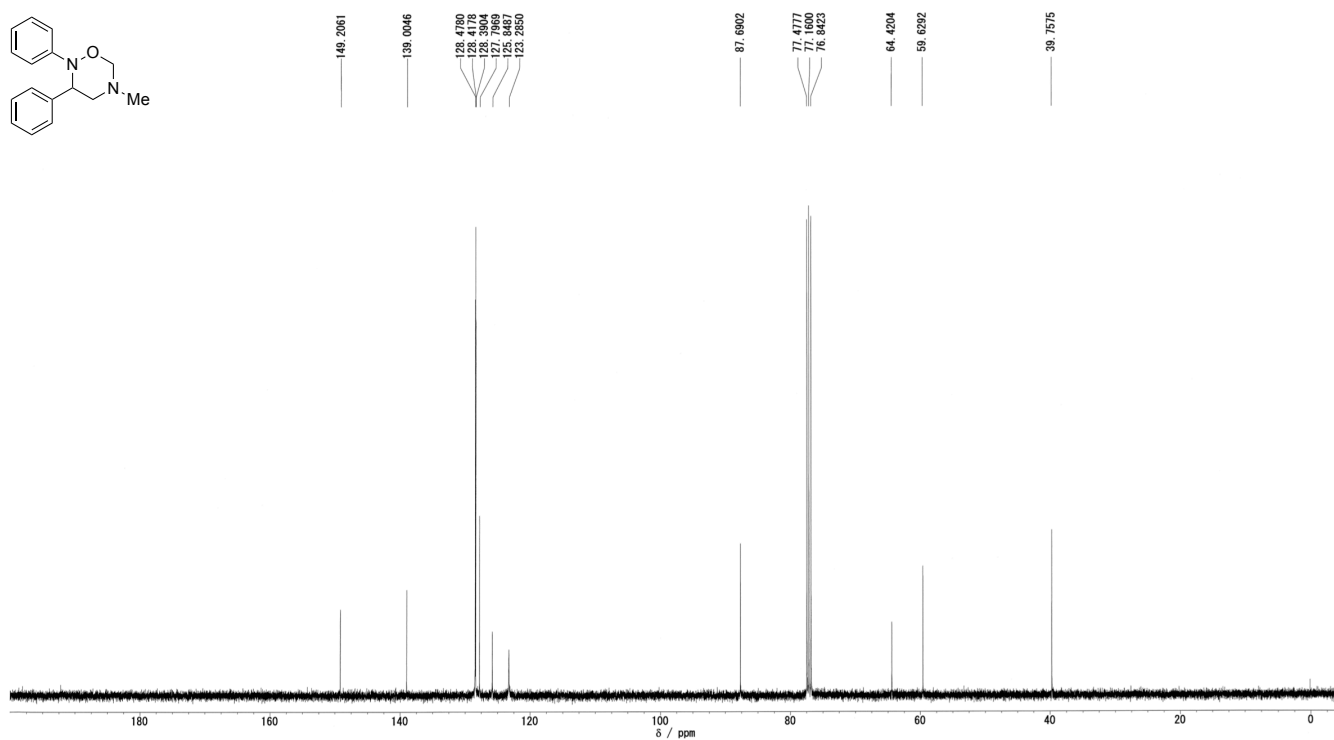
¹³C NMR spectrum of (±)-2-(*tert*-butyl)-5-methyl-3-phenyl-1,2,5-oxadiazinane (**3ma**)



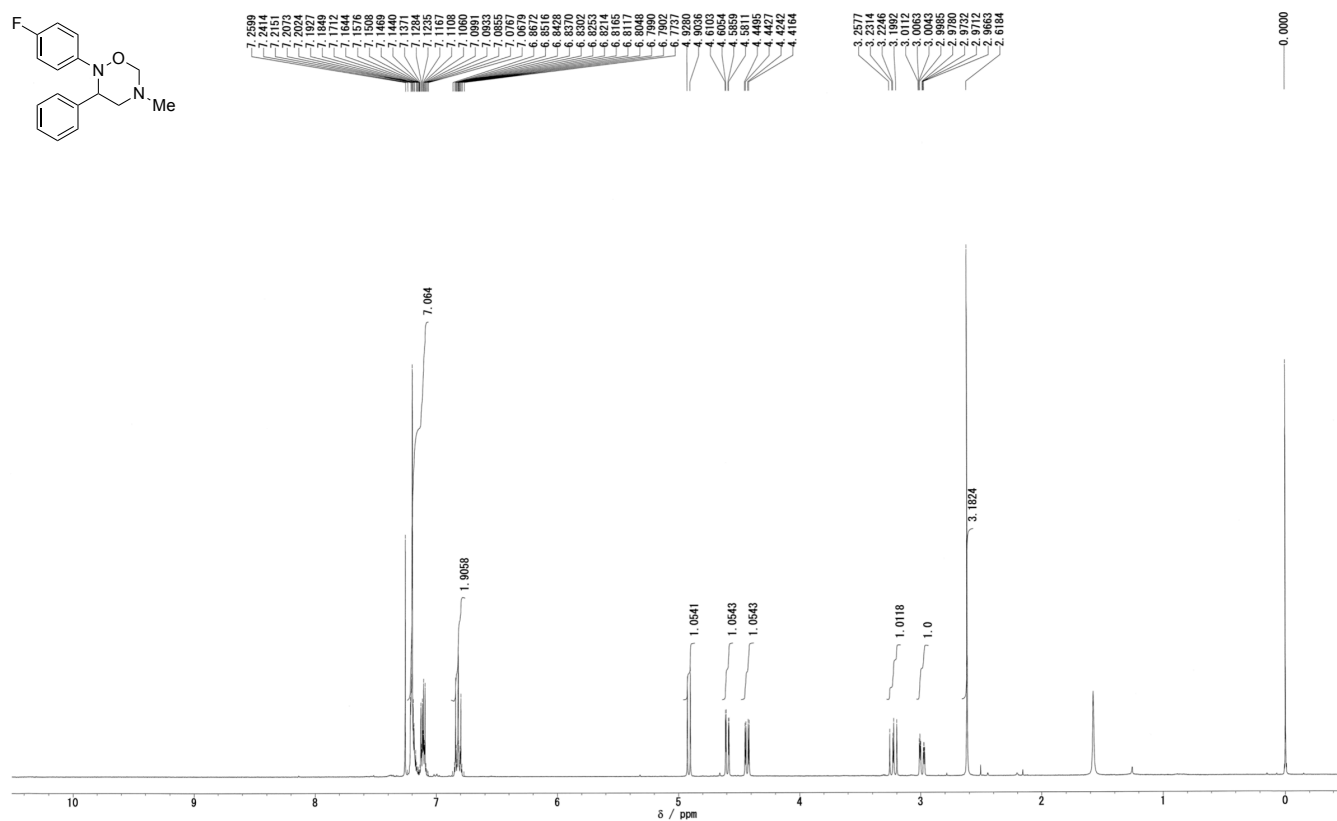
¹H NMR spectrum of (±)-5-methyl-2,3-diphenyl-1,2,5-oxadiazinane (**3na**)



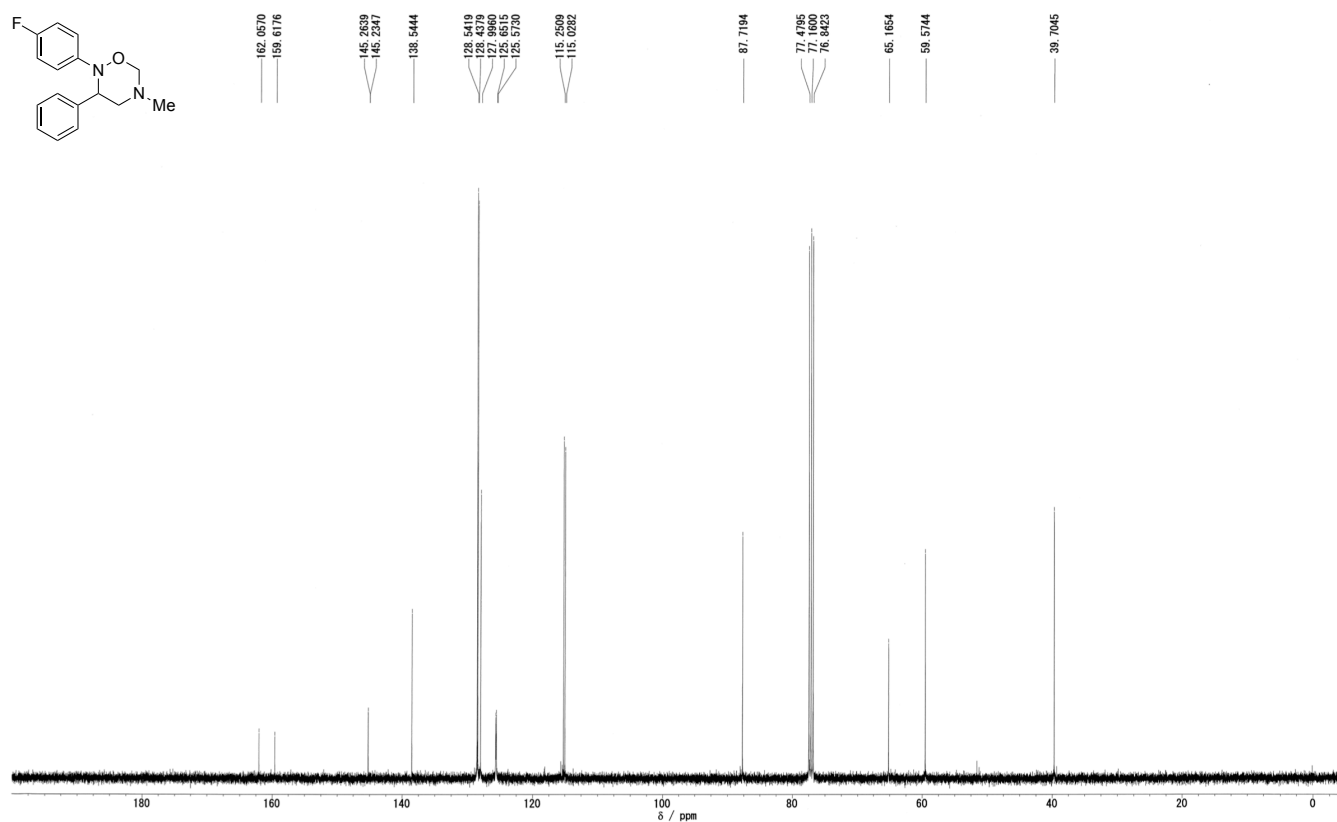
¹³C NMR spectrum of (±)-5-methyl-2,3-diphenyl-1,2,5-oxadiazinane (**3na**)



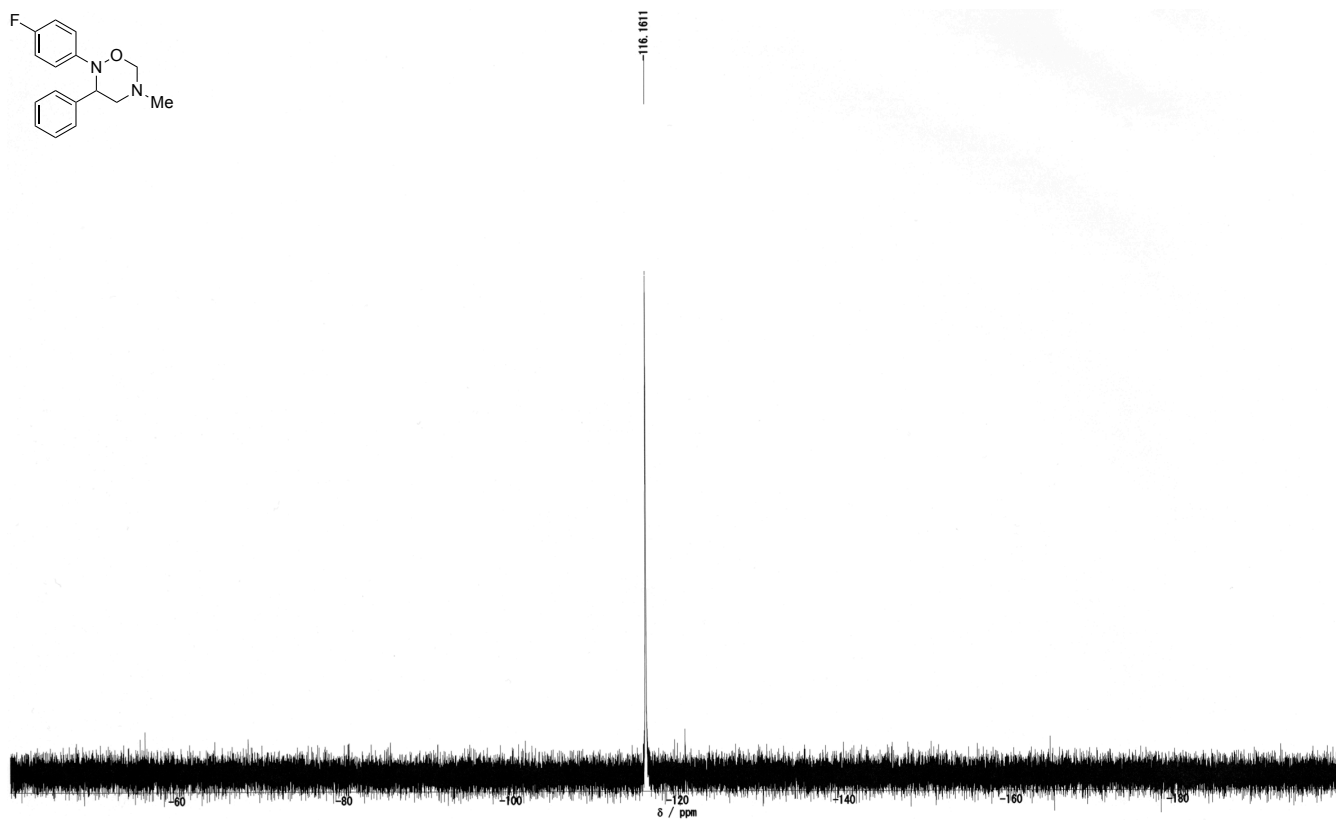
¹H NMR spectrum of (±)-2-(4-fluorophenyl)-5-methyl-3-phenyl-1,2,5-oxadiazinane (**30a**)



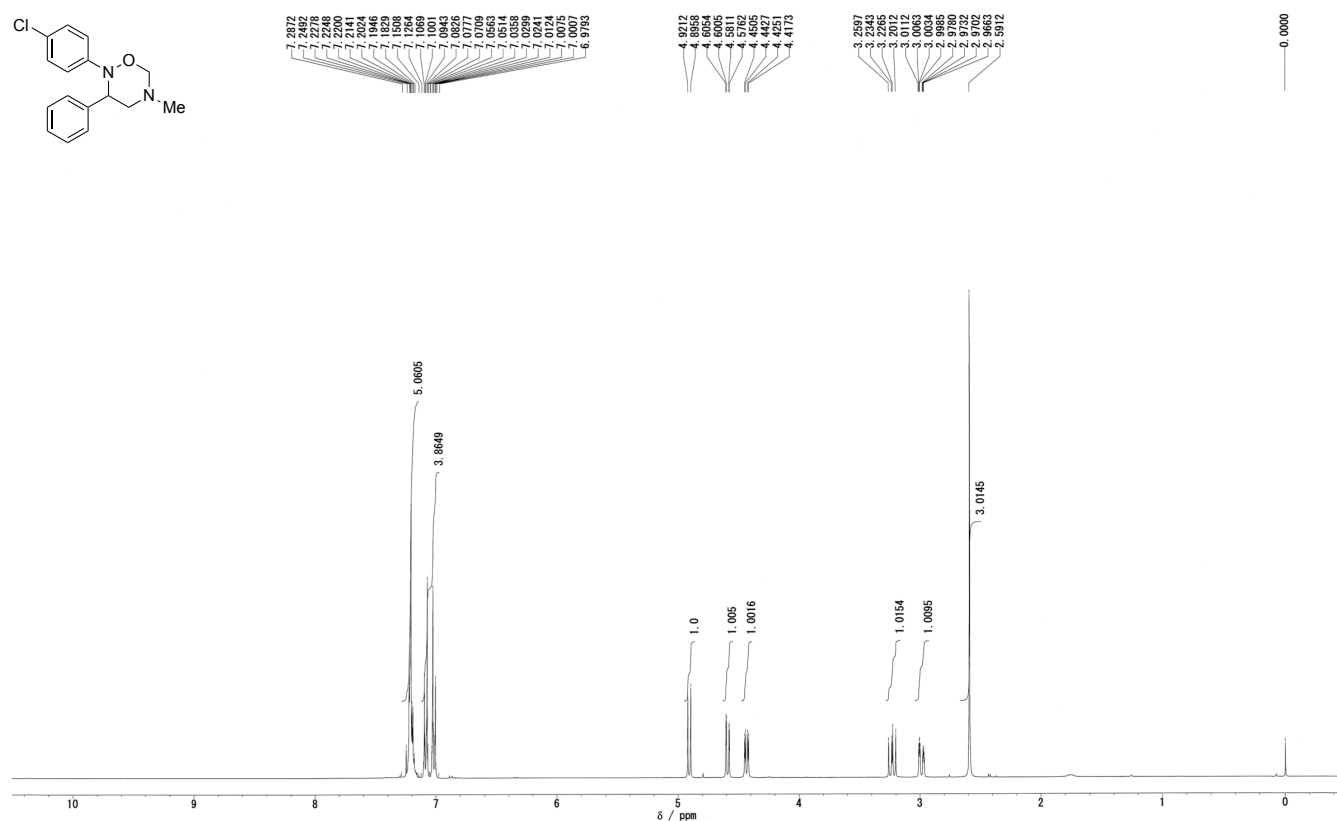
¹³C NMR spectrum of (±)-2-(4-fluorophenyl)-5-methyl-3-phenyl-1,2,5-oxadiazinane (**30a**)



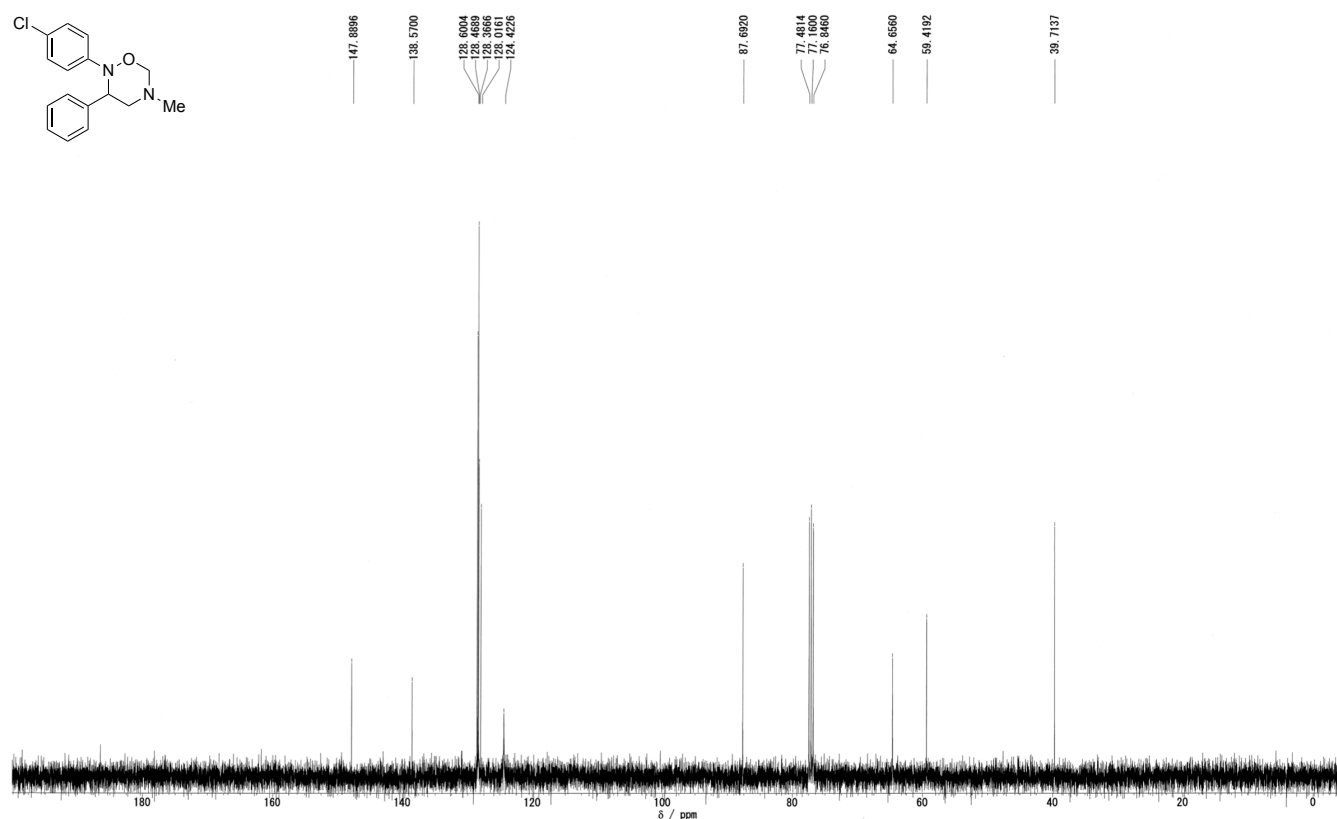
¹⁹F NMR spectrum of (±)-2-(4-fluorophenyl)-5-methyl-3-phenyl-1,2,5-oxadiazinane (**3oa**)



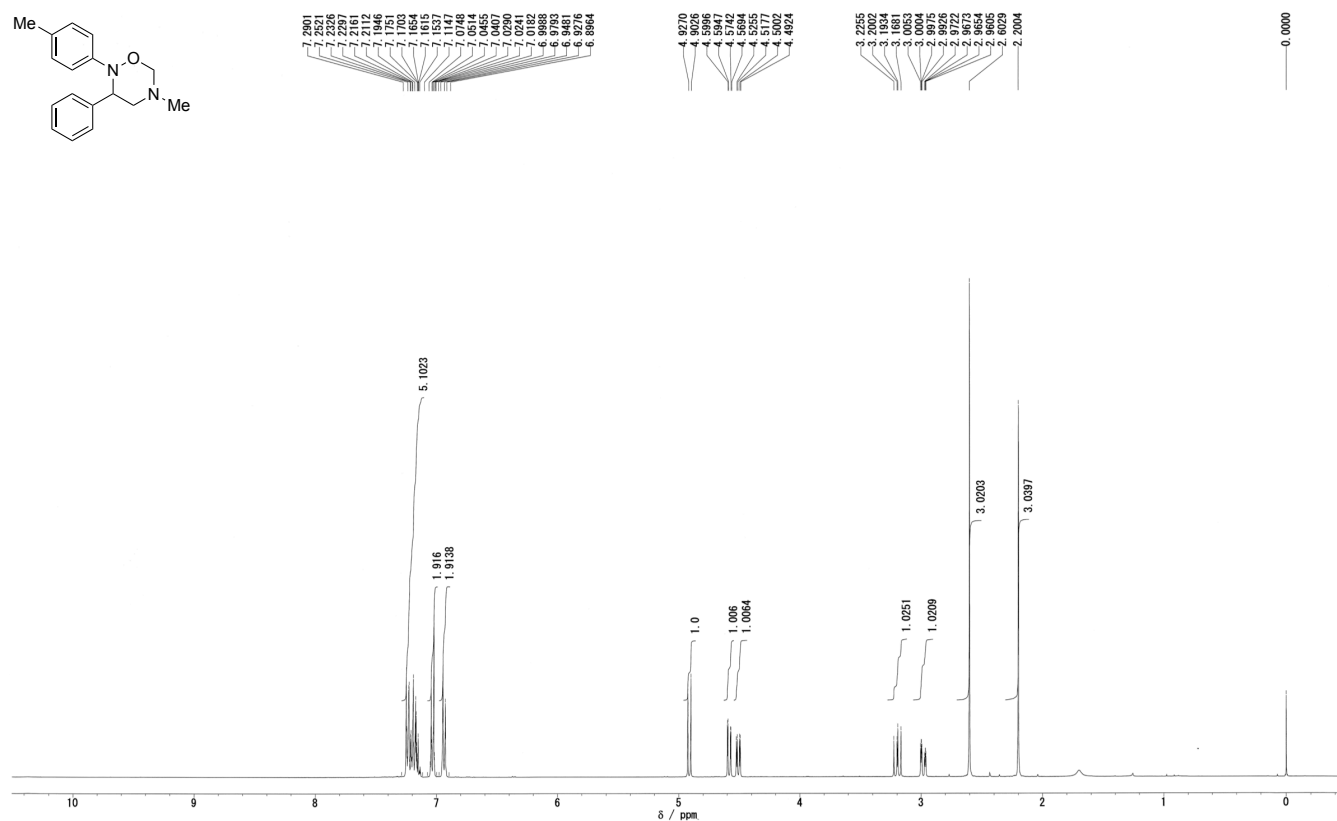
¹H NMR spectrum of (±)-2-(4-chlorophenyl)-5-methyl-3-phenyl-1,2,5-oxadiazinane (**3pa**)



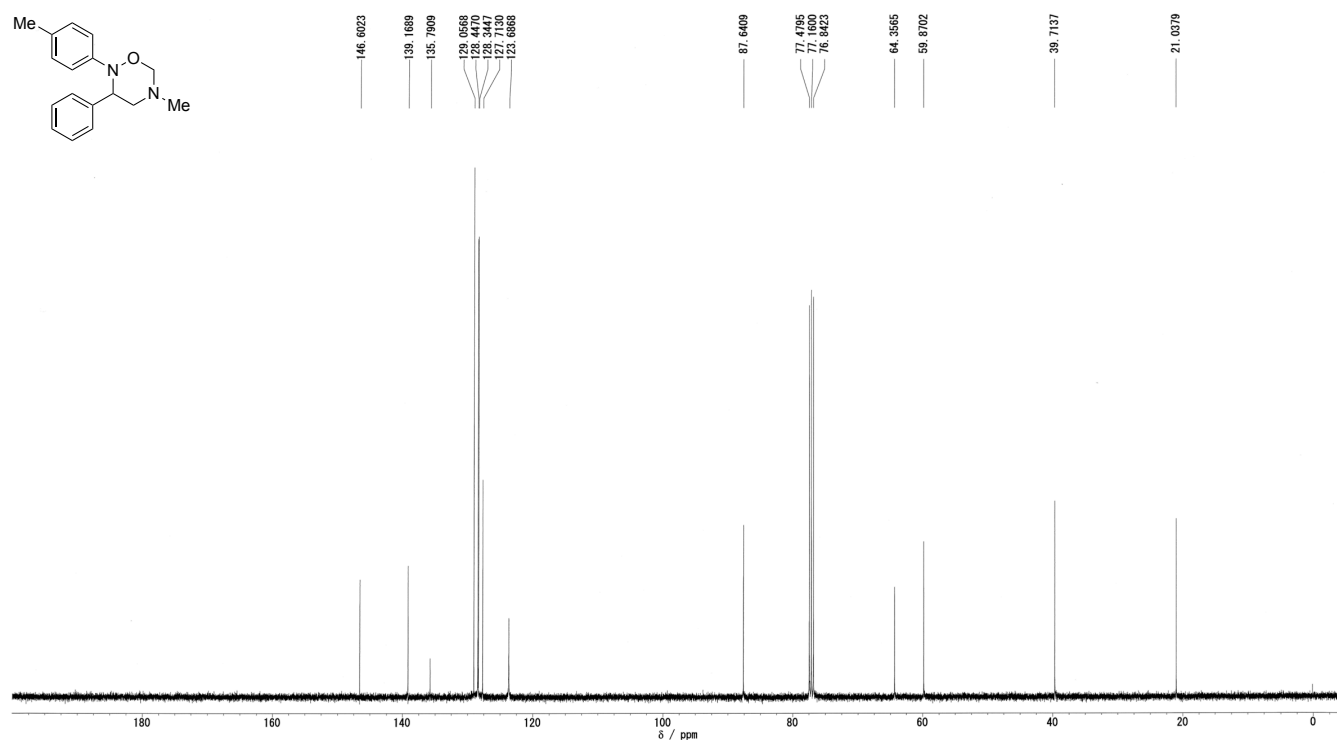
¹³C NMR spectrum of (±)-2-(4-chlorophenyl)-5-methyl-3-phenyl-1,2,5-oxadiazinane (**3pa**)



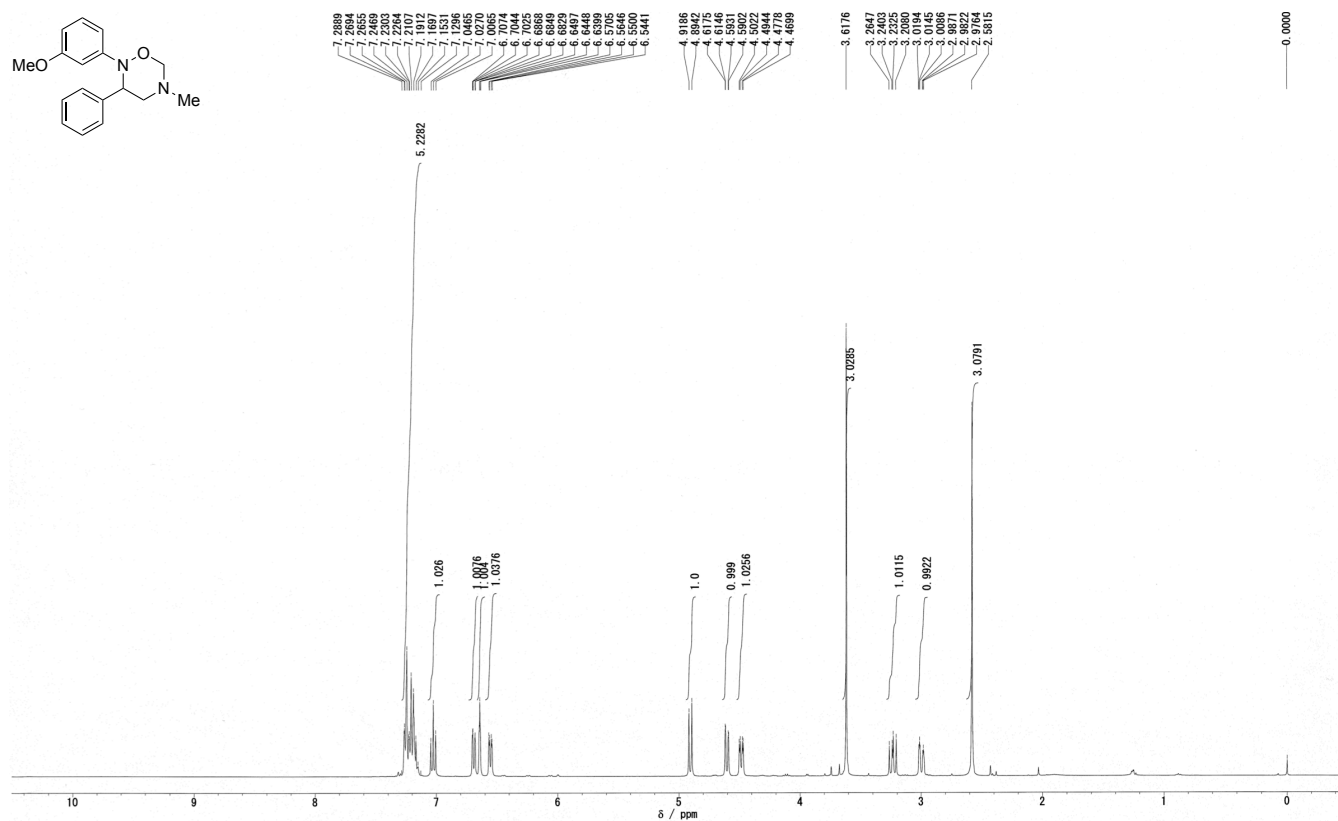
¹H NMR spectrum of (±)-5-methyl-3-phenyl-2-(p-tolyl)-1,2,5-oxadiazinane (**3qa**)



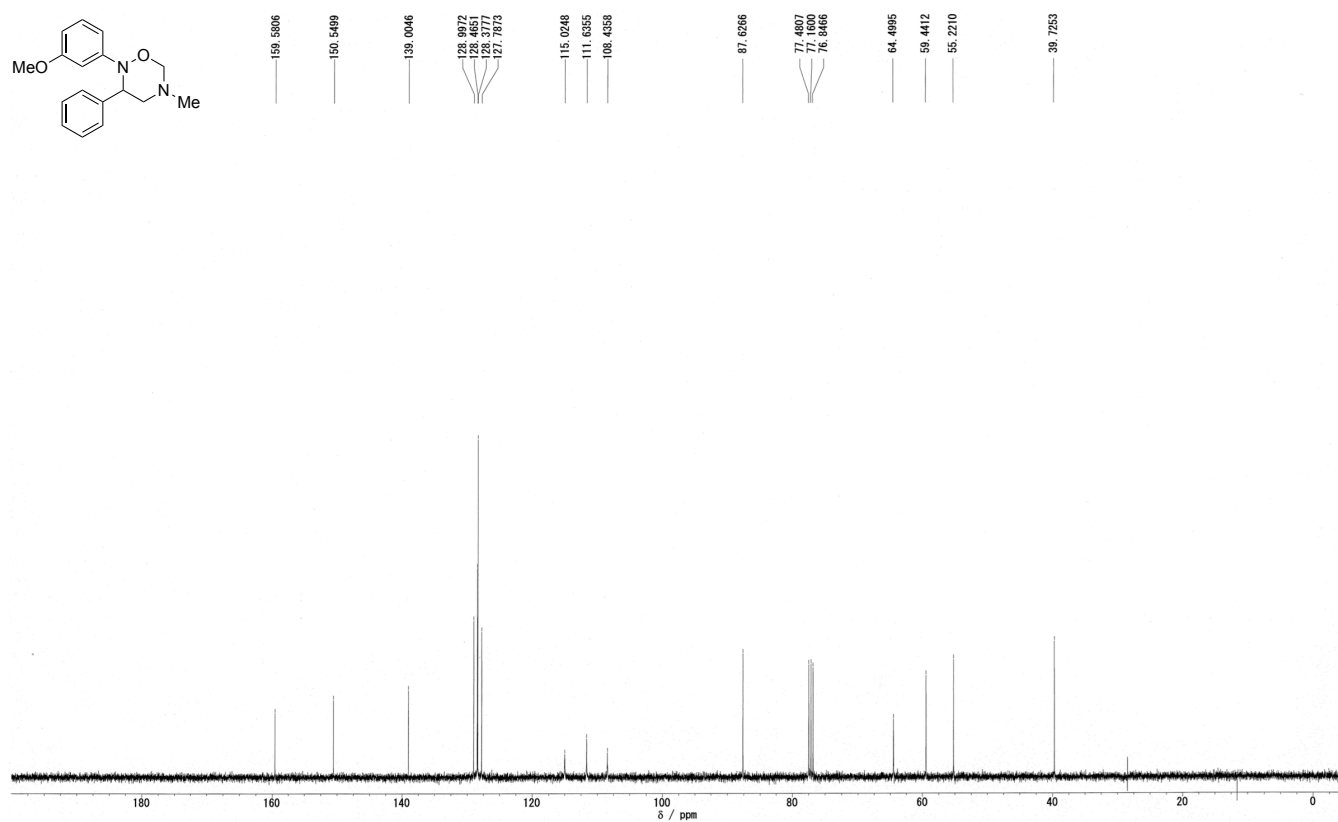
¹³C NMR spectrum of (±)-5-methyl-3-phenyl-2-(p-tolyl)-1,2,5-oxadiazinane (**3qa**)



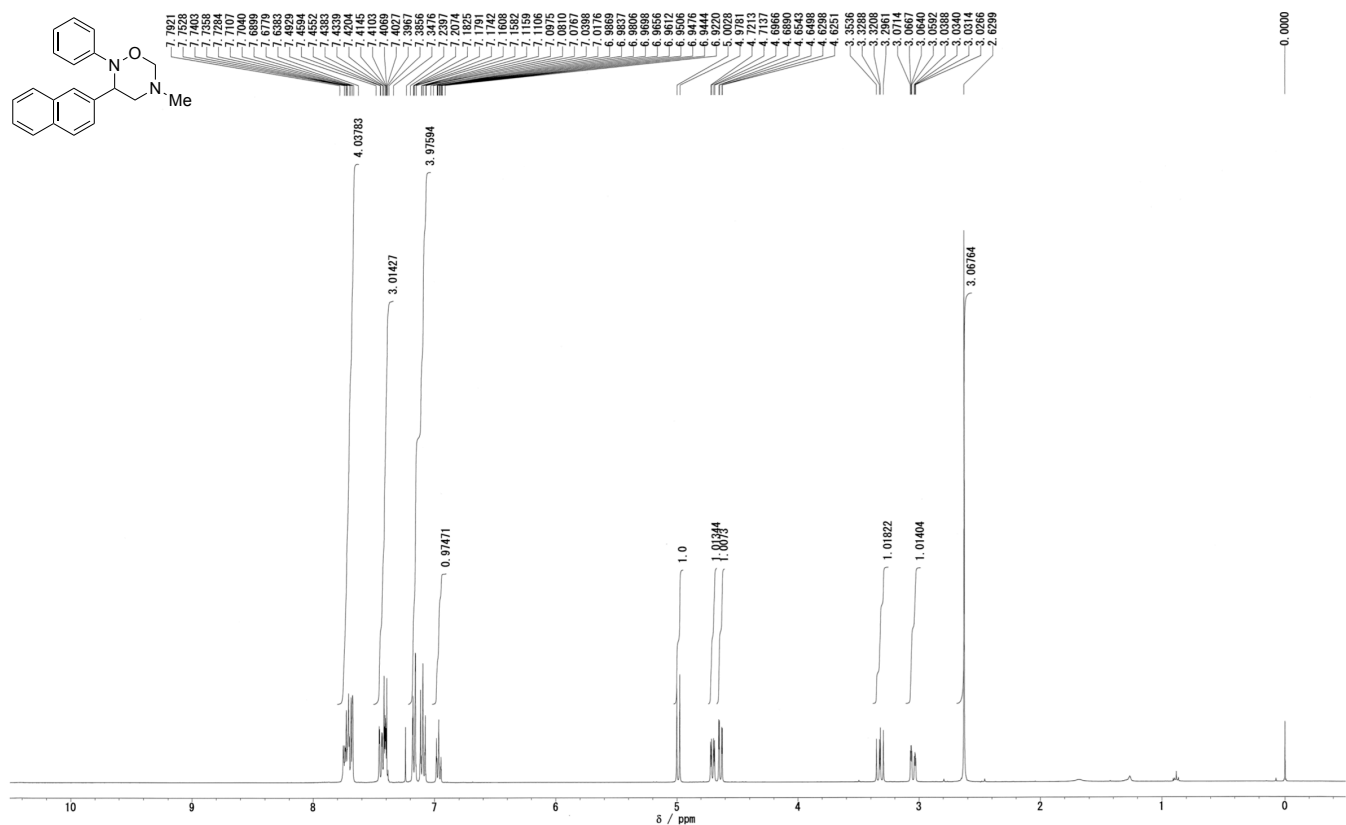
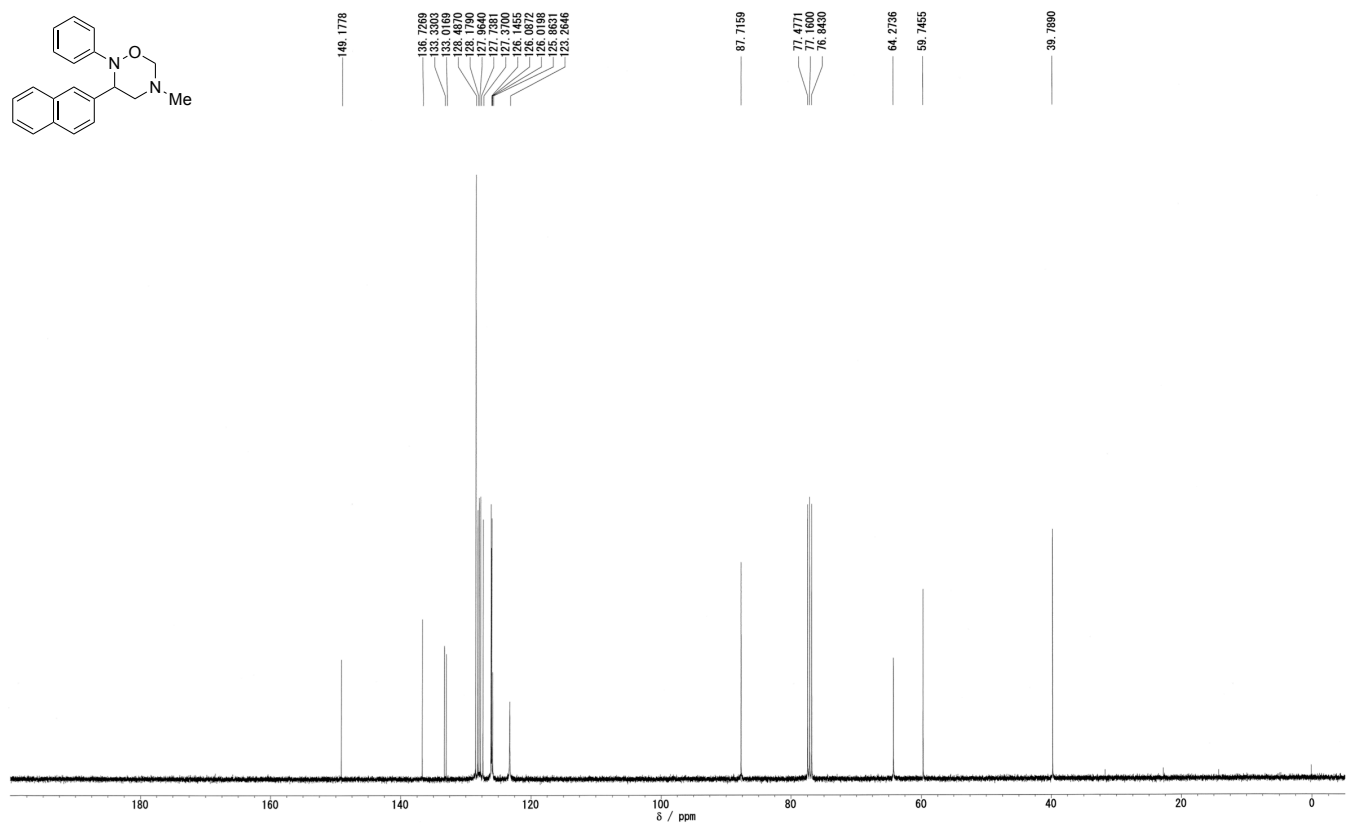
¹H NMR spectrum of (±)-2-(3-methoxyphenyl)-5-methyl-3-phenyl-1,2,5-oxadiazinane (**3ra**)



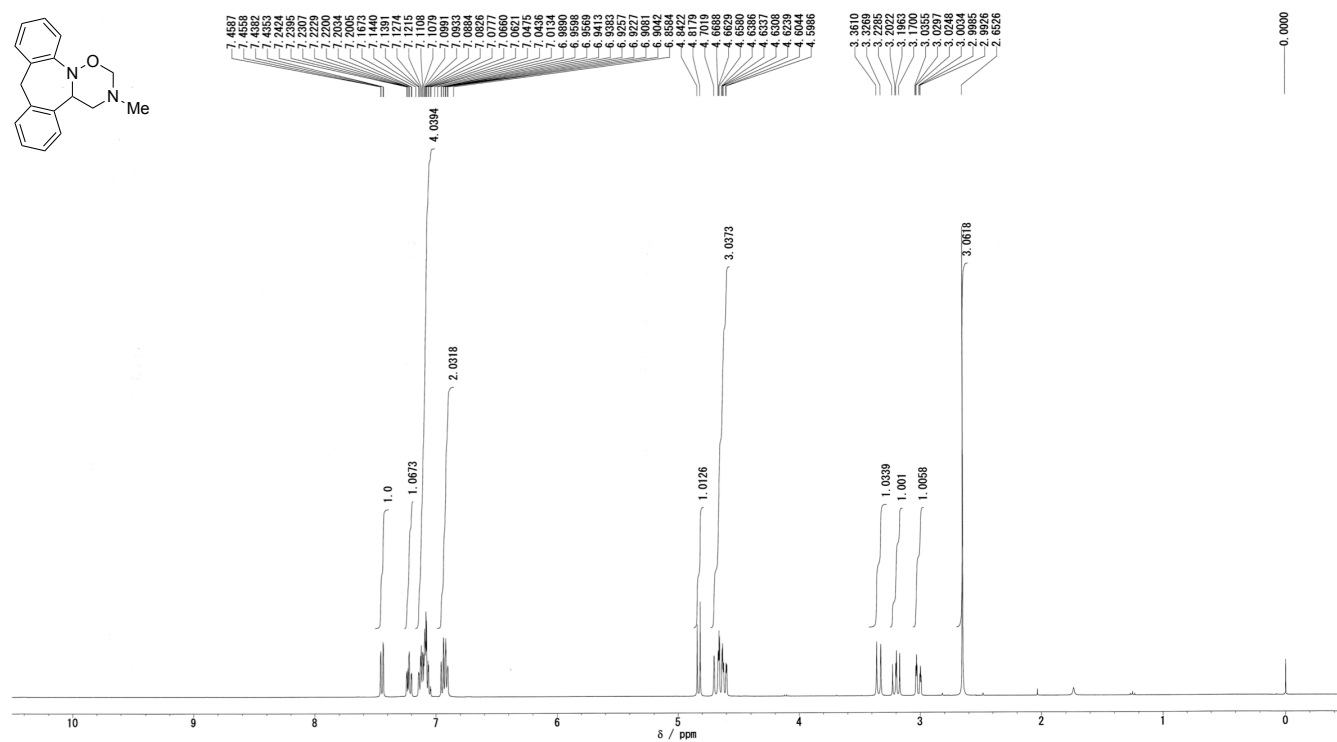
¹³C NMR spectrum of (±)-2-(3-methoxyphenyl)-5-methyl-3-phenyl-1,2,5-oxadiazinane (**3ra**)



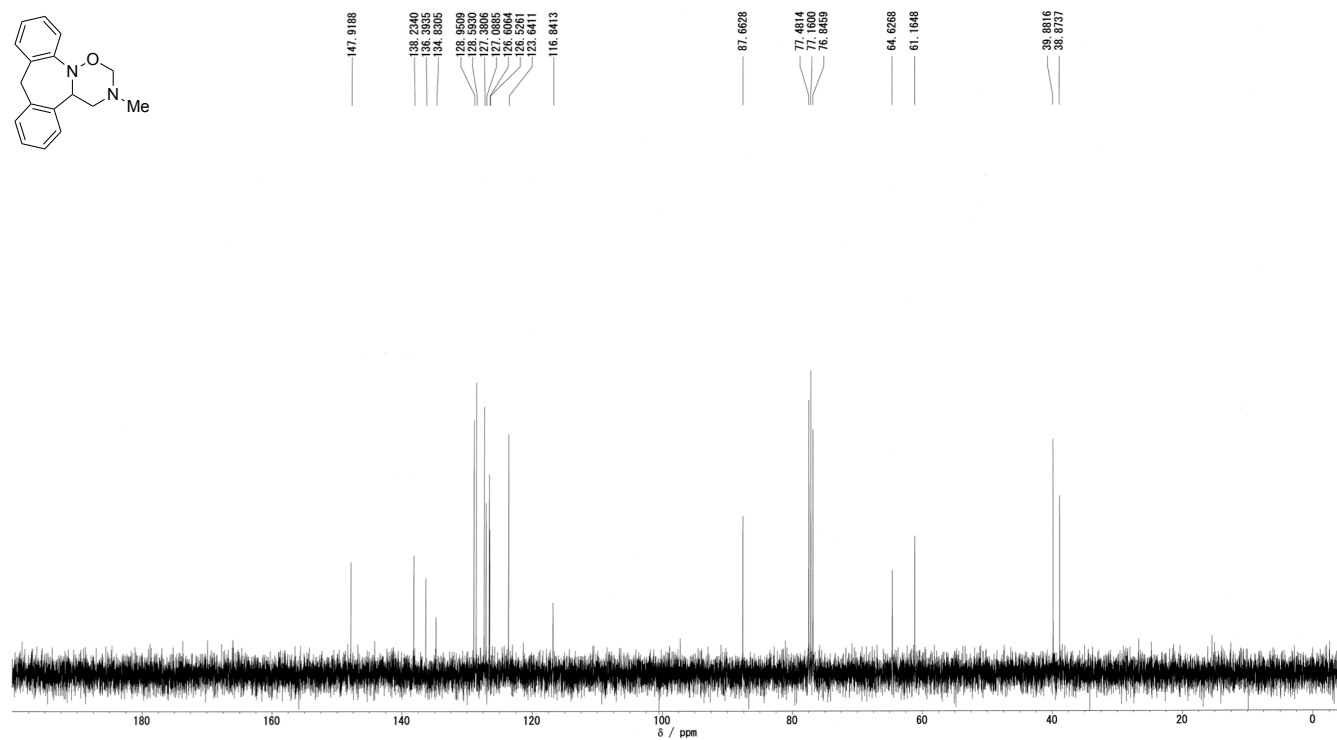
¹H NMR spectrum of (±)-5-methyl-3-(naphthalen-2-yl)-2-phenyl-1,2,5-oxadiazinane (**3sa**)

¹³C NMR spectrum of (±)-5-methyl-3-(naphthalen-2-yl)-2-phenyl-1,2,5-oxadiazinane (**3sa**)

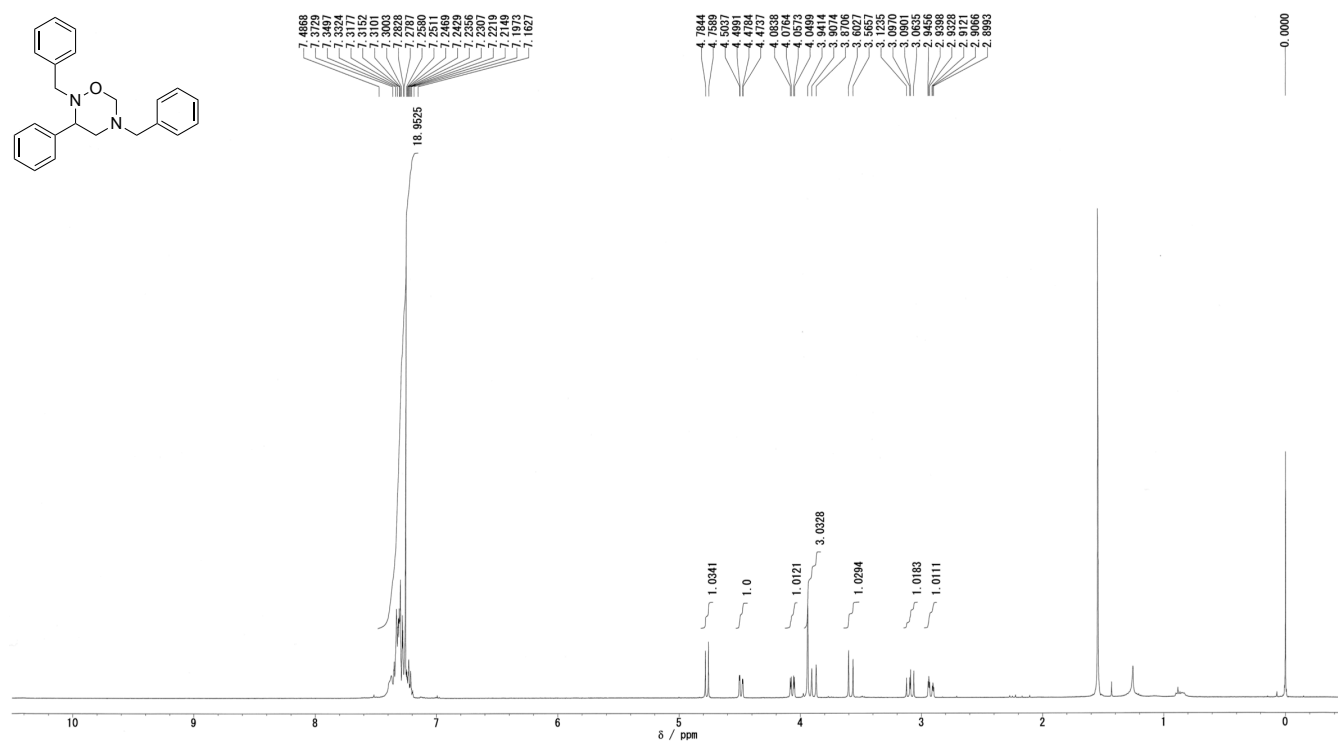
¹H NMR spectrum of (±)-3-methyl-3,4,4a,9-tetrahydro-2H-dibenzo[c,f][1,2,5]oxadiazino[2,3-a]azepine (**3ua**)



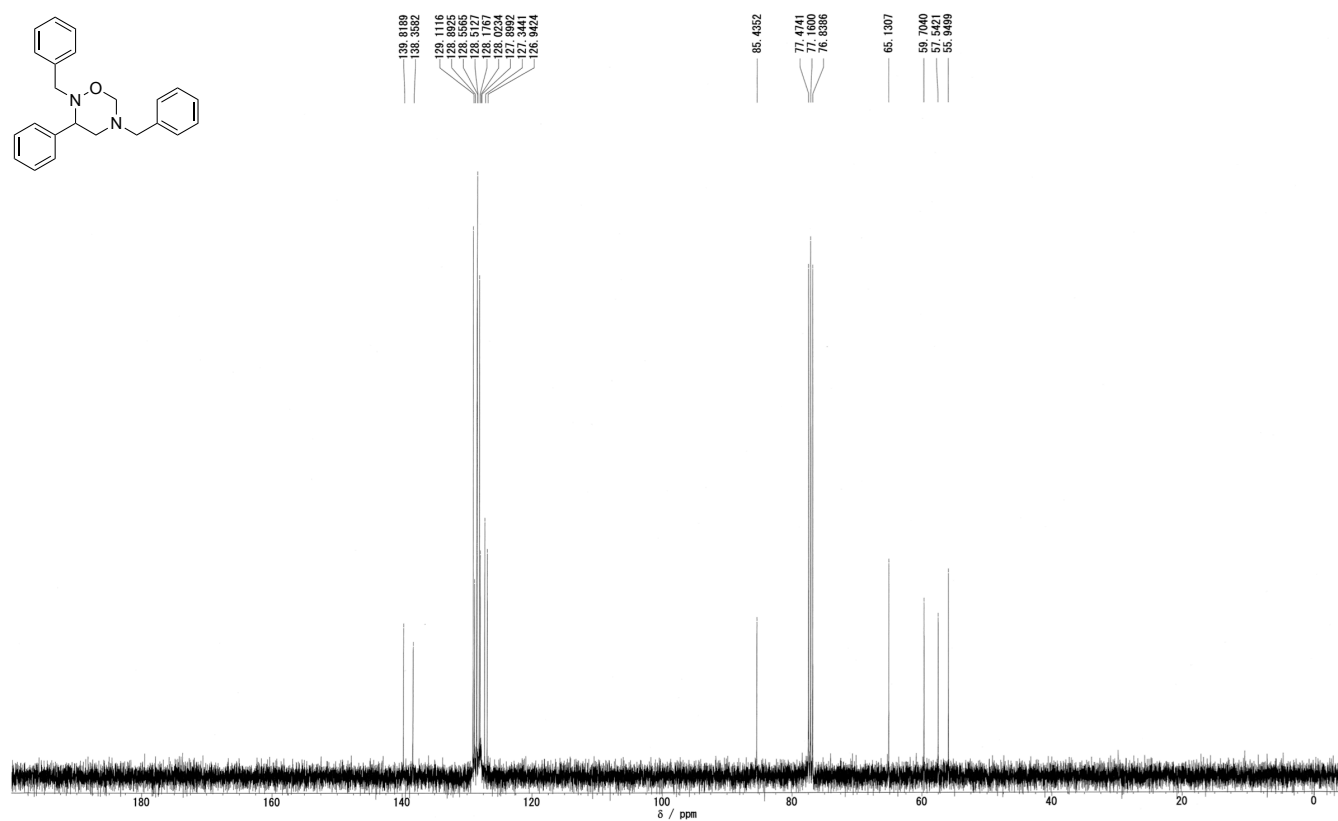
¹³C NMR spectrum of (±)-3-methyl-3,4,4a,9-tetrahydro-2H-dibenzo[c,f][1,2,5]oxadiazino[2,3-a]azepine (**3ua**)



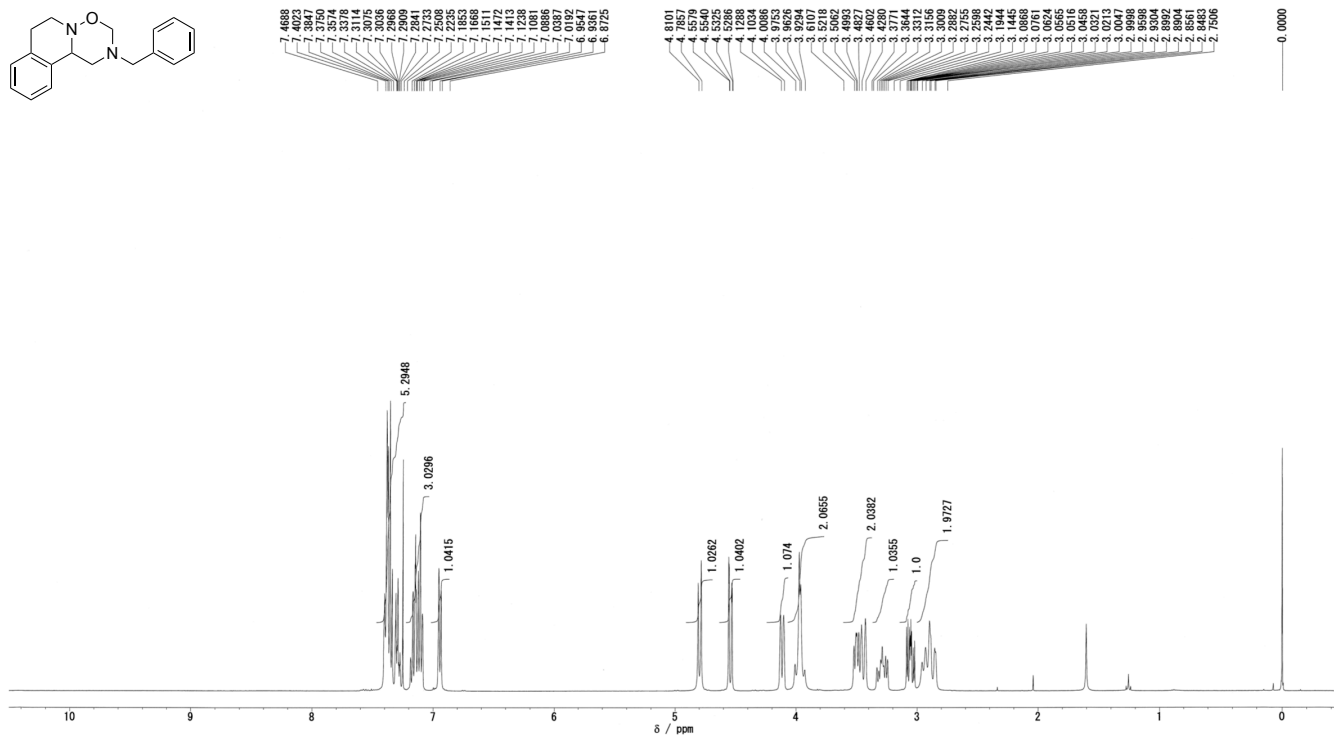
¹H NMR spectrum of (±)-2,5-dibenzyl-3-phenyl-1,2,5-oxadiazinane (**3ab**)



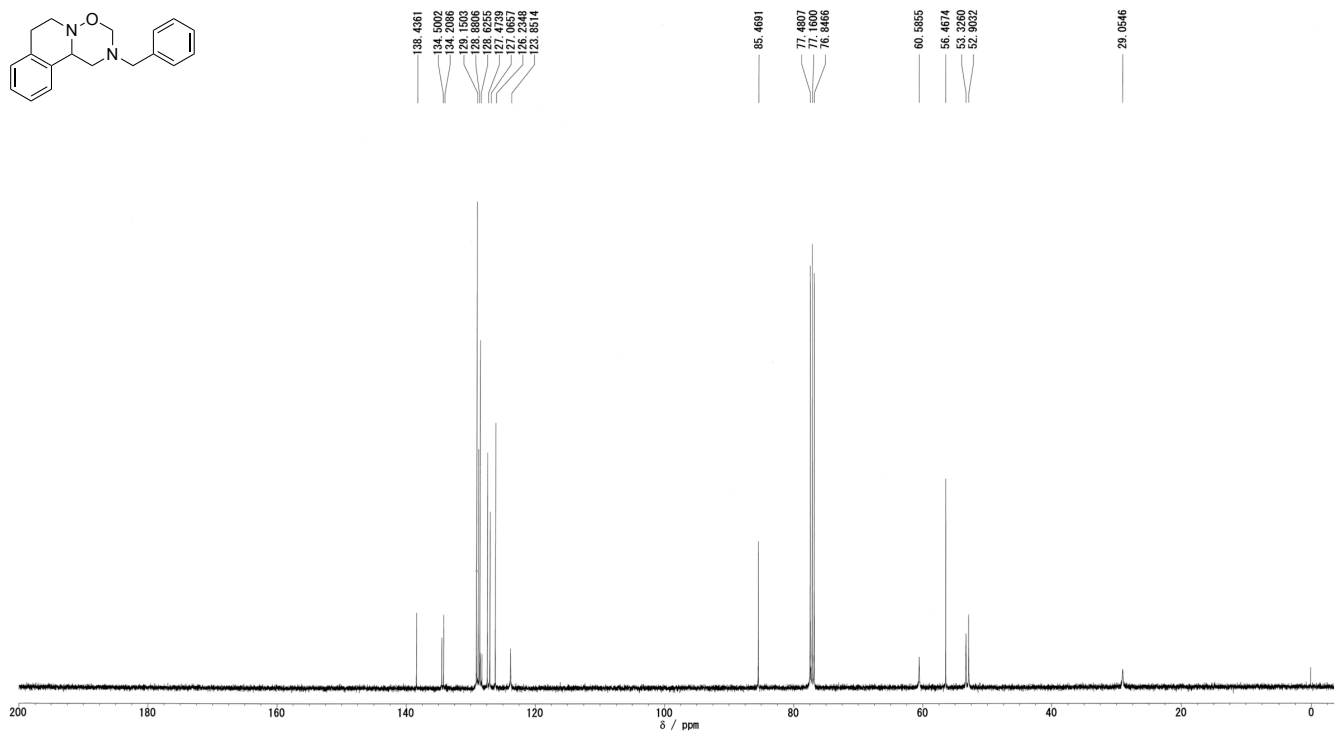
¹³C NMR spectrum of (±)-2,5-dibenzyl-3-phenyl-1,2,5-oxadiazinane (**3ab**)



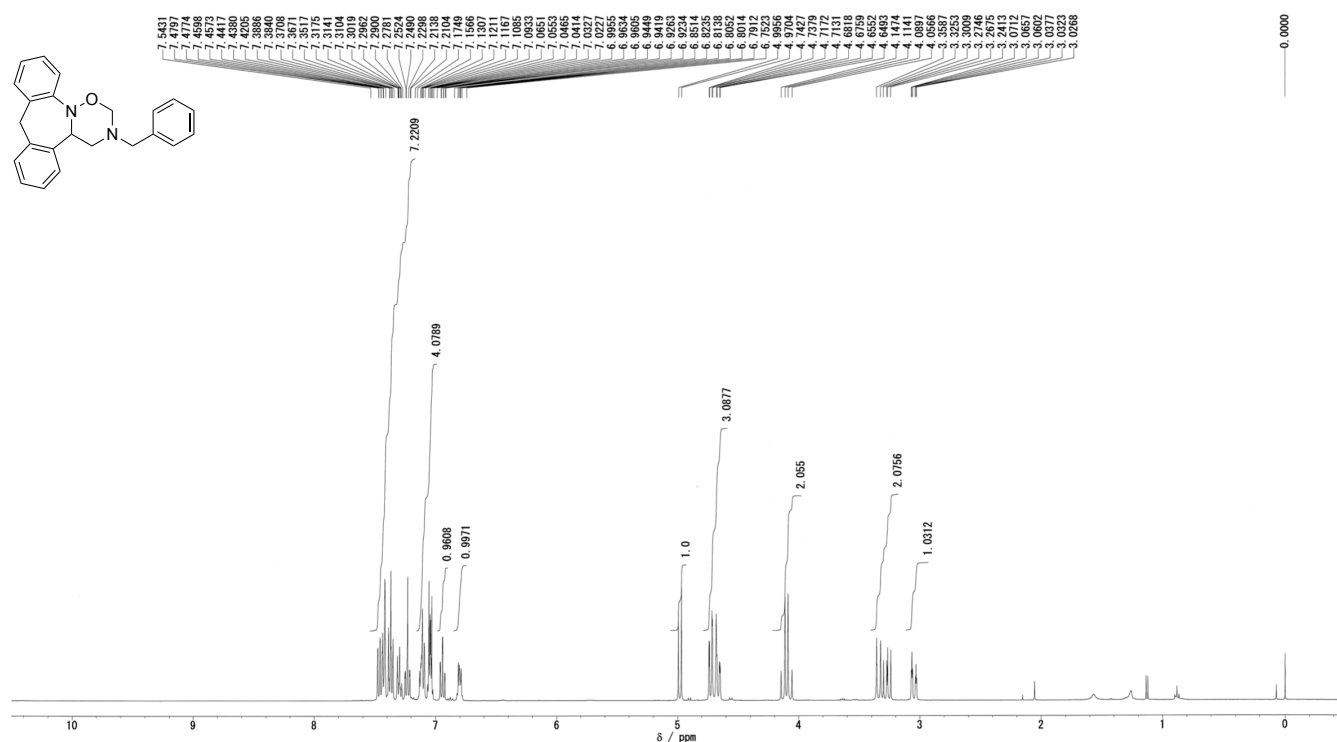
¹H NMR spectrum of (±)-2-benzyl-1,2,3,6,7,11b-hexahydro-[1,2,5]oxadiazino[3,2-a]isoquinoline (**3tb**)



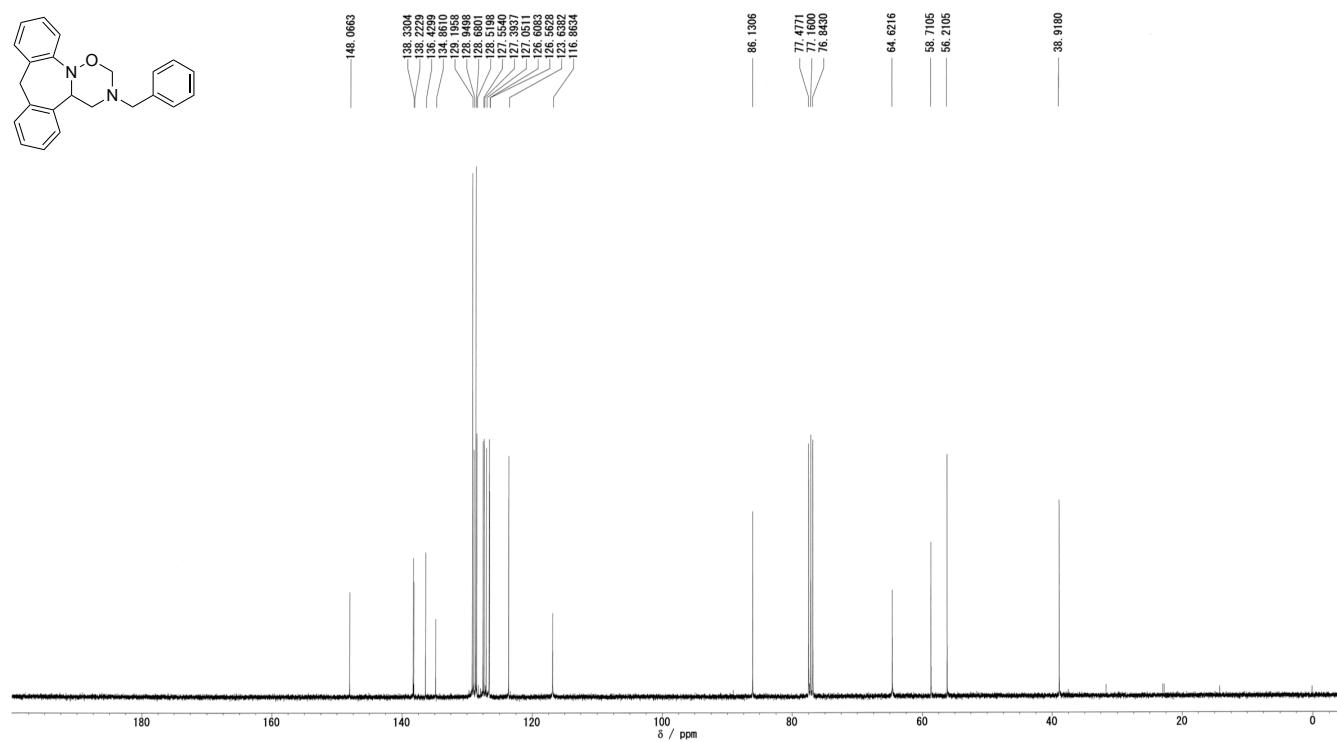
¹³C NMR spectrum of (±)-2-benzyl-1,2,3,6,7,11b-hexahydro-[1,2,5]oxadiazino[3,2-a]isoquinoline (**3tb**)



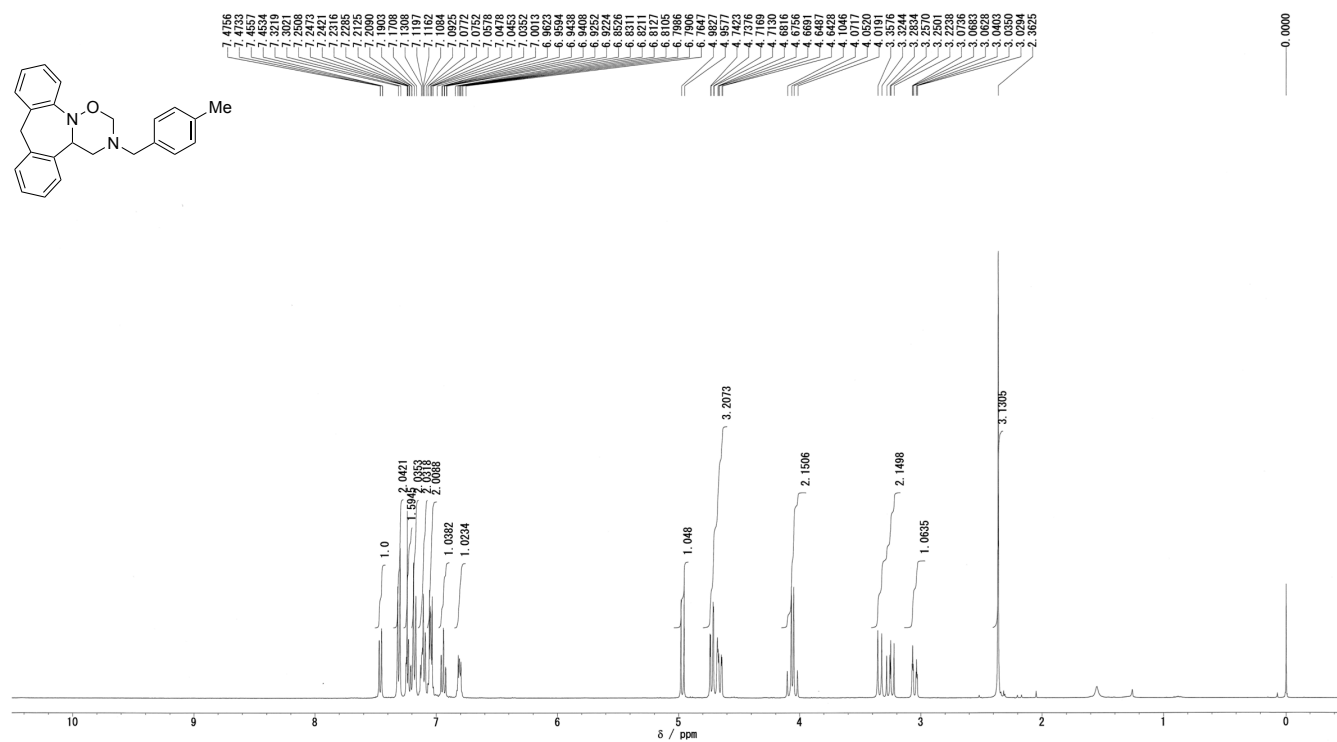
¹H NMR spectrum of (±)-3-benzyl-3,4,4a,9-tetrahydro-2H-dibenzo[c,f][1,2,5]oxadiazino[2,3-a]azepine (**3ub**)



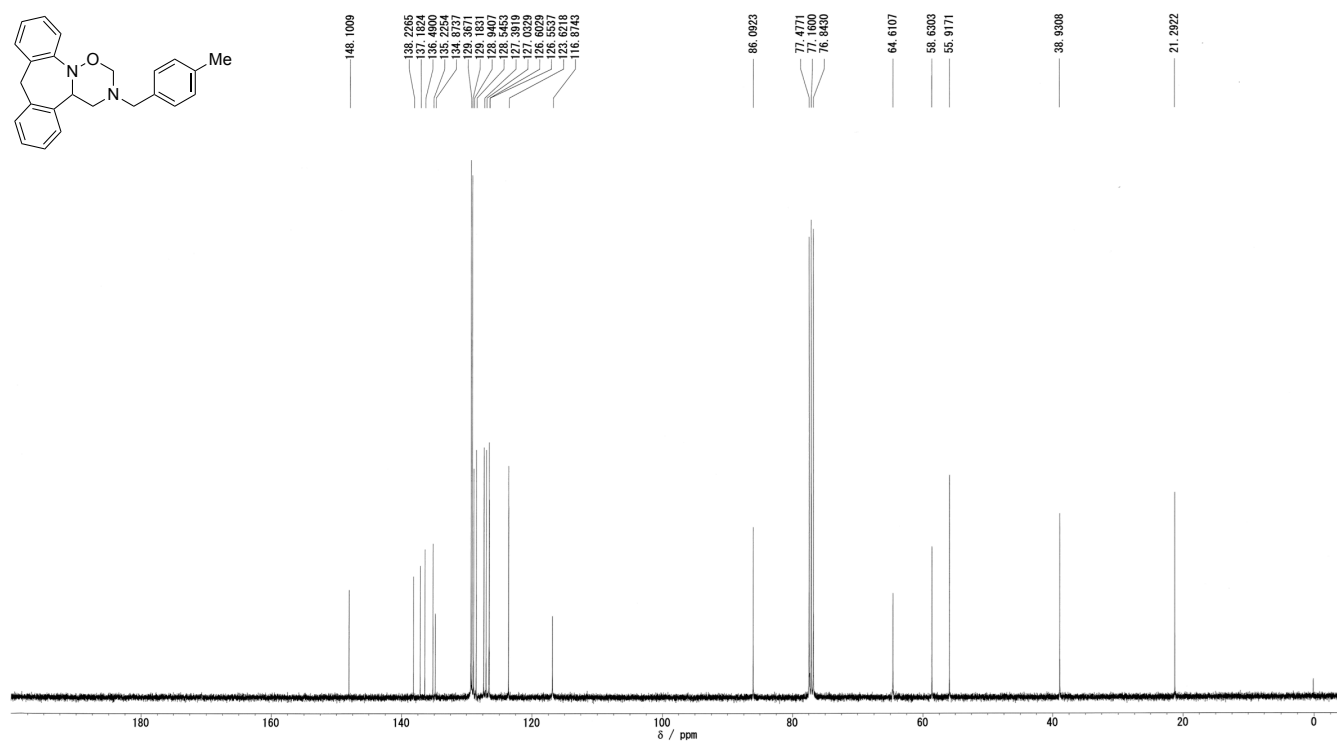
¹³C NMR spectrum of (±)-3-benzyl-3,4,4a,9-tetrahydro-2H-dibenzo[c,f][1,2,5]oxadiazino[2,3-a]azepine (**3ub**)


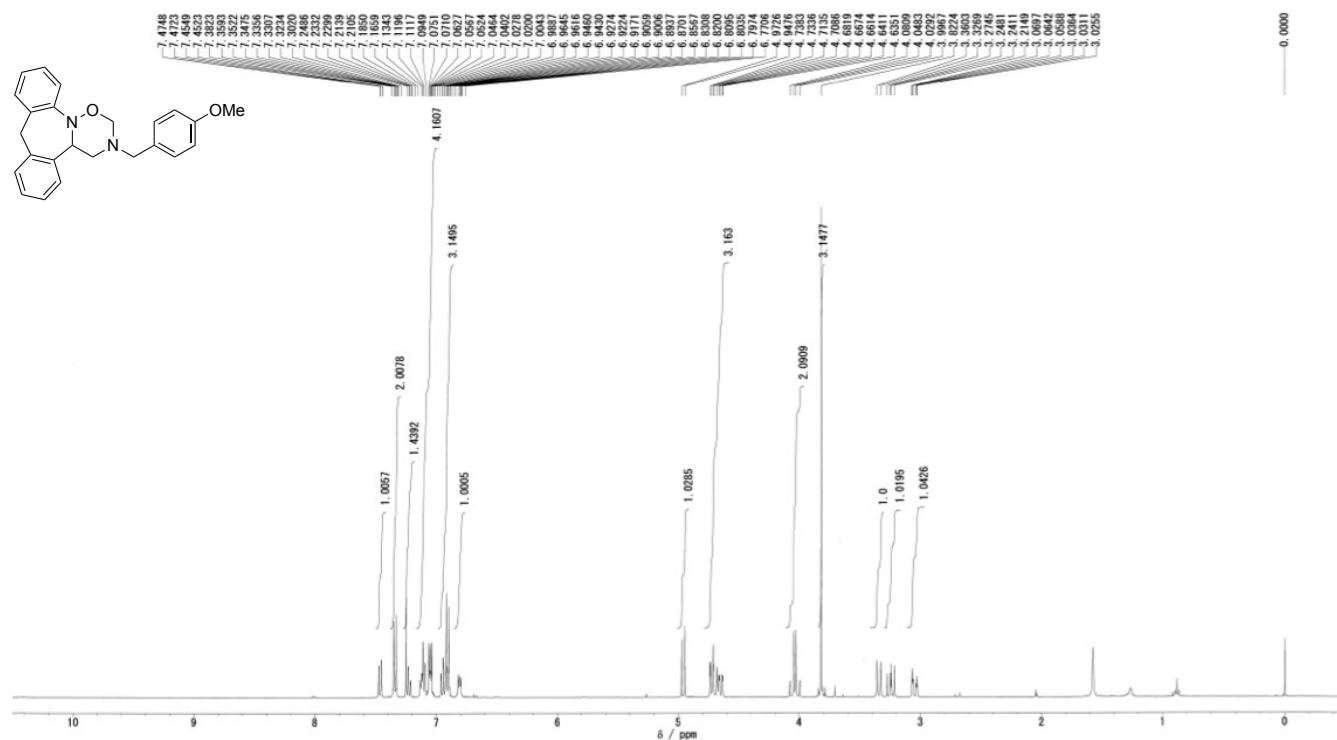
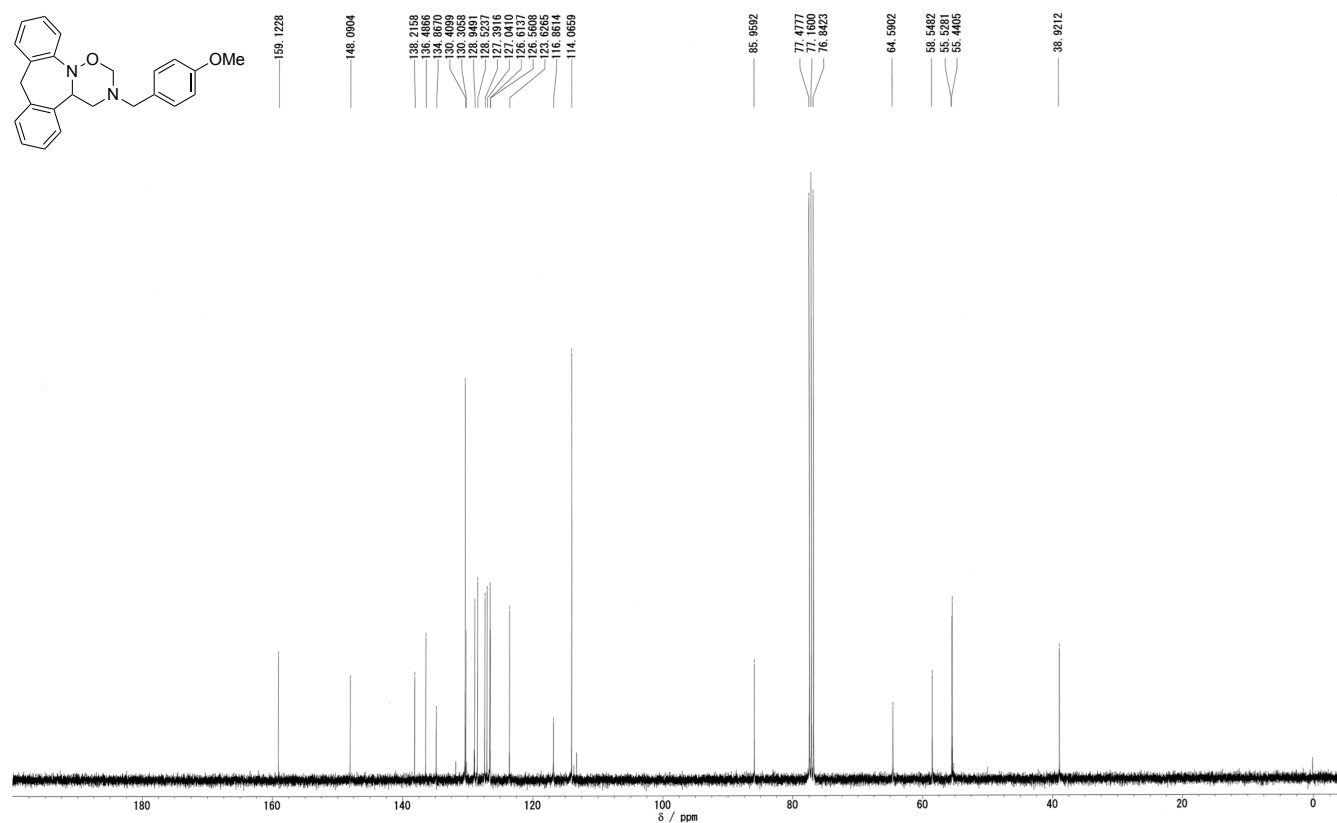


¹H NMR spectrum of (±)-3-(4-methylbenzyl)-3,4,4a,9-tetrahydro-2H-dibenzo[c,f][1,2,5]oxadiazino[2,3-a]azepine (**3uc**)

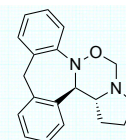
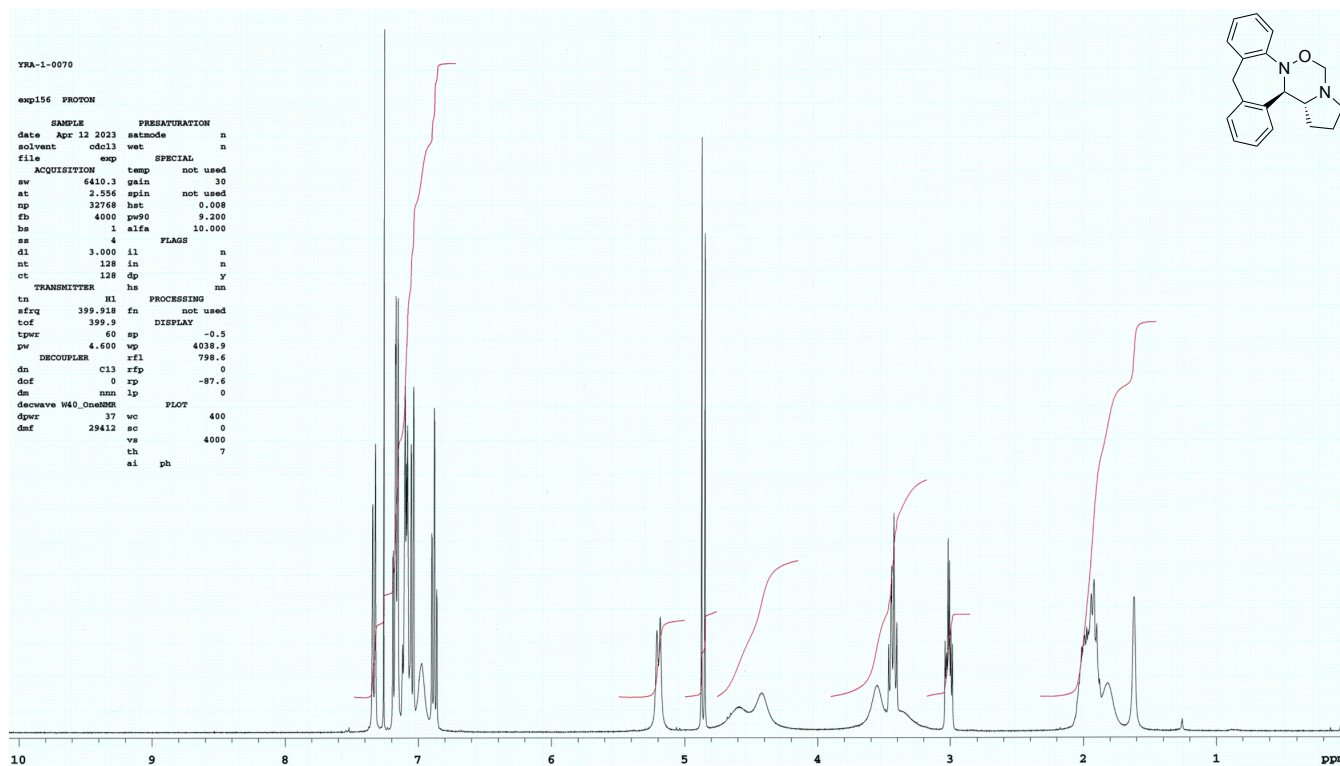


¹³C NMR spectrum of (±)-3-(4-methylbenzyl)-3,4,4a,9-tetrahydro-2H-dibenzo[c,f][1,2,5]oxadiazino[2,3-a]azepine (**3uc**)

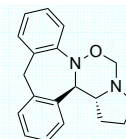
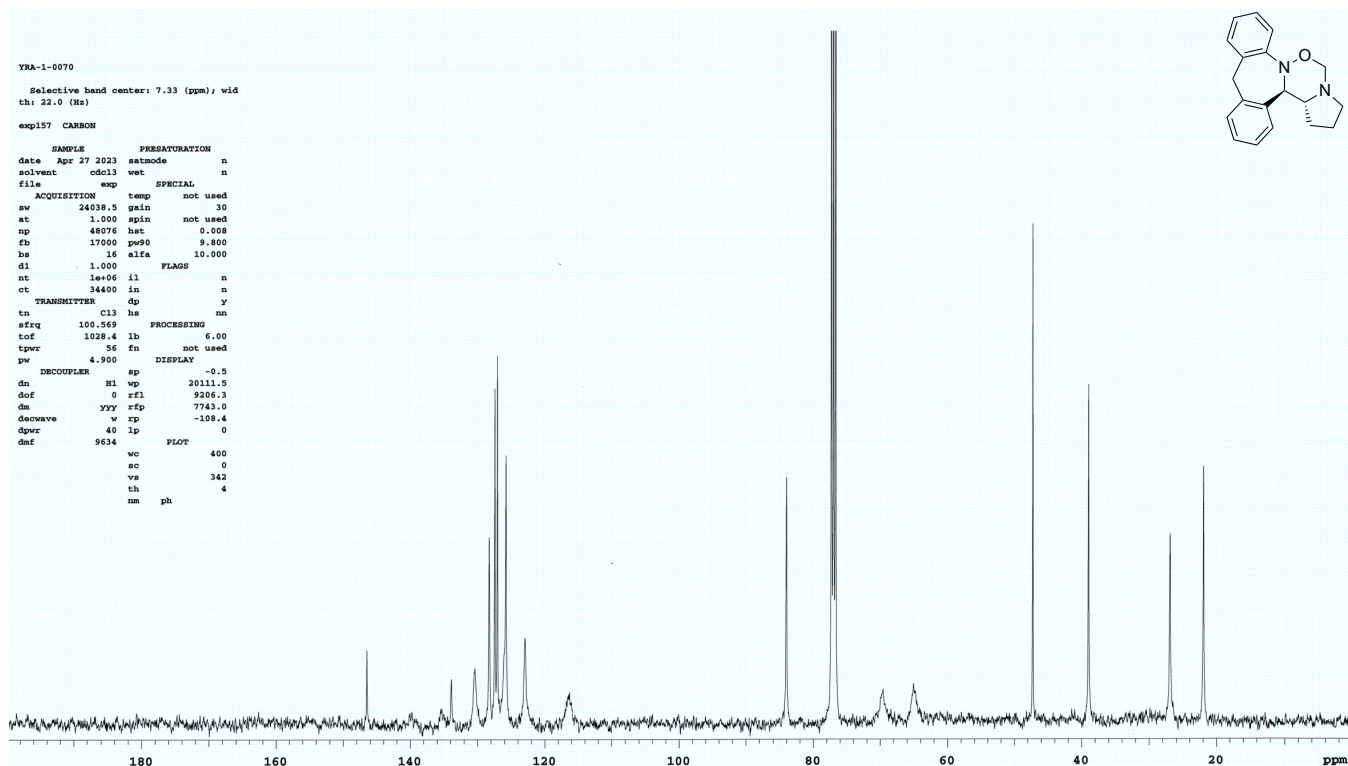



COc1ccc(cc1)CN2CCOc3c2ccc4ccccc34COc1ccc(cc1)CN2CC3C4C5C6C7C8C9C10C11C12C13C14C15C16C17C18C19C20C21C22C23C24C25C26C27C28C29C30C31C32C33C34C35C36C37C38C39C40C41C42C43C44C45C46C47C48C49C50C51C52C53C54C55C56C57C58C59C60C61C62C63C64C65C66C67C68C69C70C71C72C73C74C75C76C77C78C79C80C81C82C83C84C85C86C87C88C89C90C91C92C93C94C95C96C97C98C99C100C101C102C103C104C105C106C107C108C109C110C111C112C113C114C115C116C117C118C119C120C121C122C123C124C125C126C127C128C129C130C131C132C133C134C135C136C137C138C139C140C141C142C143C144C145C146C147C148C149C150C151C152C153C154C155C156C157C158C159C160C161C162C163C164C165C166C167C168C169C170C171C172C173C174C175C176C177C178C179C180C181C182C183C184C185C186C187C188C189C190C191C192C193C194C195C196C197C198C199C200C201C202C203C204C205C206C207C208C209C210C211C212C213C214C215C216C217C218C219C220C221C222C223C224C225C226C227C228C229C230C231C232C233C234C235C236C237C238C239C240C241C242C243C244C245C246C247C248C249C250C251C252C253C254C255C256C257C258C259C260C261C262C263C264C265C266C267C268C269C270C271C272C273C274C275C276C277C278C279C280C281C282C283C284C285C286C287C288C289C290C291C292C293C294C295C296C297C298C299C300C301C302C303C304C305C306C307C308C309C310C311C312C313C314C315C316C317C318C319C320C321C322C323C324C325C326C327C328C329C330C331C332C333C334C335C336C337C338C339C340C341C342C343C344C345C346C347C348C349C350C351C352C353C354C355C356C357C358C359C360C361C362C363C364C365C366C367C368C369C370C371C372C373C374C375C376C377C378C379C380C381C382C383C384C385C386C387C388C389C390C391C392C393C394C395C396C397C398C399C400C401C402C403C404C405C406C407C408C409C410C411C412C413C414C415C416C417C418C419C420C421C422C423C424C425C426C427C428C429C430C431C432C433C434C435C436C437C438C439C440C441C442C443C444C445C446C447C448C449C450C451C452C453C454C455C456C457C458C459C460C461C462C463C464C465C466C467C468C469C470C471C472C473C474C475C476C477C478C479C480C481C482C483C484C485C486C487C488C489C490C491C492C493C494C495C496C497C498C499C500C501C502C503C504C505C506C507C508C509C510C511C512C513C514C515C516C517C518C519C520C521C522C523C524C525C526C527C528C529C530C531C532C533C534C535C536C537C538C539C540C541C542C543C544C545C546C547C548C549C550C551C552C553C554C555C556C557C558C559C560C561C562C563C564C565C566C567C568C569C570C571C572C573C574C575C576C577C578C579C580C581C582C583C584C585C586C587C588C589C590C591C592C593C594C595C596C597C598C599C600C601C602C603C604C605C606C607C608C609C610C611C612C613C614C615C616C617C618C619C620C621C622C623C624C625C626C627C628C629C630C631C632C633C634C635C636C637C638C639C640C641C642C643C644C645C646C647C648C649C650C651C652C653C654C655C656C657C658C659C660C661C662C663C664C665C666C667C668C669C670C671C672C673C674C675C676C677C678C679C680C681C682C683C684C685C686C687C688C689C690C691C692C693C694C695C696C697C698C699C700C701C702C703C704C705C706C707C708C709C710C711C712C713C714C715C716C717C718C719C720C721C722C723C724C725C726C727C728C729C730C731C732C733C734C735C736C737C738C739C740C741C742C743C744C745C746C747C748C749C750C751C752C753C754C755C756C757C758C759C760C761C762C763C764C765C766C767C768C769C770C771C772C773C774C775C776C777C778C779C780C781C782C783C784C785C786C787C788C789C790C791C792C793C794C795C796C797C798C799C800C801C802C803C804C805C806C807C808C809C810C811C812C813C814C815C816C817C818C819C820C821C822C823C824C825C826C827C828C829C830C831C832C833C834C835C836C837C838C839C840C841C842C843C844C845C846C847C848C849C850C851C852C853C854C855C856C857C858C859C860C861C862C863C864C865C866C867C868C869C870C871C872C873C874C875C876C877C878C879C880C881C882C883C884C885C886C887C888C889C890C891C892C893C894C895C896C897C898C899C900C901C902C903C904C905C906C907C908C909C910C911C912C913C914C915C916C917C918C919C920C921C922C923C924C925C926C927C928C929C930C931C932C933C934C935C936C937C938C939C940C941C942C943C944C945C946C947C948C949C950C951C952C953C954C955C956C957C958C959C960C961C962C963C964C965C966C967C968C969C970C971C972C973C974C975C976C977C978C979C980C981C982C983C984C985C986C987C988C989C990C991C992C993C994C995C996C997C998C999

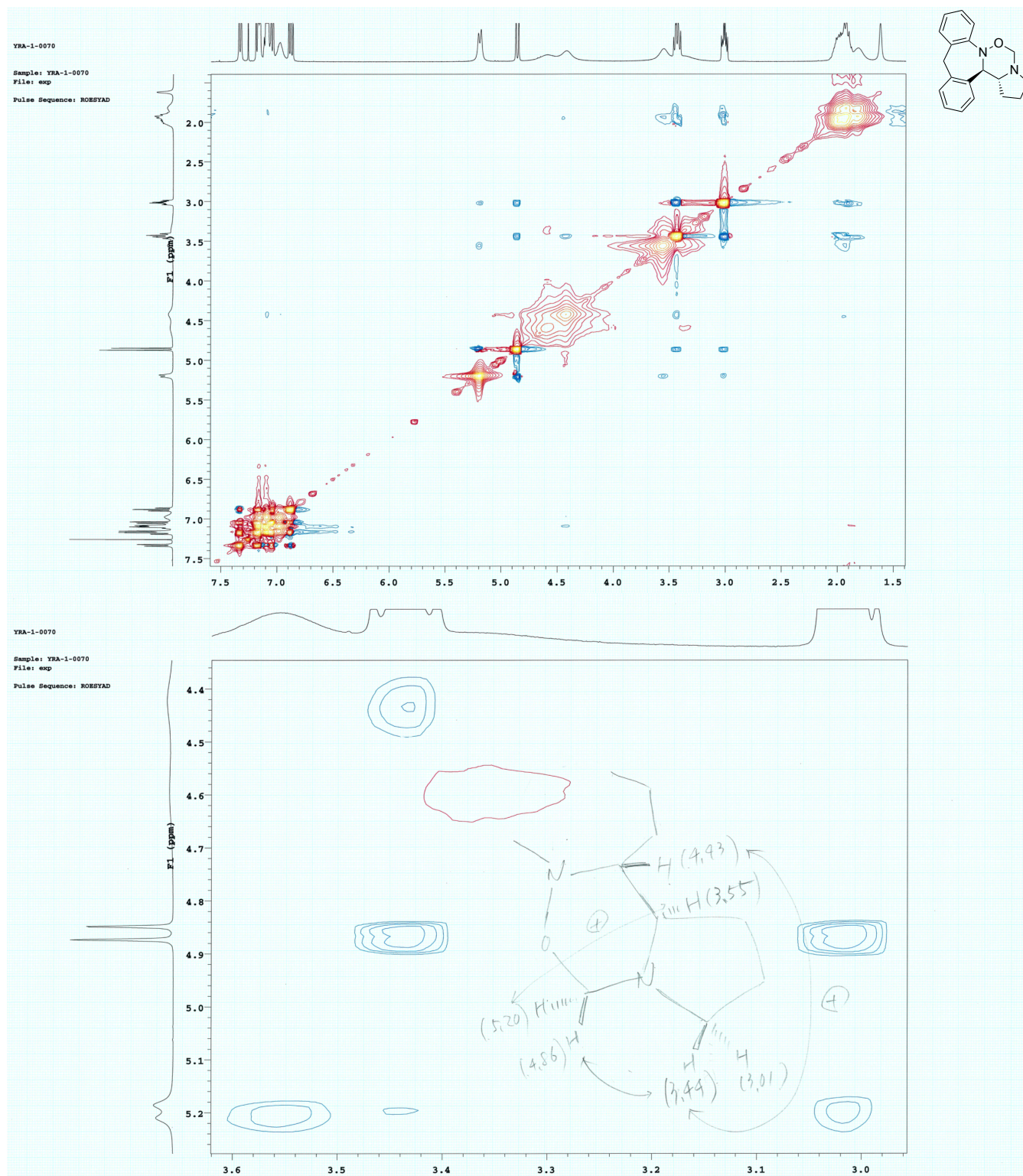
¹H NMR spectrum of (±)-1,2,3,3a,3b,8-hexahydro-15*H*-dibenzo[*c,f*]pyrrolo[2',1':4,5][1,2,5]oxadiazino[2,3-*a*]azepine (**3ue**)

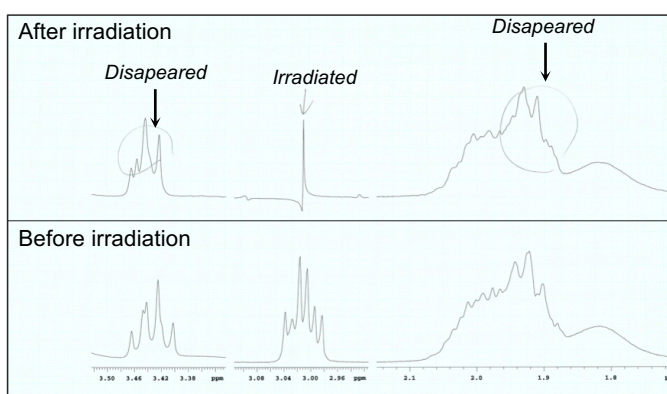
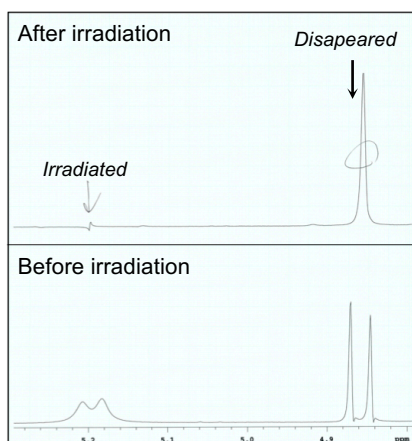
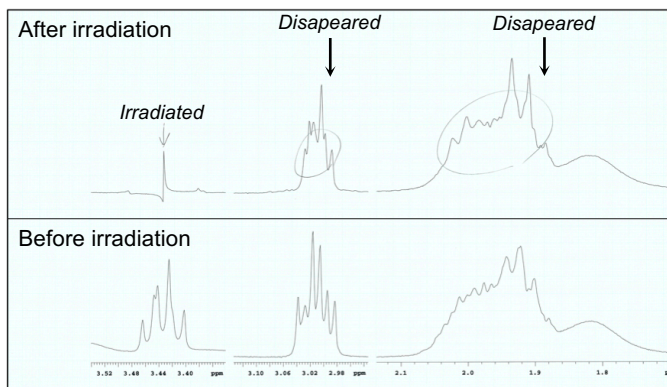
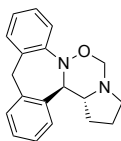


¹³C NMR spectrum of (±)-1,2,3,3a,3b,8-hexahydro-15*H*-dibenzo[*c,f*]pyrrolo[2',1':4,5][1,2,5]oxadiazino[2,3-*a*]azepine (**3ue**)

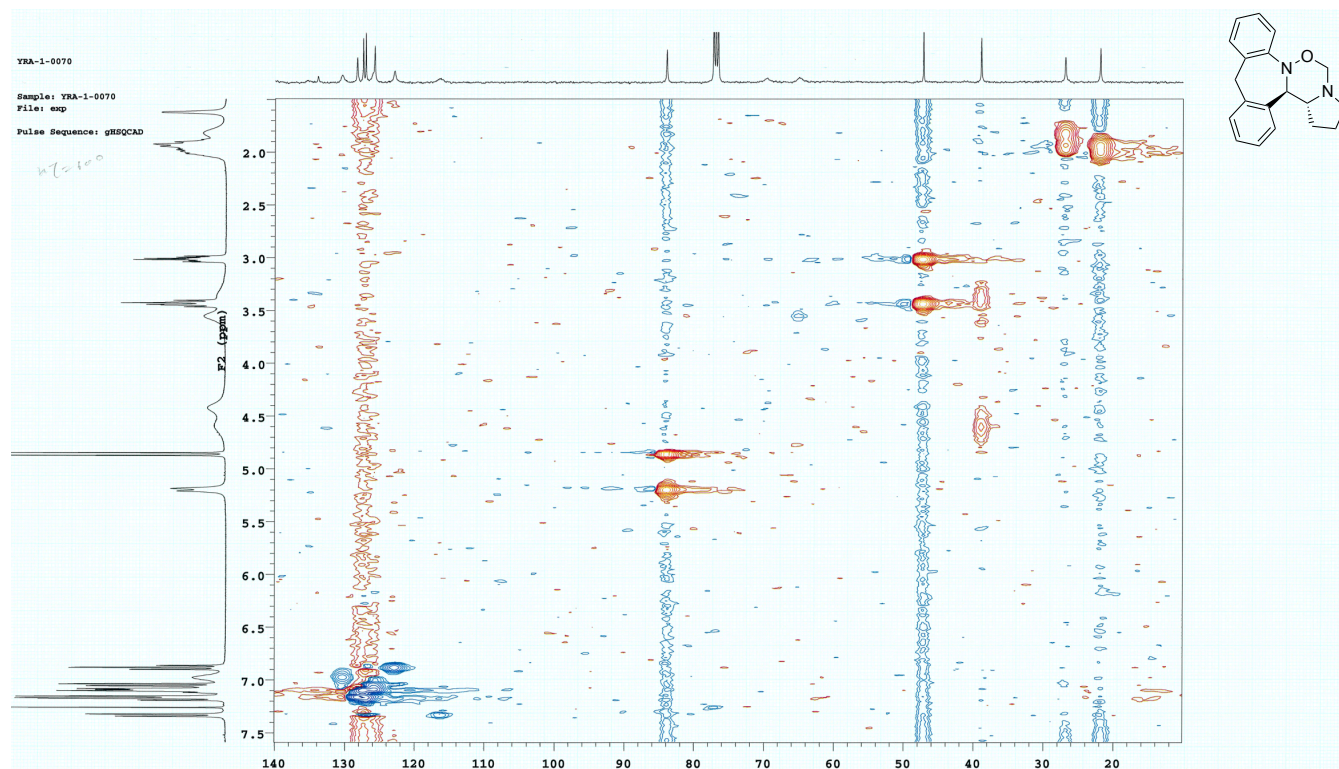


^1H - ^1H ROESY spectrum of (\pm)-1,2,3,3a,3b,8-hexahydro-15*H*-dibenzo[*c,f*]pyrrolo[2',1':4,5][1,2,5]oxadiazino[2,3-*a*]azepine (**3ue**)

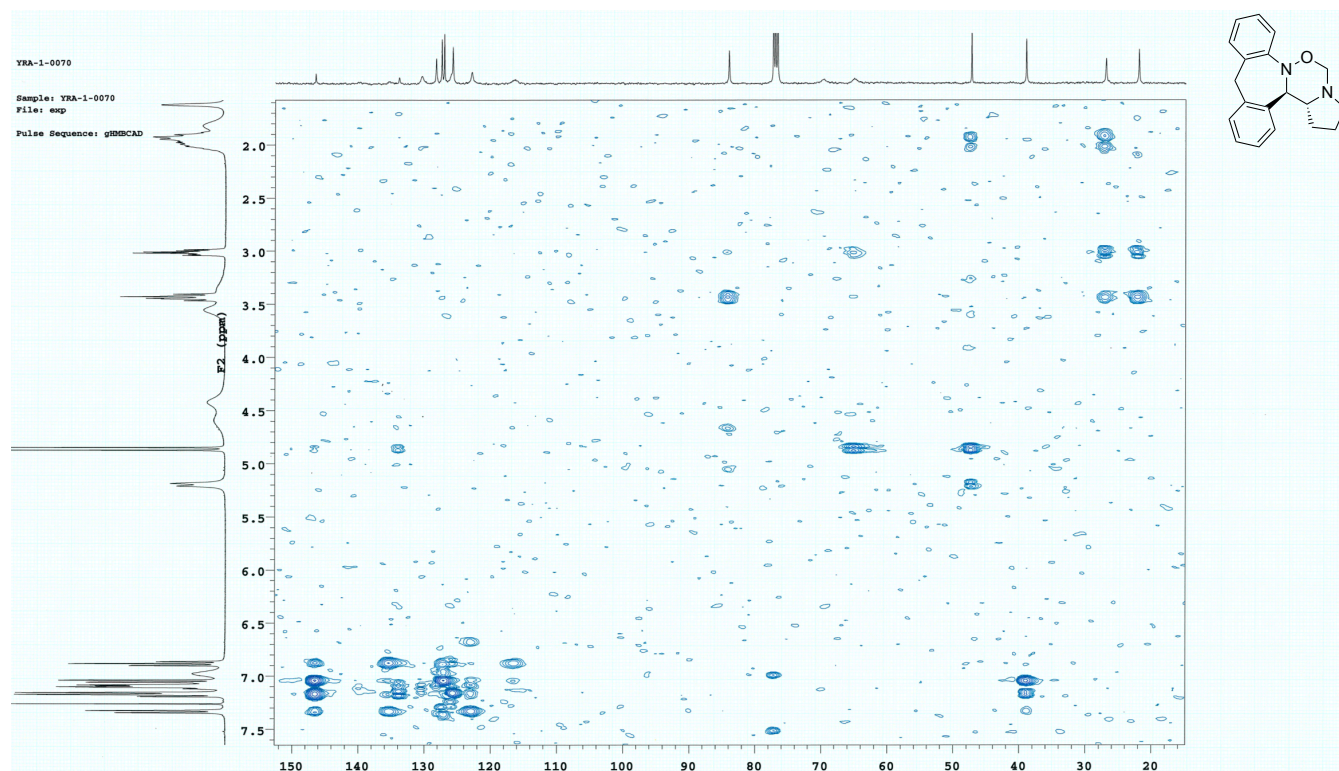




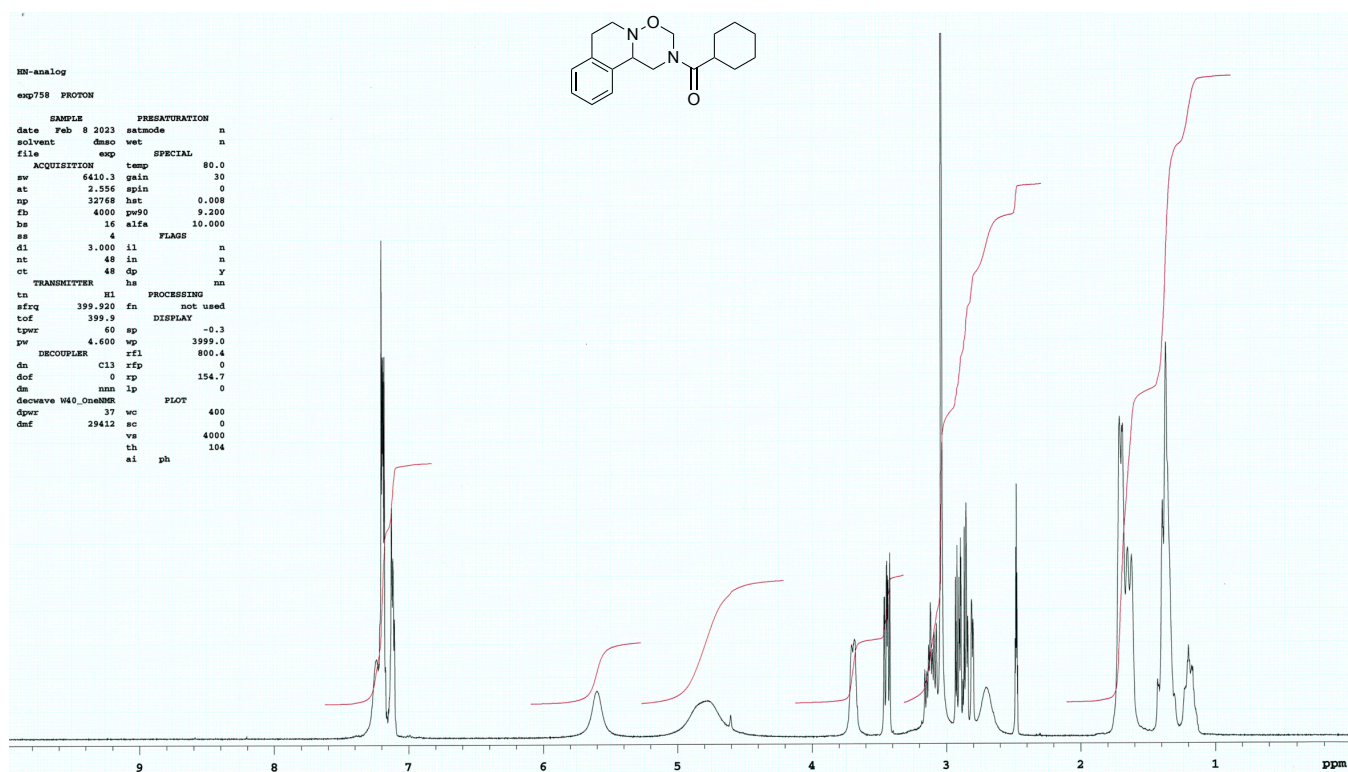
HSQC spectrum of (±)-1,2,3,3a,3b,8-hexahydro-15*H*-dibenzo[*c,f*]pyrrolo[2',1':4,5][1,2,5]oxadiazino[2,3-*a*]azepine (**3ue**)



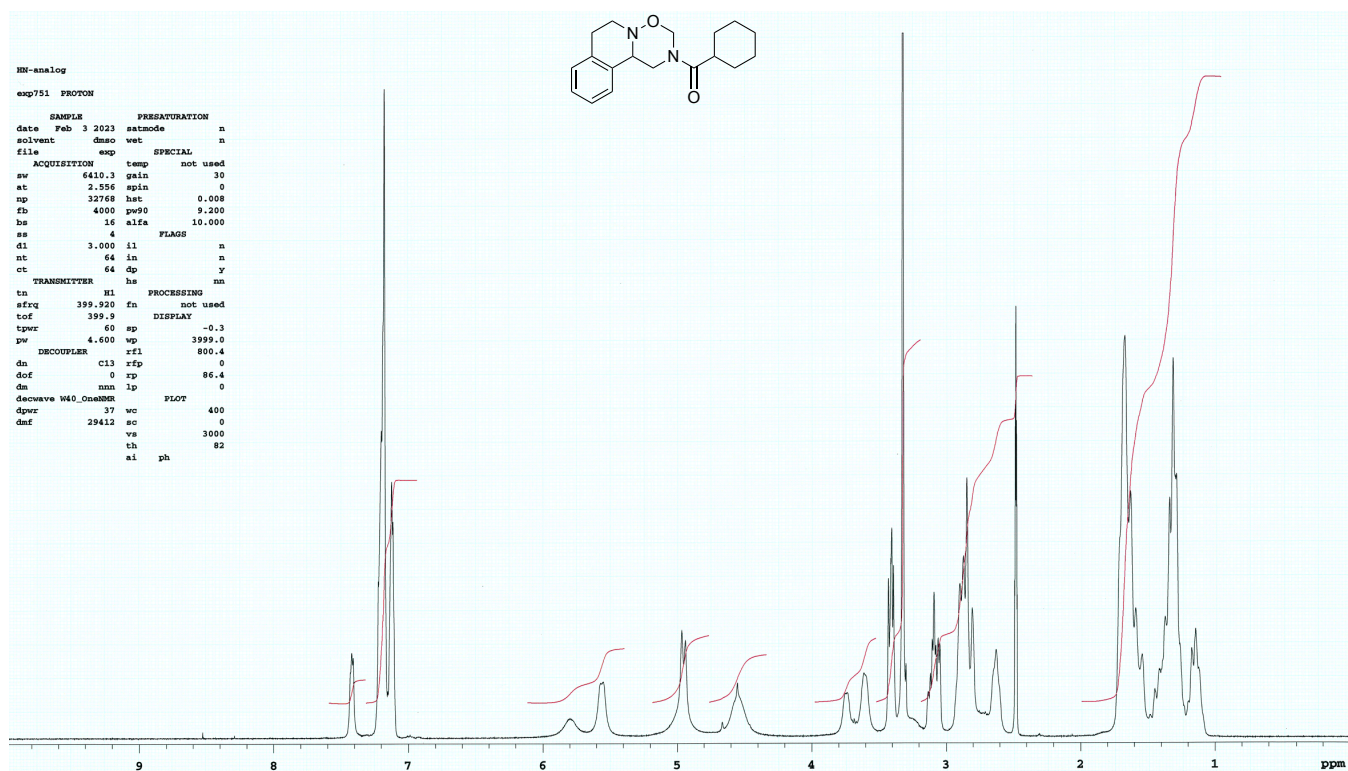
HMBC spectrum of (±)-1,2,3,3a,3b,8-hexahydro-15*H*-dibenzo[*c,f*]pyrrolo[2',1':4,5][1,2,5]oxadiazino[2,3-*a*]azepine (**3ue**)



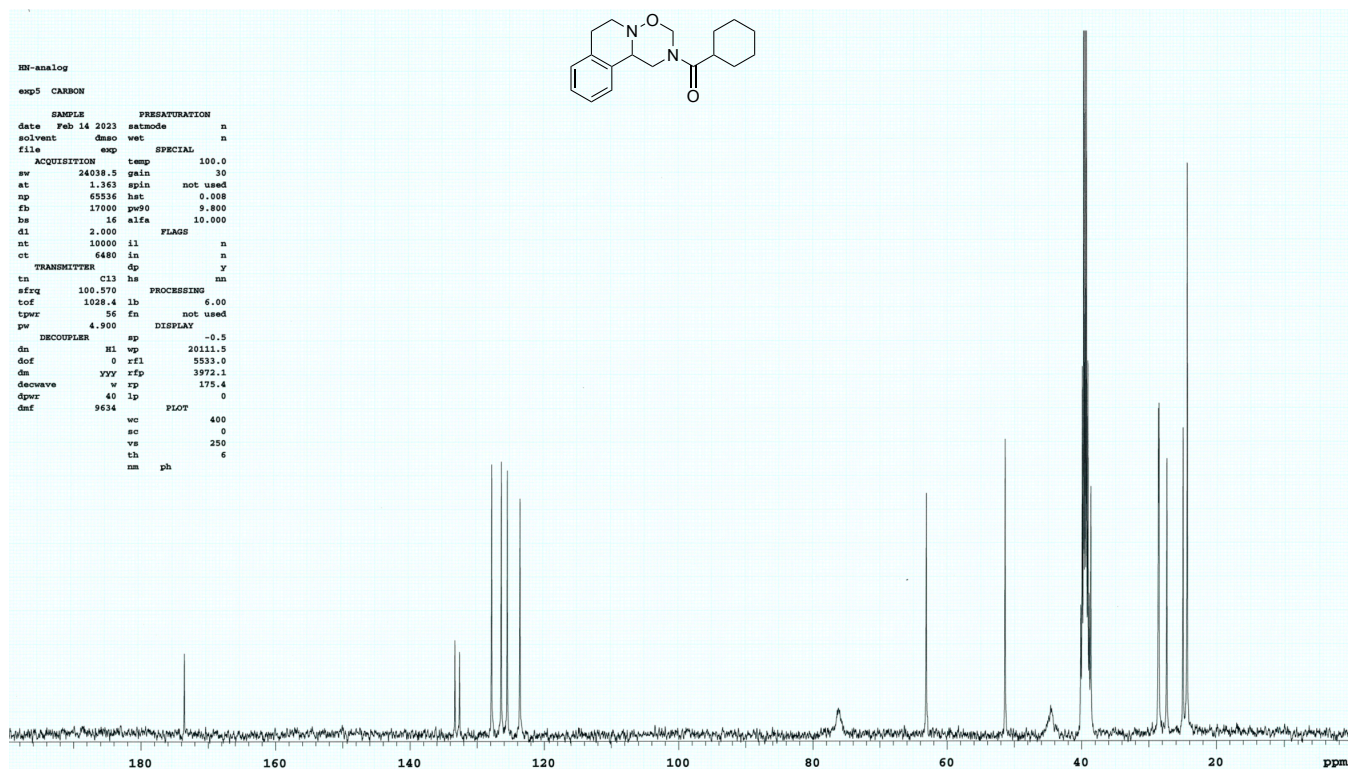
¹H NMR spectrum of (±)-cyclohexyl(1,6,7,11b-tetrahydro-[1,2,5]oxadiazino[3,2-a]isoquinolin-2(3*H*)-yl)methanone (**4**) at 100 °C



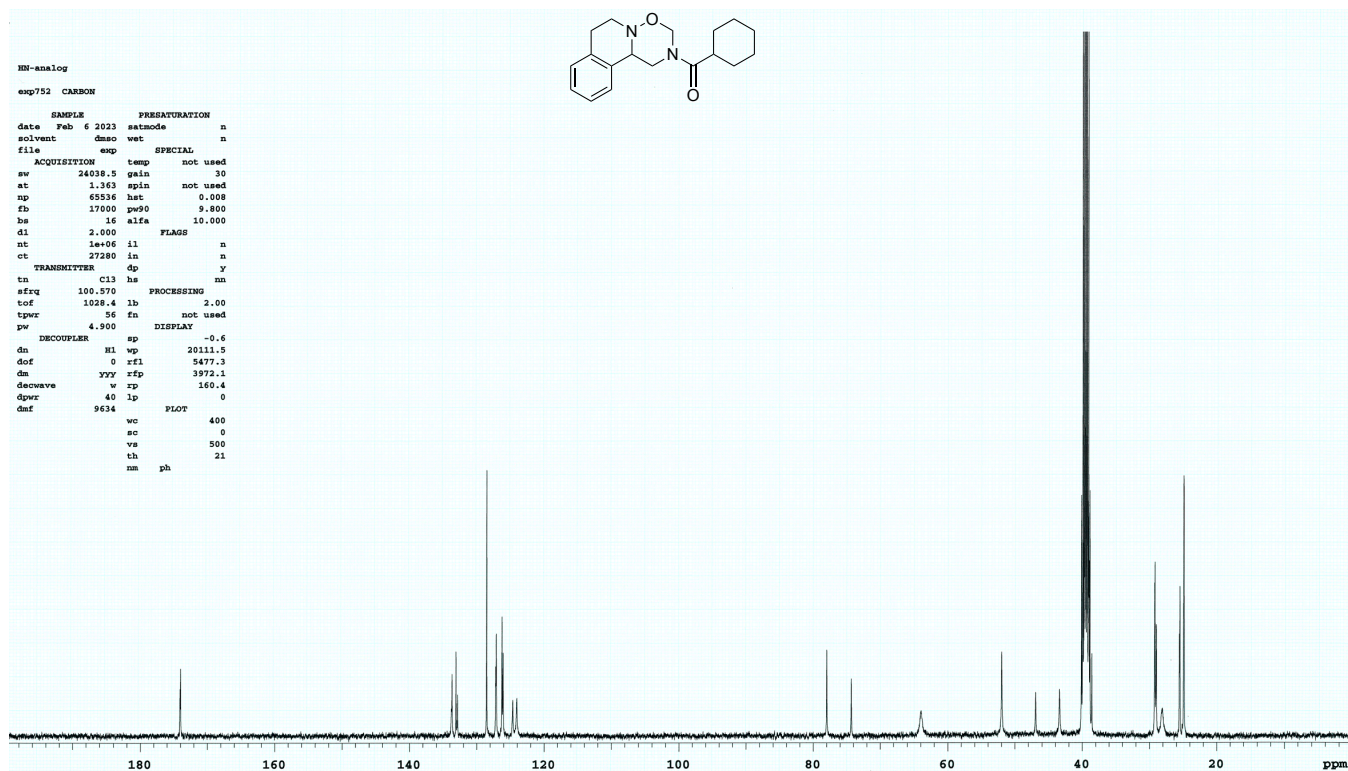
¹H NMR spectrum of (±)-cyclohexyl(1,6,7,11b-tetrahydro-[1,2,5]oxadiazino[3,2-a]isoquinolin-2(3*H*)-yl)methanone (**4**) at rt



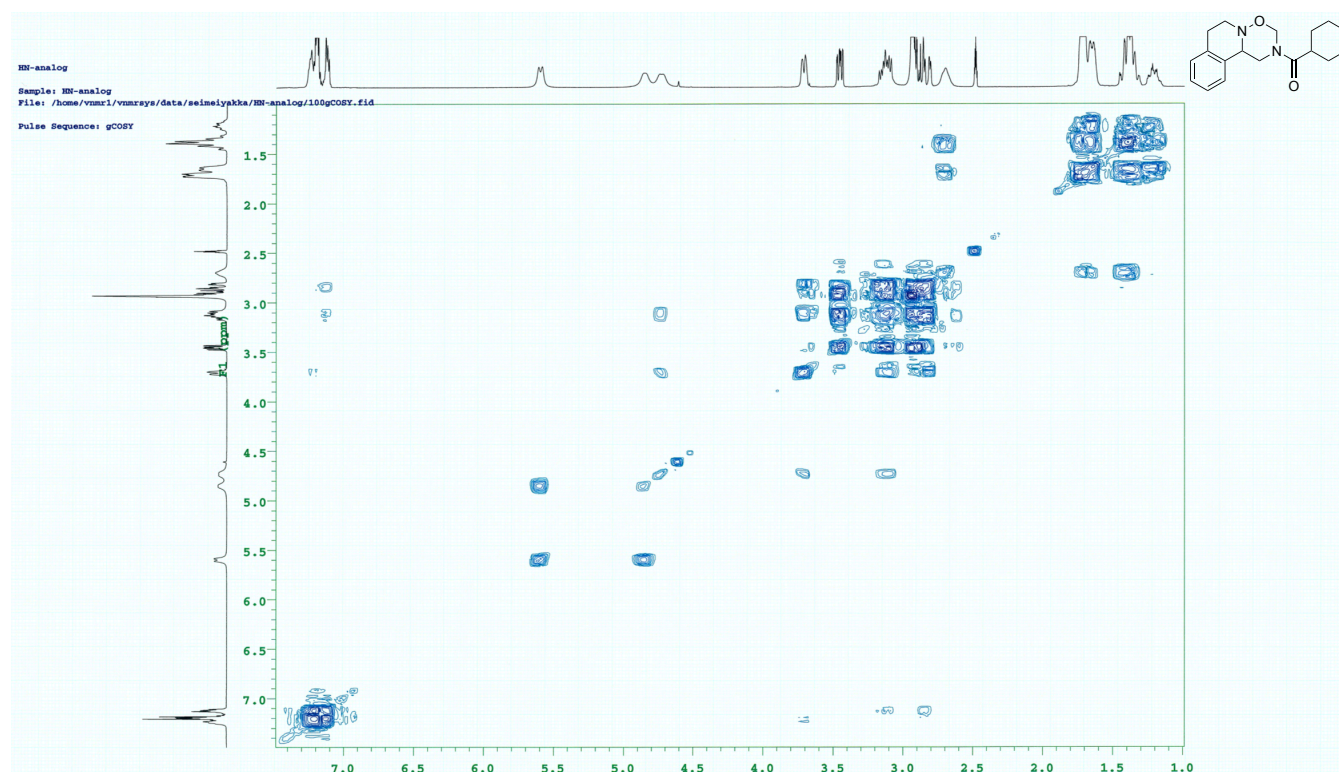
¹³C NMR spectrum of (±)-cyclohexyl(1,6,7,11b-tetrahydro-[1,2,5]oxadiazino[3,2-a]isoquinolin-2(3*H*)-yl)methanone (**4**) at 100 °C



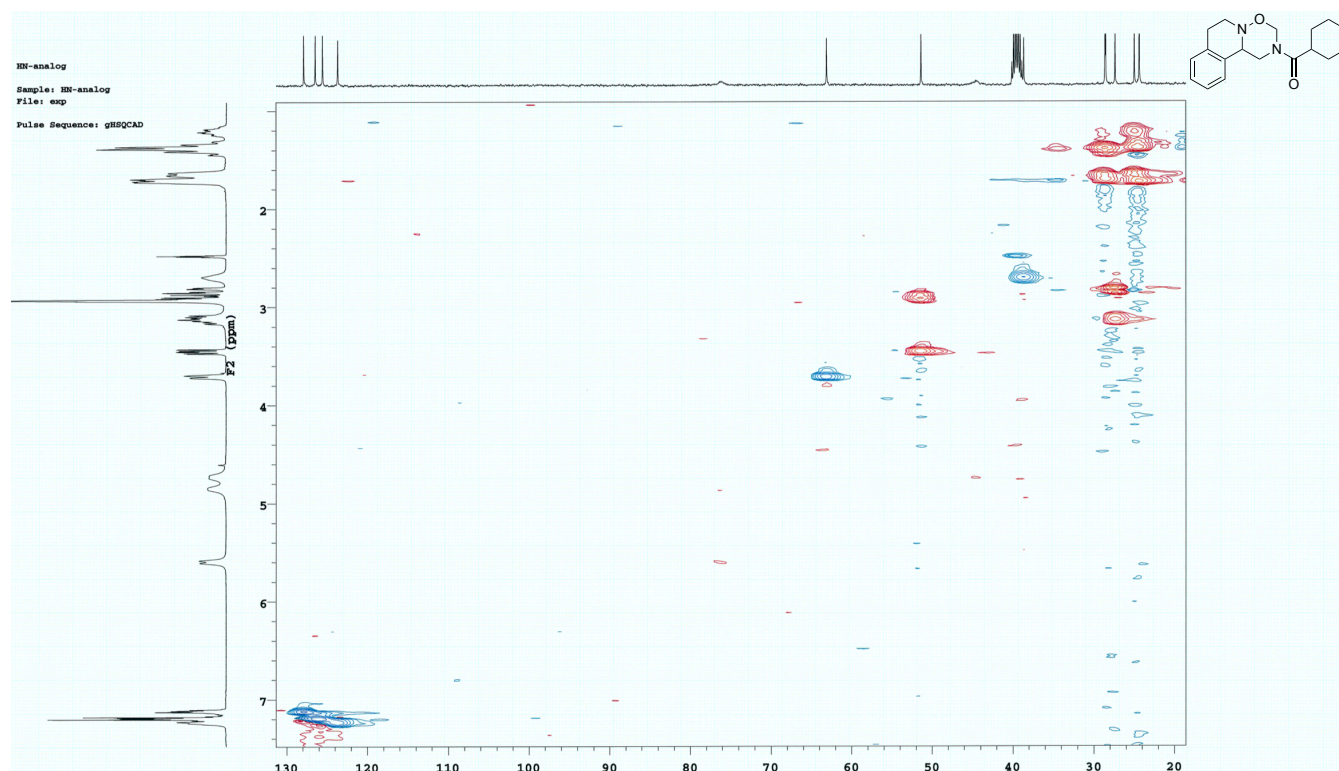
¹³C NMR spectrum of (±)-cyclohexyl(1,6,7,11b-tetrahydro-[1,2,5]oxadiazino[3,2-a]isoquinolin-2(3*H*)-yl)methanone (**4**) at rt



^1H - ^1H COSY spectrum of (\pm)-cyclohexyl(1,6,7,11b-tetrahydro-[1,2,5]oxadiazino[3,2-a]isoquinolin-2(3*H*)-yl)methanone (**4**) at 100 °C



HSQC spectrum of (\pm)-cyclohexyl(1,6,7,11b-tetrahydro-[1,2,5]oxadiazino[3,2-a]isoquinolin-2(3*H*)-yl)methanone (**4**) at 100 °C



9. Quenching Experiment

Emission of Ir^{III} complex **VIII** (excited at 380 nm, monitored at 475 nm) was quenched by nitron **1a**, *N,N,N',N'*-tetramethyldiaminomethane (**2**) in CH₂Cl₂. The Stern-Volmer plots is shown in Scheme 3 (a) in the article. The emission from the excited states of **VIII** was measured on Molecular Devices SpectraMax M5. The emission was quenched with **1a** and *N,N,N',N'*-tetramethyldiaminomethane (**2**) in Ar-saturated CH₂Cl₂. The relative emission intensities at 475 nm (excited at 380 nm) were determined with various concentrations of the quenchers. The Stern-Volmer relationship (equation 1) was obtained between the concentration of the quencher (Q) and the relative emission intensity (I_0/I), where I_0 and I represent the intensity in the absence and the presence of a quencher, respectively.

$$I_0/I = K_{SV}[Q] + 1 \quad (\text{eq. 1})$$

The slopes in the Stern-Volmer plots correspond to the Stern-Volmer constants (K_{SV}). The quenching fraction of emission (η (%)) is calculated according to equation 2. The parameters for the quenching of emission of **VIII** are summarized in Table S1.

$$\eta = \{1 - I/I_0\} * 100 = \{K_{SV}[Q]/(K_{SV}[Q] + 1)\} * 100 \quad (\text{eq. 2})$$

Table S1. Quenching fraction (η) of the emission of Ir^{III} complex **VIII** in CH₂Cl₂.

Quencher	Concentration (mM)	K_{SV} (M ⁻¹)	K_{SV} [Q]	η (%)
Nitron 1a	50	1.01×10^4	5.05×10^2	99.8
<i>N,N,N',N'</i> -tetramethyldiaminomethane (2)	500	2.86×10^3	1.43×10^3	99.9

10. Determination of Quantum Yield

The quantum yield of the reaction of nitron **1a** with *N,N,N',N'*-tetramethyldiaminomethane (**2**) was determined by using K₃[Fe(C₂O₄)₃] as the actinometer.^{6,7} The photolysis of K₃[Fe(C₂O₄)₃] (0.15 M) was carried out in a room with dim light, as depicted in the previously reported literature from our group.¹ The volume of the solution in the photon flux reaction was adjusted to 1 mL. A plot of moles of Fe²⁺ vs. irradiation time gave the average value of the three slopes of 5.277×10^{-8} . After that, the average value of the three slopes was divided by the quantum yield ($\Phi_{std} = 1.14$) of the actinometer (0.15 M) at 405 nm, followed by the absorbed fraction of 1.0 to give 4.629×10^{-8} einsteins s⁻¹. The plot of the formation of product **3aa** shown in Scheme 3 (b) in the article was drawn resulting from the following experiment. The mixture of nitron **1a** (10.0 mg, 4.73×10^{-2} mmol), *N,N,N',N'*-tetramethyldiaminomethane (**2**) (0.473 mmol), and Ir^{III} complex **VIII** (2.37×10^{-3} mmol), CH₂Cl₂ (946 μ L), and a stirring bar was placed in a quartz cuvette (path length: 1.00 cm) with a silicon septum and deaerated by bubbling with Ar for 15 min. After irradiation with a definite time, the reaction solution was evaporated to dryness. The residue was dissolved in CDCl₃ with 1,1,2,2-tetrachloroethane as an internal standard and was transferred to an NMR tube. The resulting amount of 1,2,5-oxaziadinane **3aa** was determined with the ¹H NMR spectrum. The plots of the moles of **3aa** versus irradiation times gave the slope of 1.053×10^{-8} . The absorbance at 405 nm was >2, which corresponded to the absorbed fraction of >0.999. Finally, the quantum yield (Φ_r) of the formation of **3aa** was determined to be 0.23 according to equation 3.

$$\phi_r = \frac{(\text{Rate of product formation})}{(\text{Photon flux})} \quad (\text{eq. 3})$$

11. Determination of Redox Potential and Excited-State Potential of Ir^{III} complex

11.1. Ir^{III} complex VIII

Electrochemical measurements were conducted using a glassy carbon electrode and a coiled platinum as the working and the counter electrodes, respectively. A reference electrode was Ag/AgNO₃ in CH₃CN, and the scan rate was 100 mV/s. Sample solutions were prepared by dissolving a sample (1 mM) in an electrolyte solution of [(Bu)₄N][PF₆] in CH₃CN (0.1 M, 8 mL) (Figure S3). The reference electrode was calibrated before measurements using an external ferrocene standard. Electrochemical data of Ir^{III} complex VIII are depicted in Table S2.

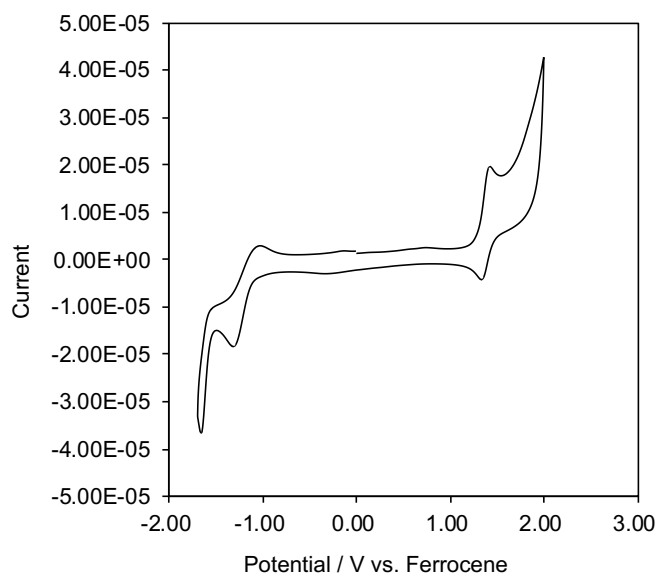


Figure S3. Cyclic voltammogram of Ir^{III} complex VIII.

Table S2. Electrochemical data (potential in V vs. Fc/Fc⁺) of VIII in CH₃CN at 298 K.

VIII	Fc/Fc ⁺	Ir ^{III} /Ir ^{II}	Ir ^{III} /Ir ^{II} vs. Fc/Fc ⁺	Ir ^{III} /Ir ^{IV}	Ir ^{III} /Ir ^{IV} vs. Fc/Fc ⁺
$E_{1/2}$	+0.085	-1.18	-1.26	+1.38	+1.30
E_p	—	-1.03	-1.12	+1.43	+1.34
E_n	—	-1.32	-1.40	+1.34	+1.25

Excited-state potentials are estimated using the Rehm-Weller equations as given (equation 5 and 6):

$$E^{0*}_{Ox} = E^{0'}_{Ox} - E^{0-0} \quad (\text{eq. 5})$$

$$E^{0*}_{Red} = E^{0'}_{Red} + E^{0-0} \quad (\text{eq. 6})$$

Where E^{0*} and $E^{0'}$ represent the excited state potential and the ground state potential, respectively. E^{0-0} means the 0-0 transition frequency of Ir^{III} complex VIII, which was revealed as 2.67 V in the previous report.¹ E_{Ox} represents the Ir^{III}/Ir^{IV} couples, and E_{Red} to the Ir^{II}/Ir^{III} couple. Therefore, excited state potentials (potential in V vs. Fc/Fc⁺) of VIII in CH₃CN at 298 K are depicted in Table S3.

Table S3. Excited-state potentials (E^*) (potential in V vs. Fc/Fc⁺) of VIII in CH₃CN at 298 K.

VIII	*Ir ^{III} /Ir ^{II} vs. Fc/Fc ⁺	*Ir ^{III} /Ir ^{IV} vs. Fc/Fc ⁺
E^*	+1.41	-1.37

11.2. Ir^{III} complex IX

The absorption spectrum and emission spectrum of Ir^{III} complex IX in MeCN are shown in Figure S4.

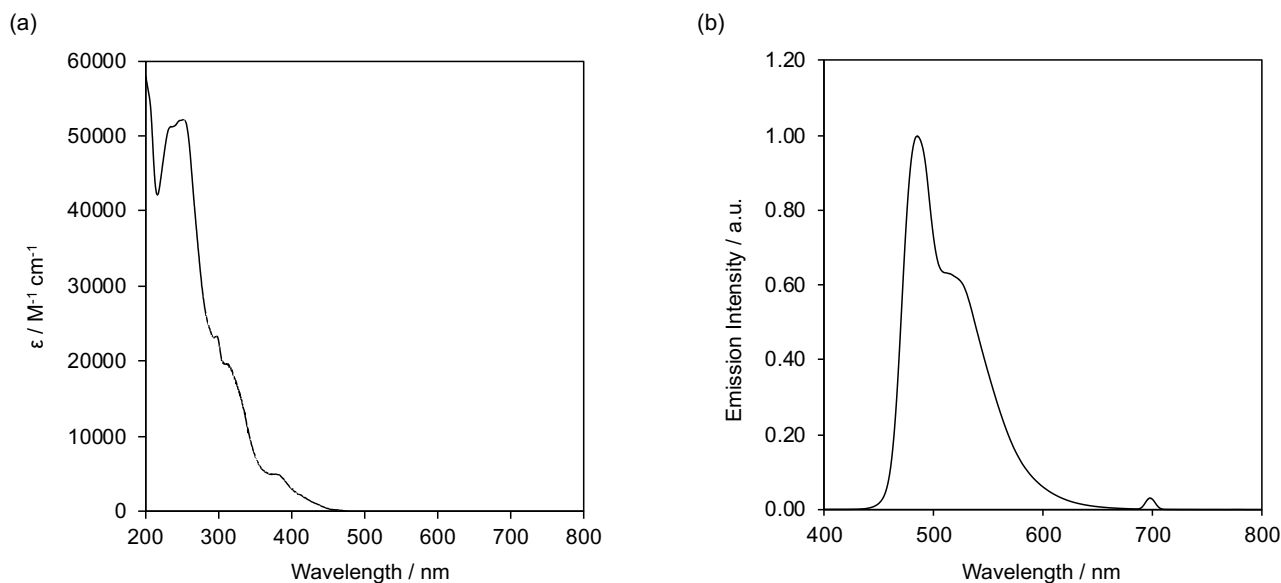


Figure S4. (a) Absorption spectrum of Ir^{III} complex IX at 296 K (5.34×10^{-6} M in MeCN). (b) Emission spectrum of Ir^{III} complex IX at 296 K (5.34×10^{-6} M in MeCN).

The emission spectrum of novel Ir^{III} complex IX at 77 K in propionitrile/*n*-butyronitrile was measured in accordance with the previously reported method⁸ to reveal that the maximum emission peak was observed at 2.63 eV (471 nm) as 0-0 transition frequency (Fig. S5a). Electrochemical measurements were conducted using a glassy carbon electrode and a coiled platinum as the working and the counter electrodes, respectively. A reference electrode was Ag/AgNO₃ in CH₃CN, and the scan rate was 100 mV/s. Sample solutions were prepared by dissolving a sample (1 mM) in an electrolyte solution of [(Bu)₄N][PF₆] in CH₃CN (0.1 M, 8 mL) (Figure S5b). The reference electrode was calibrated before measurements using an external ferrocene standard. Electrochemical data of Ir^{III} complex IX are depicted in Table S4.

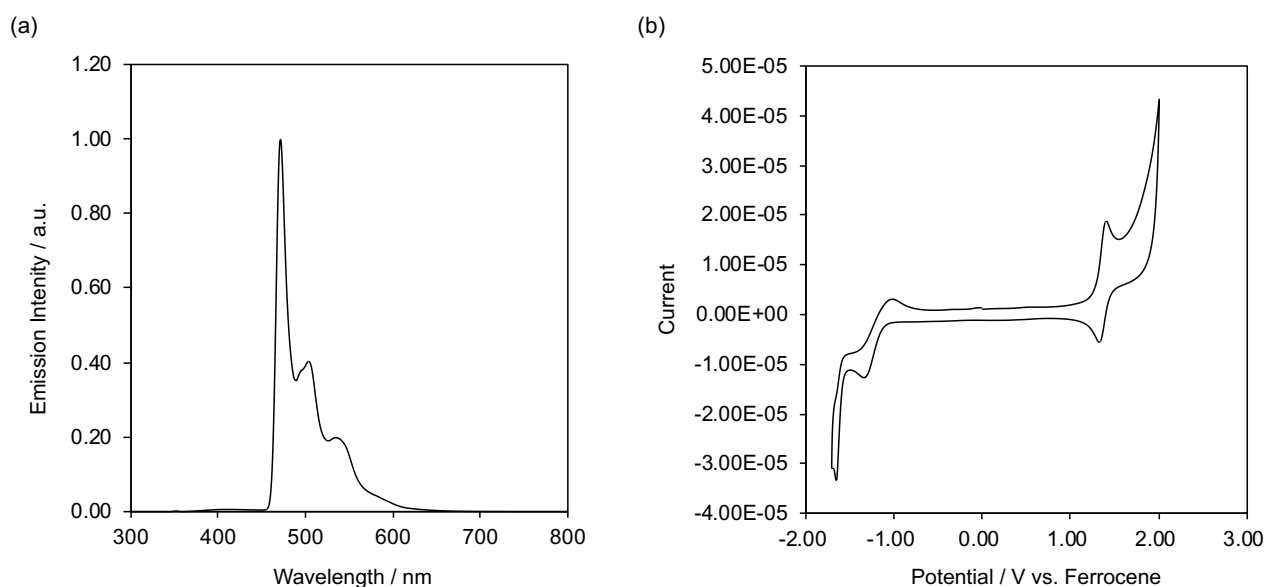


Figure S5. (a) Emission spectrum of Ir^{III} complex IX at 77 K in propionitrile/*n*-butyronitrile. (b) Cyclic voltammogram of Ir^{III} complex IX.

Table S4. Electrochemical data (potential in V vs. Fc/Fc⁺) of **IX** in CH₃CN at 298 K.

IX	Fc/Fc ⁺	Ir ^{III} /Ir ^{II}	Ir ^{III} /Ir ^{II} vs. Fc/Fc ⁺	Ir ^{III} /Ir ^{IV}	Ir ^{III} /Ir ^{IV} vs. Fc/Fc ⁺
$E_{1/2}$	+0.085	-1.18	-1.26	+1.36	+1.28
E_p	—	-1.02	-1.10	+1.40	+1.32
E_n	—	-1.34	-1.42	+1.32	+1.24

Excited-state potentials are estimated using the Rehm-Weller equations depicted in equation 5 and 6. The 0-0 transition frequency of Ir^{III} complex **IX**, which is revealed as 2.63 V. Therefore, excited state potentials (potential in V vs. Fc/Fc⁺) of **IX** in CH₃CN at 298 K are depicted in Table S5.

Table S5. Excited-state potentials (E^*) (potential in V vs. Fc/Fc⁺) of **IX** in CH₃CN at 298 K.

IX	*Ir ^{III} /Ir ^{II} vs. Fc/Fc ⁺	*Ir ^{III} /Ir ^{IV} vs. Fc/Fc ⁺
E^*	+1.37	-1.35

12. Computation of Dipole Moment

Structures of PZQ and **4** were optimized by B3LYP hybrid functional with 6-31G** basis set using Gaussian 16. Solvent effect of water was considered using the polarizable continuum model with the integral equation formalism variant (IEFPCM). Optimized geometries and energies are shown in Tables S6 and S7. The values of dipole moments obtained by the same calculation method are 1.97 and 3.96 debye for PZQ and **4**, respectively. The vectors of dipole moments for both compounds are shown in Figure S6.

Table S6. Optimized geometry of PZQ. Energy of PZQ is -998.512628364 a.u.

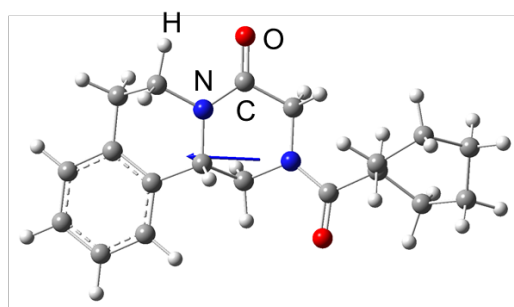
No.	Element	x (Å)	y (Å)	z (Å)
1	N	-0.749748	-0.160301	0.614772
2	C	0.592694	-0.715016	0.701638
3	C	1.500074	-0.053635	-0.343687
4	N	1.448925	1.408316	-0.167480
5	C	0.394671	2.069570	0.381451
6	C	-0.814592	1.270466	0.872658
7	C	2.597366	2.174162	-0.657441
8	C	-1.817297	-0.986162	0.357733
9	C	2.926128	-0.594000	-0.253992
10	C	4.034231	0.236782	-0.017050
11	C	3.853022	1.734915	0.091656
12	O	-1.647390	-2.191834	0.150254
13	C	3.126097	-1.971813	-0.430231
14	C	4.398338	-2.530611	-0.339047
15	C	5.497951	-1.708782	-0.078319
16	C	5.310593	-0.336997	0.070171
17	C	-3.213341	-0.360203	0.292596
18	C	-4.295322	-1.361272	0.774112
19	C	-5.669361	-1.118111	0.110493
20	C	-5.887749	0.368841	-0.194885
21	C	-4.850872	0.877922	-1.224067
22	C	-3.517419	0.099021	-1.154341
23	O	0.357682	3.295505	0.518916
24	H	-1.675160	1.720676	0.379610
25	H	-0.905707	1.483153	1.947082
26	H	0.521412	-1.785660	0.527528
27	H	1.005788	-0.543867	1.704475
28	H	1.100121	-0.301269	-1.338672
29	H	2.713357	1.995279	-1.733858
30	H	2.376995	3.228588	-0.501802
31	H	4.729779	2.249024	-0.316434
32	H	3.767311	2.039572	1.142908
33	H	2.278527	-2.615284	-0.649845
34	H	4.531121	-3.599452	-0.475976
35	H	6.495213	-2.132726	-0.008405

36	H	6.165866	0.310394	0.246799
37	H	-3.246916	0.520495	0.940987
38	H	-3.950098	-2.376217	0.561212
39	H	-4.388524	-1.277182	1.863279
40	H	-5.738230	-1.686848	-0.825947
41	H	-6.464145	-1.501946	0.759456
42	H	-6.903501	0.545322	-0.565260
43	H	-5.798722	0.939418	0.738843
44	H	-5.255558	0.788341	-2.238873
45	H	-4.663580	1.945303	-1.059138
46	H	-3.561236	-0.794876	-1.787741
47	H	-2.701964	0.713817	-1.551306

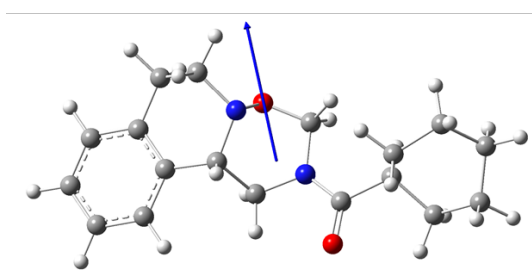
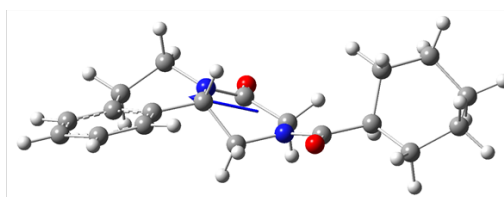
Table S7. Optimized geometry of **4**. Energy of **4** is -960.319474276 a.u.

No.	Element	x (Å)	y (Å)	z (Å)
1	N	0.691322	-0.355127	-0.560401
2	C	-0.628338	-0.961512	-0.409749
3	C	-1.515125	-0.124253	0.551662
4	N	-1.086121	1.296069	0.422089
5	C	0.647057	1.032059	-1.055892
6	C	-2.160836	2.261256	0.655658
7	C	1.817229	-1.016603	-0.153017
8	C	-2.994349	-0.409129	0.319112
9	C	-3.889200	0.603818	-0.065748
10	C	-3.393027	2.023308	-0.223476
11	O	1.761218	-2.156602	0.321983
12	C	-3.473084	-1.713915	0.511508
13	C	-4.814626	-2.024809	0.299760
14	C	-5.702555	-1.021040	-0.097010
15	C	-5.238579	0.281521	-0.267867
16	C	3.151990	-0.278316	-0.277791
17	C	3.496459	0.390419	1.074802
18	C	4.759504	1.273420	0.956839
19	C	5.777199	0.716199	-0.066841
20	C	5.671239	-0.810507	-0.167847
21	C	4.288602	-1.243735	-0.704454
22	H	1.310287	1.667216	-0.459792
23	H	0.909479	1.097171	-2.118637
24	H	-0.485098	-1.969571	-0.027126
25	H	-1.114508	-1.023582	-1.388006
26	H	-1.264209	-0.401372	1.584228
27	H	-2.424618	2.163846	1.715355
28	H	-1.746708	3.261235	0.504094

29	H	-4.183603	2.733557	0.041321
30	H	-3.127657	2.223868	-1.268659
31	H	-2.788248	-2.494216	0.834303
32	H	-5.166270	-3.041455	0.448572
33	H	-6.751728	-1.250256	-0.258876
34	H	-5.930340	1.069173	-0.556567
35	H	3.066975	0.510787	-1.031719
36	H	2.652564	0.986100	1.441128
37	H	3.651286	-0.406224	1.811797
38	H	4.472538	2.292105	0.671416
39	H	5.227016	1.349541	1.945456
40	H	5.587211	1.150697	-1.057058
41	H	6.793172	1.018543	0.209722
42	H	6.459287	-1.212538	-0.814039
43	H	5.839484	-1.245045	0.826115
44	H	4.313475	-1.292446	-1.799477
45	H	4.045229	-2.247109	-0.345119
46	O	-0.683567	1.482139	-0.974250



PZQ



4

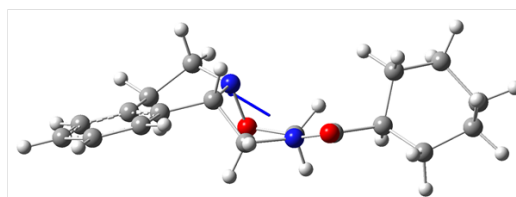


Figure S6. Vectors of dipole moments of PZQ (1.97 debye) and **4** (3.96 debye).

13. Single Crystal X-Ray Diffraction of **3ab**

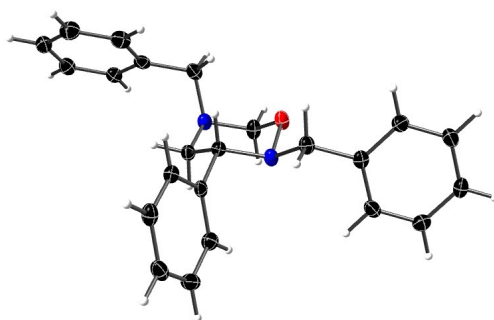


Figure S7. ORTEP drawing of **3ab** (CCDC deposition number: 2224678)

Suitable colorless crystals of **3ab** for X-ray diffraction measurements was obtained from the mixed solution of *n*-hexane and ethyl acetate at room temperature. Thermal ellipsoids are drawn at 50% probability level.

EXPERIMENTAL DETAILS

Table S8. Crystal Data.

Empirical Formula	C ₂₃ H ₂₄ N ₂ O
Formula Weight	344.46
Crystal Color, Habit	colorless, platelet
Crystal Dimensions	0.300 X 0.300 X 0.300 mm
Crystal System	monoclinic
Lattice Type	C-centered
Lattice Parameters	a = 21.6310(4) Å b = 5.52013(10) Å c = 30.7878(6) Å β = 90.895(6) ° V = 3675.80(12) Å ³
Space Group	C2/c (#15)
Z value	8
D _{calc}	1.245 g/cm ³
F ₀₀₀	1472.00
μ(CuKα)	5.955 cm ⁻¹

Table S9. Intensity Measurements

Diffractometer	R-AXIS RAPID
Radiation	CuK α (λ = 1.54187 Å) graphite monochromated
Voltage, Current	50kV, 40mA
Temperature	-180.0°C
Detector Aperture	460.0 x 256.0 mm
Data Images	180 exposures
ω oscillation Range (c=54.0, f=0.0)	80.0 - 260.0°
Exposure Rate	30.0 sec./°
ω oscillation Range (c=54.0, f=90.0)	80.0 - 260.0°
Exposure Rate	30.0 sec./°
ω oscillation Range (c=54.0, f=180.0)	80.0 - 260.0°
Exposure Rate	30.0 sec./°
ω oscillation Range (c=54.0, f=270.0)	80.0 - 260.0°
Exposure Rate	30.0 sec./°
ω oscillation Range (c=0.0, f=0.0)	80.0 - 260.0°
Exposure Rate	30.0 sec./°
Detector Position	127.40 mm
Pixel Size	0.100 mm
$2\theta_{\text{max}}$	136.4°
No. of Reflections Measured	Total: 19648 Unique: 3366 (R_{int} = 0.0253)
Corrections	Lorentz-polarization Absorption (trans. factors: 0.683 - 0.836)

Table S10. Structure Solution and Refinement

Structure Solution	Direct Methods (SIR2008)
Refinement	Full-matrix least-squares on F^2
Function Minimized	$\sum w (F_o^2 - F_c^2)^2$
Least Squares Weights	$w = 1 / [s^2(F_o^2) + (0.0430 \cdot P)^2 + 2.8001 \cdot P]$ where $P = (\text{Max}(F_o^2, 0) + 2F_c^2)/3$
$2\theta_{\text{max}}$ cutoff	136.4°
Anomalous Dispersion	All non-hydrogen atoms
No. Observations (All reflections)	3366
No. Variables	235
Reflection/Parameter Ratio	14.32
Residuals: R1 ($I > 2.00\sigma(I)$)	0.0382
Residuals: R (All reflections)	0.0426
Residuals: wR2 (All reflections)	0.0958
Goodness of Fit Indicator	1.078
Max Shift/Error in Final Cycle	0.001
Maximum peak in Final Diff. Map	$0.20 \text{ e}^-/\text{\AA}^3$
Minimum peak in Final Diff. Map	$-0.20 \text{ e}^-/\text{\AA}^3$

14. Biological Assay

Freshly isolated adult schistosomes from the infected mice were cultured in RPMI 1640 medium containing 5% fetal bovine serum and penicillin/streptomycin with or without the tested compound including **4** or PZQ at concentrations of 0.1 μ M, 1 μ M, and 10 μ M or No.4..., at 37°C in an atmosphere containing 5% CO₂.

15. ADMET Assay

15.1. Solubility and LogD

Each compound dissolved in PBS at a final concentration of 100 μ M in 1% DMSO. After shaking for 20 min, each solution was filtered using MultiScreen HTS MSSLBPC10 (Millipore) and filtrates were analyzed via UPLC (ACQUITY UPLC, Waters), using BEH C18 column (1.7 μ m, 2.1 \times 50 mm, Waters) with photodiode array detection (wavelength was 280 nm), and the solubility (%) of each compound was calculated by comparing the peak area with that of each well-dissolved (100 μ M in 5% DMSO) solution. Mobile phase A = 10mM ammonium acetate/5% acetonitrile/water, B = 10mM ammonium acetate/5% water/acetonitrile, and gradient system as follows: 0 min-2% B, 1.0 min-98% B. The flow rate was 0.8 mL/min. The logD (pH7.4) values were also calculated by comparing the retention times with that of standard compounds with a known logD value.

15.2. Caco-2 Assay

A caco-2 permeability assay was performed as follows. Briefly, 25 μ M each compound/HBSS solution was added to the upper wells of cultured Caco-2 cells in a trans-well-plate, and HBSS with 1% BSA was added to the lower wells. After incubation for 2 h, the solution on the top plate and the bottom plate was collected. Acetonitrile was added to the solution, which was vortexed and centrifuged at 3500 rpm for 20 min. The supernatant was analyzed by LC-MS/MS, and the apparent permeability coefficient (Papp) was calculated. The class "high" means that the Papp of compound was higher than the Papp of propranolol.

15.3. LC-MS/MS Analysis

LC-MS/MS analysis was performed using an ACQUITY UPLC® system (Waters) fitted with a cooling autosampler and a column oven with temperature control. Mass spectrometry was performed using a Waters Xevo TQ-S tandem quadrupole mass spectrometer (QQ-MS; Waters). Chromatographic separation was performed on an ACQUITY UPLC® BEH C18 1.7 μ m column (50 mm \times 2.1 mm; Waters). The mobile phase A was 0.1% formic acid in water (v/v), and acetonitrile containing 0.1% formic acid was used as mobile phase B. The flow rate was set at 0.5 mL/min. The sample injection volume was 5 μ L. The injected sample was eluted from the column with the following gradient program: 1.8-min linear gradient in solvent B from 2% to 98%, 0.7-min linear gradient in solvent B from 98% to 2%, and 2.5-min hold at 2% B. Positive electrospray ionization was used to generate the parental ions.

15.4. Acid Stability Assay

For the acid stability assay, 5 μ M each compound was added to acidic (dissolution test solution 1, pH1.2) or neutral (phosphate-buffered saline, pH7.4) buffers, respectively. After incubation at 37°C for 0, 1, and 5 hours at 37 °C, acetonitrile was added to each mixture, which was vortexed and centrifuged at 3500 rpm for 20 min. The supernatant was analyzed by LC-MS/MS, and the ratio of unchanged chemical compound at 1 or 5 hr compared to the unchanged each compound at 0 hr as 100% was calculated.

15.5. Metabolic Stability in Microsomes

For the metabolic stability assay, 500 μ M each compound was mixed with liver microsomes (Sekisui XenoTech, LLC, final concentration 0.2 mg protein/mL), coenzyme group (1.3 mM NADPH, 3.3 mM G-6-P: Sigma, 3.3 mM MgCl₂: Wako), and 0.45U/mL G6PDH (Oriental Yeast) at 37 °C, for 0 min and 60 min. Acetonitrile was added to each mixture, which was vortexed and centrifuged at 3500 rpm for 20 min. The supernatant was analyzed by LC-MS/MS, and the ratio of unchanged chemical compound at 60 min compared to the unchanged each compound at 0 min as 100% was calculated.

15.6. Cytotoxicity Assay

The Hela cells were plated to the 96 well microplate at 1,000 cells/well and incubated in the culture medium. Each compound was treated with 10, 20, and 30 μM for 2 days, then WST-8 reagent was added and measured at 405 nm. Cytotoxicity was calculated using the cell viability of DMSO-treated wells as 100%.

15.7. Cardiotoxicity Assay

The human iPS cell-derived cardiomyocytes, iCell[®] Cardiomyocytes² (FUJIFILM Cellular Dynamics, Inc.) were plated to the gelatin-coated 96 well half-area microplate (Corning[®] 3882) at 30,000 cells/well and incubated in the culture medium. After 9 days of cells maintenance, cells were stained with EarlyTox[™] Cardiotoxicity Kit (Molecular Devices, LLC.), and were set on FDSS system (Hamamatsu photonics K.K.) for Ca^{2+} transient measurements, made pre and after compound treatment.

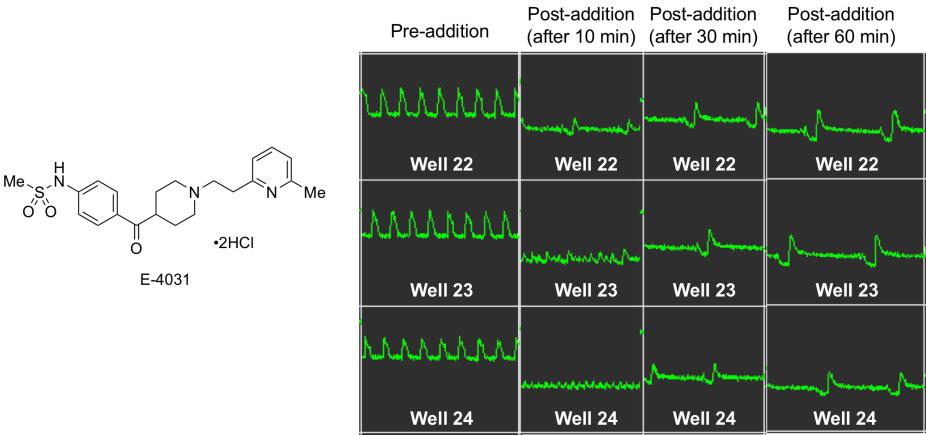


Figure S8. Time-course evaluation of the cardiotoxic effects of the hERG channel blocker E-4031.

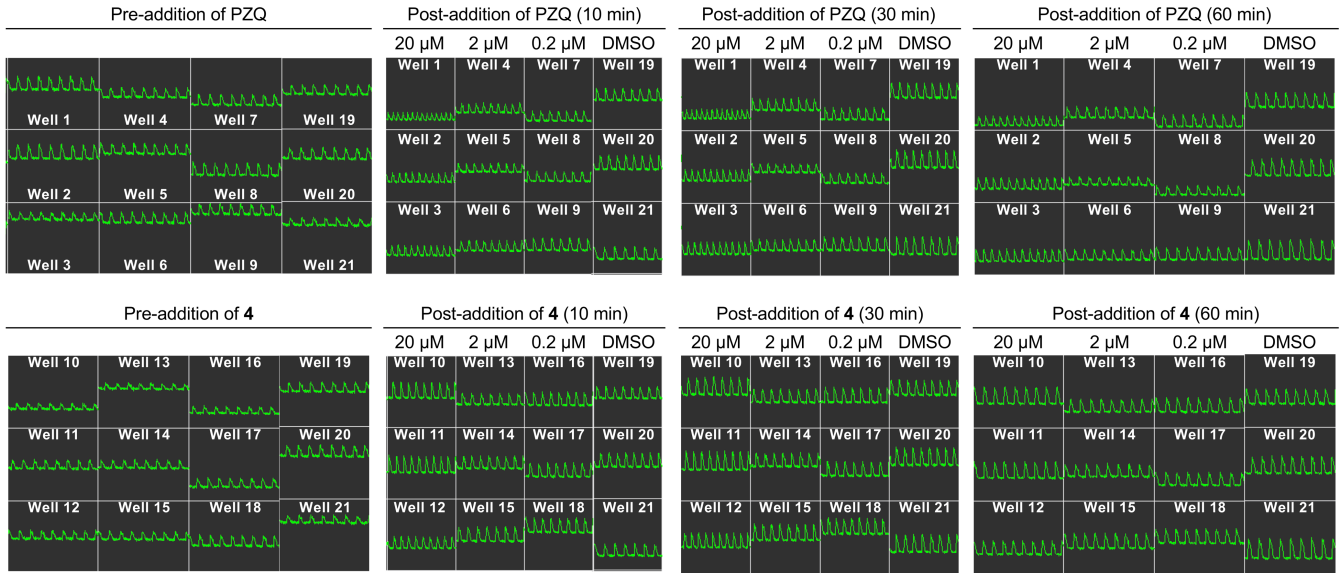


Figure S9. Time-course evaluation of the cardiotoxic effects of PZQ and 4.

16. References

- 1 K. Itoh, N. Ishii, A. Takashino, A. Hara, S. Kon, T. Mizuguchi, F. Karaki, S. Hirayama, Y. Shibagaki, K. Nagai, N. Sato, K. Tokunaga, M. Suzuki, M. Hashimoto, H. Fujii, *J. Photochem. Photobiol. A: Chem.*, 2022, **434**, 114293.
- 2 D. M. Schultz, J. W. Sawicki, T. P. Yoon, *Beilstein J. Org. Chem.*, 2015, **11**, 61–65.
- 3 H. Li, J. Oppenheimer, M. R. Smith III, R. E. Maleczka Jr. *Tetrahedron Lett.*, 2016, **57**, 2231–2232.
- 4 (a) C. Gella, È. Ferrer, R. Alibés, F. Busqué, P. de March, M. Figueredo, J. Font, *J. Org. Chem.*, 2009, **74**, 6365–6367; (b) K. S. Chan, M. L. Yeung, W.-K. Chan, R.-J. Wang, T. C. W. Mak, *J. Org. Chem.*, 1995, **60**, 1741–1747.
- 5 (a) Y. Xie, B. Qian, P. Xie, H. Huang *Adv. Synth. Catal.*, 2013, **355**, 1315–1322; (b) K. Itoh, A. Takashino, A. Ohtsuka, M. Kobe, S. Sawamura, R. Kato, S. Hirayama, F. Karaki, T. Mizuguchi, N. Sato, K. Tokunaga, Y. Toda, H. Suga, H. Ishida, H. Fujii, *ChemPhotoChem*, 2020, **4**, 388–392.
- 6 M. Montalti, A. Credi, L. Prodi, M. T. Gandolfi, in *Handbook of Photochemistry*, 3rd ed., CRC Press, Boca Raton, 2006, pp. 601–616.
- 7 G. J. Choi, Q. Zhu, D. C. Miller, C. J. Gu, R. R. Knowles, *Nature*, 2016, **539**, 268–271.
- 8 K. P. S. Zononi, B. K. Kariyazaki, A. Ito, M. K. Brennaman, T. J. Meyer, N. Y. M. Iha, *Inorg. Chem.*, 2014, **53**, 4089–4099.